Optimizing process design and control development for free-radical polymerization in continuous reactors

Juan Miguel García Méndez

Universidad Nacional de Colombia
Facultad de Ingeniería y Arquitectura
Departamento de Ingeniería Química
Manizales, Colombia
2023

Optimizing process design and control development for free-radical polymerization in continuous reactors

Juan Miguel García Méndez

Thesis or degree project presented as a partial requirement to qualify for the title of:
Maestría en ingeniería - Ingeniería química

Director:
Óscar Andrés Prado Rubio, PhD

Co-Director:
Alneira Cuellar Burgos, PhD

Research area:
Process optimal design and control-Polymers
Grupo de Investigación en Aplicación de Nuevas Tecnologías (GIANT)

Universidad Nacional de Colombia
Facultad de Ingeniería y Arquitectura
Departamento de Ingeniería Química
Manizales, Colombia
2023

“You can really do anything you set your mind to. Just look around you!”

Irvin Guevara

“It's all about not breaking, when you're already broken”

Joel Segura

“May your heart stay faithful and your will relentless. The sun will shine again. Do not fall prey to despair, and do not be led astray”.

Daniel "Ithzerian" Goldberg

Agradecimientos

Quiero agradecer a mis padres Luz Mariela y Alvaro por apoyarme en la realización de este trabajo, a mi hermano mayor Felipe por ser mi mejor amigo, por influir tanto en mis gustos personales como en mi forma de ser. Mi familia es el motivo más grande por el cual realice este trabajo, espero que este trabajo los haga sentir orgullosos de mí y de ustedes mismos ya que ustedes me criaron para ser la persona que soy el día de hoy. También a mí mismo por tanta valentía, paciencia y dedicación a lo largo de esta aventura.

A mi director de tesis, el profesor Oscar Andrés Prado rubio por darme la oportunidad de realizar este trabajo bajo su tutela, ya que de algún modo no fui el mejor estudiante en el momento de conocernos, a pesar de todo me permitió tener como tutor a uno de los mejores profesores que he tenido el gusto de conocer en toda mi vida. Por su motivación, por su energía, entrega a este proyecto y a la docencia. A mi co-directora la profesora Alneira Cuéllar Burgos, por todo el conocimiento brindado, por su disposición a trabajar en un área que tampoco es de su correspondencia y a estar dispuesta hacer equipo para poder sacar este bonito trabajo adelante.

Agradezco a mis amigos en la universidad, a Diego por ser siempre mi amigo a pesar de no ser la mejor persona del mundo, a Leyton por aceptarme tal cual la persona que soy, a Dani por ser mi amigo de maestría por escucharme y atenderme. Agradecer a los integrantes de nuestro grupo de investigación, a Luis, a Laura, a Oscar, a Julio, a Ebtisan, a Jason, no solo por los buenos momentos que pasamos juntos si no por toda su ayuda para que este trabajo se pudiera realizar. También agradecer a todas las personas con las que tuve la fortuna de compartir en esta maestría, Carlos, Maria Alejandra, Junior, Jhon, y a muchos otros que hicieron parte de este proceso de aprendizaje y crecimiento personal.

Finalmente quiero agradecer a toda mi familia, mis primos, mis tías y tíos, por siempre estar ahí y brindarme muchos momentos felices de mi vida, a todas las personas que ya no están y que de algún modo me sigue apoyando a pesar de ello, a mi niña hermosa porque nunca le importo que tipo de persona era, siempre

estaba feliz de verme y que se conformaba con una simple caricia, espero que ahora estes en un lugar muy feliz.

Abstract

Optimizing process design and control development for free-radical polymerization in continuous reactors

The polymeric industry has been exhibiting remarkable economic growth, in recent years due to increasing product demand. Just like other processes with remarkable development, the polymeric industry carries environmental and economic problems with the generation of a substantial amount of waste. An important percentage of the waste generated by polymerization processes is the off-specification product due to a lack of process control. Also, polymerization processes are challenging, where complex interactions of mass and energy are handled, thus intricate mathematical models are obtained, whose solution might not be straightforward. Those depend on the polymer type and the synthesis methods used in the process, in some cases presenting simplification compared with other polymerization systems. Among the most interesting polymers, there is polystyrene, which is highly used in the industry for production versatility, and relevant markets, among others.

The most employed production route is through bulk polymerization by free radicals due to the properties, kinetic mechanisms and operation of the polymerization reactor are still highly studied. Also, separation is not required after the reaction, simplifying the flowsheet. For this kind of system, a high process understanding leads to better design and enhanced control which are essential to ensure the production of a high-quality final product. Due to its relevance, polystyrene is highly investigated to cope with production limitations such as poor temperature and viscosity control.

Having those problems in mind, this research aims improving the environmental impact and economic potential in a complex system as such the bulk polymerization by free radicals, through optimal design and implementing of advanced control structures (focused on polystyrene but potentially appliable for any polymer produced by this process). Herein, two systems are investigated for bulk polymerization by free radicals of polystyrene using different reactor configurations. The first study case is based on a continuous stirred-tank reactor (CSTR) from the literature. The second study case investigates potential process improvements

when the reaction takes place in a plug flow reactor (PFR), taking some elements to the CSTR study case.

In order to determine the best production scenarios, optimal design is performed using a global approach through a genetic algorithm (GA), obtaining an optimal point to perform the reaction. Employing an optimization with two objective functions, providing a robust selection for the optimal point (operation point). Evaluating two technical criteria, namely efficiency and economic aspects, assessed by the productivity and the operational cost. Giving a robust design to obtain the operational point in the system, accomplishing physics characteristics desired for the final product (mass average molecular weight) and the reactor (conversion). Taking as case study a relatively big pilot scale reactor (reactor volume of 3000 L), results show an operational cost of 521932.83 USD/year and productivity of 6.21e-5 mol/L*h for the CSTR case, also, conversion values of 0.38 and mass average molecular weight values of 72436.24 g/mol. On the other hand, for the PFR with a total volume of 9470.19 L, operational cost and productivity values of 86171.80 USD/year and 0.0024 mol/L*h are obtained, respectively and conversion values of 0.61 and 70869.58 of mass average molecular weight.

Subsequently, the control structure design and implementation are performed. A comparison is done between linear controllers and two advanced controllers, namely the proportional-integral-derivative (PID) control, linear-quadratic-regulator (LQR) control, and linear-quadratic-Gaussian (LQG) control. Controller performance is assessed through well-established performance indexes such as settling time, rise time, time to first peak, and overshoot during setpoint tracking and disturbance rejection tests. Nevertheless, the comparison is not only used for the controllers but instead the systems in general, evaluating important performance indexes (*e.g.* cost evaluation, productivity, production time, among others). For both case studies, the best controller performance is obtained with LQG controller, the more advanced controller implemented. With settling times 2 times faster than the other two controllers in the CSTR case. For the PFR case values of 6 times faster the settling time for PID controller.

Particularly, it is advantageous to use a Kalman filter (within the LQG controller) to calculate the response of unmeasured variables in the system using physically measurable variables (limitation that PID control has). In this case, the moments of molecular weight distribution (physically unmeasurable) were calculated through the mass average molecular weight (measurable). It is worth mentioning that no information about the implementation LQG controllers in this process was found in the literature, so the findings presented here are novel. Then, the investigated approach prove a powerful tool to overcome the monitoring limitations. Also, despite the best control structure are the advanced controllers, the use of basic controllers

as the PID, shows a good performance in both reactors compared with the system in open loop (no control implementation).

The findings found in this thesis showed an improvement in environmental impact and economic potential for bulk polymerization by free radicals of polystyrene in a continuous process. This was accomplished by first by employing a systematic methodology for design and performance evaluation that copes with the particular challenges of the polymerization process. Secondly, by using diverse control strategies beyond conventional simple loops in conjunction with the optimal design. Therefore, the model-based approach proposed in this research provided relevant system understanding reflected in improved process design and control.

Finally, this research has shown the benefit of considering optimal design and advanced control in the development of future polymerization processes, driving enhanced system performance towards more sustainable processes.

Keywords: Optimal Polystyrene production, PID, LQR, LQG, CSTR, PFR, simulation, optimization, GA optimization.

Resumen

Optimización del diseño de procesos y desarrollo de controles para la polimerización por radicales libres en reactores continuos

La industria polimérica ha estado exhibiendo un crecimiento económico notable en los últimos años debido a la creciente demanda de productos. Al igual que otros procesos con notable desarrollo, la industria polimérica conlleva problemas ambientales y económicos con la generación de una cantidad sustancial de residuos. Un porcentaje importante de los residuos que se generan en los procesos de polimerización es el producto fuera de especificación por falta de control del proceso. Además, son desafiantes los procesos de polimerización, donde se manejan interacciones complejas de masa y energía, obteniendo así modelos matemáticos intrincados, cuya solución puede no ser sencilla. Éstos dependen del tipo de polímero y de los métodos de síntesis utilizados en el proceso, presentando en algunos casos una simplificación en comparación con otros sistemas de polimerización. Entre los polímeros más interesantes, se encuentra el poliestireno, muy utilizado en la industria por su versatilidad productiva y mercados relevantes, entre otros.

La ruta de producción más empleada es mediante polimerización en masa por radicales libres debido a que las propiedades, los mecanismos cinéticos y el funcionamiento del reactor de polimerización son altamente estudiados. Además, no se requiere separación después de la reacción, lo que simplifica el diagrama de flujo. Para este tipo de sistema, un alto conocimiento del proceso conduce a un mejor diseño y control, que son esenciales para garantizar la producción de un producto final de alta calidad. Debido a su relevancia, el poliestireno se investiga mucho para hacer frente a las limitaciones de producción, como el control deficiente de la temperatura y la viscosidad.

Teniendo en cuenta estos problemas, esta investigación pretende mejorar el impacto ambiental y el potencial económico de un sistema complejo como es la polimerización en masa por radicales libres, mediante el diseño óptimo y la implementación de estructuras de control avanzadas (centradas en poliestireno pero potencialmente aplicables a cualquier polímero producido por este proceso). En este documento, se investigan dos sistemas para la polimerización en masa mediante radicales libres de poliestireno utilizando diferentes configuraciones de reactor. El primer caso de estudio se basa en un reactor de tanque agitado continuo (CSTR) de la literatura. El segundo caso de estudio investiga posibles mejoras en

el proceso cuando la reacción tiene lugar en un reactor de flujo pistón (PFR), implementando algunos elementos al caso de estudio CSTR.

Para determinar los mejores escenarios de producción, se realiza un diseño óptimo mediante un enfoque global a través de un algoritmo genético (GA), obteniendo un punto óptimo para realizar la reacción. Emplear una optimización con dos funciones objetivo, proporcionando una selección robusta para el punto óptimo (punto de operación). Evaluando dos criterios técnicos, a saber, la eficiencia y los aspectos económicos, evaluados por la productividad y el costo operativo. Dando un diseño robusto para obtener el punto operativo en el sistema, cumpliendo con las características físicas deseadas para el producto final (peso molecular promedio másico) y el reactor (conversión). Tomando como caso de estudio un reactor a escala piloto relativamente grande (volumen de reactor de 3000 L), los resultados muestran un costo operativo de 521932,83 USD/año y una productividad de 6,21e-5 mol/L*h para el caso CSTR, además, valores de conversión de 0,38 y valores de peso molecular promedio en masa de 72436,24 g/mol. Por otro lado, para el PFR con un volumen total de 9470.19 L, se obtienen valores de costo operativo y productividad de 86171.80 USD/año y 0.0024 mol/L*h, respectivamente y valores de conversión de 0.61 y 70869.58 de peso molecular promedio en masa.

Posteriormente se realiza el diseño e implementación de la estructura de control. Se realiza una comparación entre controladores lineales y dos controladores avanzados, a saber, el control proporcional-integral-derivativo (PID), el control de regulador lineal-cuadrático (LQR) y el control lineal-cuadrático-gaussiano (LQG). El rendimiento del controlador se evalúa mediante índices de rendimiento bien establecidos, como el tiempo de asentamiento, el tiempo de elevación, el tiempo de pico y el sobreimpulso durante las pruebas de seguimiento del punto de ajuste y rechazo de perturbaciones. Sin embargo, la comparación no sólo se utiliza para los controladores sino para los sistemas en general, evaluando importantes índices de desempeño (por ejemplo, evaluación de costos, productividad, tiempo de producción, entre otros). Para ambos casos de estudios, el mejor rendimiento del controlador se obtiene con el controlador LQG, el controlador más avanzado implementado. Con tiempos de asentamiento 2 veces más rápidos que los otros dos controladores en el caso CSTR. Para el caso del PFR, los valores son 6 veces más rápidos que el tiempo de asentamiento del controlador PID.

Particularmente, es ventajoso usar un filtro de Kalman (dentro del controlador LQG) para calcular la respuesta de variables no medidas en el sistema usando variables físicamente medibles (limitación que tiene el control PID). En este caso, los momentos de distribución del peso molecular (físicamente no medibles) se calcularon a través del peso molecular promedio en masa (medible). Cabe mencionar que no se encontró en la literatura información sobre la implementación

de controladores LQG en este proceso, por lo que los hallazgos aquí presentados son novedosos. Entonces, el enfoque investigado demuestra ser una herramienta poderosa para superar las limitaciones del monitoreo. Además, a pesar de que la mejor estructura de control son los controladores avanzados, el uso de controladores básicos como el PID, muestra un buen desempeño en ambos reactores en comparación con el sistema en lazo abierto (sin implementación de control).

Los hallazgos encontrados en esta tesis mostraron una mejora en el impacto ambiental y el potencial económico de la polimerización en masa mediante radicales libres de poliestireno en un proceso continuo. Esto se logró primero empleando una metodología sistemática para el diseño y la evaluación del desempeño que hace frente a los desafíos particulares del proceso de polimerización. En segundo lugar, mediante el uso de diversas estrategias de control más allá del lazo simple convencionale junto con el diseño óptimo. Por lo tanto, el enfoque basado en modelos propuesto en esta investigación proporcionó una comprensión relevante del sistema que se refleja en un mejor diseño y control de procesos.

Finalmente, esta investigación ha demostrado el beneficio de considerar un diseño óptimo y un control avanzado en el desarrollo de futuros procesos de polimerización, impulsando un mejor rendimiento del sistema hacia procesos más sostenibles.

Palabras clave: Producción óptima de Poliestireno, PID, LQR, LQG, CSTR, PFR, simulación, optimización, optimización GA.

Contents

Figures

Tables

1. Introduction

1.1. Research motivation

The fast-growing world population has an increasing demand for energy and products which drives research to provide further developments in a sustainable way. In particular, product development satisfying the world's needs, such as polymers, is still in growth due to their mechanical and technical properties useful in many areas. For this reason, the constant research on polymers increases the spectrum of applications in different areas, from domestic use to large scale industry (Koltzenburg, Maskos and Nuyken, 2017). Some relevant applications of polymers are listed in Table 1-1.

The rising demand for the production of polymers around the world since the first appearance in 1950 is growing rapidly, at the beginning, the production was approximately 1.5 million tons, now the world production is around 359 million tons (Garside, 2019). In 2014, China and Europe were the principal producers with 31% and 16% of the world production, respectively. Besides, Latin America is in the sixth position with only 4% without significant changes since 2006 (PlasticsEurope, 2009; PlasticEurope, 2020).

Polymers also conventionally called “plastics” are sensitive to temperature (thermoplastic), so these products could be warped at high temperatures (Johnson *et al.*, 1994). Thermoplastics usually are the most produced polymer in the global market and also the most studied polymers in the industry, such as polypropylene (PP) and polyethylene of low density (LDPE) (Mundoplast, 2017). Due to their wide range of applications corresponding to more than 80% of the worldwide production of polymers (Figure 1-1).

Table 1-1: Common uses of polymers in different fields.

Field	Application example	Reference
Detergent industry	Surfactants.	(Tejedor, 2014)
Packaging industry	Water bottle, Kellogg's packing, supermarket bags.	(Postobón, 2020)
Automotive industry	Dashboard, Mirrors, Headlights.	(Riduco S.A., 2010)
Electricity	Connection cables, transistors, boards.	(Johnson *et al.*, 1994)
Construction	PVC tubes, gutters, skylight, additive in concrete.	(González Madariaga, 2008)
Aerospace industry	Interior wall panels, aircraft doors, luggage compartments, fuselages.	(Ghori *et al.*, 2018)
Furnishing industry	Wood-plastic composites.	(Stark and Matuana, 2007)
Textile industry	Synthetic fibers as nylon and Dacron.	(Casatextil, 2018)
Sport industry	Accessories as the helm in skate and bike.	(Falabella, 2020)
Electronic devices	Frame in computers and cellphones.	(American Chemistry Council, 2020)

From global production, a significant number of polymeric products are classified as single-use plastics. This kind of products are generally wasted after being used, producing tremendous environmental pollution (Schnurr *et al.*, 2018). To counteract this problem, governments have proposed the implementation of fines or forbidding plastics (Schnurr *et al.*, 2018). However, it does not entirely fix the problem, since the main problem is not the plastic as such. The constraint is the consumer who does not follow the environmental measures as protocols designed by the local environmental entities, generating environmental pollution. On the other hand,

recycling these kind of materials has been proposed, despite the polymers just can reprocess a few times (Rojas González and Ríos Aranzazu, 2018). Despite important, that approach is insufficient to deal with the environmental problem. More recently, there is a world trend of sustainable development, where biopolymers could satisfy the different properties required for the polymers industry. However, many biopolymers cannot be produced at a large scale to supply actual world demand and present production limitations comparable to the petrochemical polymers.

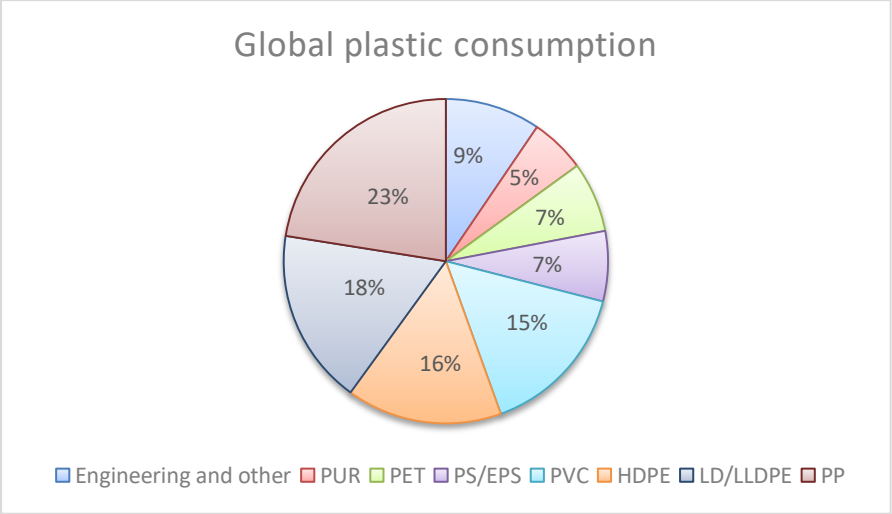

Figure 1-1: Global plastic consumption adapted from Plasteurope, (2012). PUR (polyurethane), PET (Polyethylene terephthalate), PS (polystyrene), EPS (expandable polystyrene), PVC (Polyvinyl chloride), HDPE (High-density polyethylene), LD (Low-density polyethylene), LLDPE (Linear low-density polyethylene), PP (Polypropylene).

In the last decade, the polymer industry has been subject to great pressure due to the strengthening of environmental policies, especially for the large amount of waste generated by polymeric materials, thus demanding to optimize the process to decrease this waste. During production, large amount of wasted plastic is generated during the stage of polymerization processes as off-specification products. This product is generated by disturbances in the process, which implies a loss of resources, energy, and thus process economic potential loss.

As many other processes at large scale, there is a need to reduce off-specification manufacture and the polymer industry is not the exception, creating polymers

without the correct specification thus deflecting the properties required in the final product. These properties are modified mostly by the final molecular weight of the sample and temperature in the process (Asteasuain *et al.*, 2006; Alvarez and Odloak, 2012; Patil, Maia and Ricardez Sandoval, 2015).

The molecular weight in continuous processes of polymerization is frequently used as a scheduling process, which consists in produce various grades of product throughout the plant production, switching between one polymerization grade to another. The continuous polymerization processes frequently used continuous reactors in series to achieve a high yield, thus to operate with a schedule to reach a different gamma of polymers grades non-stopping the process (España, Gobierno de Marino, 2007). The reaction scheduling depends on the desired polymerization grade of the final product (*i.e.* associated with the molecular weight) (Patil, Maia and Ricardez Sandoval, 2015). However, monitoring the molecular weight is challenging, since this is an analytical process that can take 30 minutes as the size exclusion chromatography, so exist a delay between the real-time variable and the measured variable (Asteasuain *et al.*, 2006).

Alternatively, the reaction behavior could be controlled by the temperature, due to the temperature affect directly the energy balances, States, ranges and stability in reactors (Almeida, Wada and Secchi, 2008; Patil, Maia and Ricardez Sandoval, 2015; Wang, Tan and Wu, 2019). Even poor control in this variable can carry some problems in the specification of products since polymers are thermoplastic. Therefore, the presence of high temperatures during production f some important properties loss of the final product.

Despite the multiple efforts to solve this problem, this is a relevant research are where advances are made every day in these technical problems for polymerization processes. Particularly, it is necessary to reduce the off-specification generated during the polymerization. If the waste amount is not controlled, it implies a rise in the environmental and economic problems, since in many cases a considerable profit loss in the polymerization processes. Automatic control is an interesting alternative to solve the problem, increasing the process performance, reducing energy consumption, and the amount of product outside the specifications (Patil, Maia and Ricardez Sandoval, 2015). The automatic control anticipates changes in the process, attempting to hold some important variables in the process enhancing the process.

The findings of this thesis contribute understanding the optimal the behavior of the optimal reactor design making a trade off between productivity and cost of styrene production system, provides insights into control structures designed for polymerization processes and criteria evaluating the controller performance which make the process suitable. Using these strategies, it is expected to reduce the industrial production times of material off-specification, thus improving the environmental impact and the economic potential of an industrial polymerization process. To accomplish the control system development, it is necessary to use a systematic methodology for design and performance evaluation, which copes with the particular challenges of the polymerization process. Therefore, a model-based approach is proposed where simulations are used to emulate and understand the process behavior. Subsequently, time and frequency domain analyses are performed to design, implement and evaluate control structures, diverse controllers must be implemented beyond conventional single loops.

1.2. Methods of synthesis

Polymers synthesis methods are anionic polymerization, coordination polymerization, cationic polymerization and radical polymerization. Herein, radical polymerization is further explained due to the extensive studies in polymers reactions by this method of synthesis. The reaction steps are described in the following subsections, starting from the monomer until the desired polymerization degree.

1.1.1 Step polymerization reaction

Step polymerization works without the presence of an initiator. Herein, the monomer units have functional groups that can react with each other. Reactions are slower, and growth is skipping rather than unit-to-unit, where oligomers bind to each other (Braun *et al.*, 2013).

1.1.2 Chain polymerization reaction

Chain polymerization occurs when activated species react with a monomer molecule to give an intermediate. Subsequently, that intermediate successively reacts with monomer molecules to give new intermediates. The reaction becomes a manifold repetition of the monomer addition until reaches the termination where the active center disappears (Braun *et al.*, 2013). The potential routes are:

a) Anionic polymerization

It is a chain reaction where an atom or group with a negative charge and a pair of unshared electrons react. When the initiators are nucleophilic reagents that incorporate into the monomer to produce a carbanion. Then, this carbanion is added to the monomer molecules where the polymer will grow to termination when the polymer takes a proton from the solvent. An example of anionic polymerization is polyvinyl chloride (PVC) production. The scheme of an anionic reaction is shown below (Johnson *et al.*, 1994).

- Initiation

$$N^- + M \rightarrow NM^- \tag{1.1}$$

- Propagation

$$NM^- + M \rightarrow NMM^- + M \cdots N(M)_n^- \tag{1.2}$$

- Termination

$$N(M)_n^- \rightarrow (M)_n + N^- \tag{1.3}$$

b) Coordination polymerization

Coordination polymerization reactions are carried out with organometallic catalysts, which occur in the presence of gaseous monomers and heterogeneous polymerization conditions. Generally, the hydrocarbon solvents used in these reactions and many of the most effective catalysts are insoluble, making it difficult to investigate the precise nature of polymerization chemistry. An example of anionic polymerization is polyethylene (PE) production using Ziegler-Natta catalysts (Johnson *et al.*, 1994).

c) Cationic polymerization

This is a reaction of monomers with carbon-carbon double bonds, where the initiators must be species of high electronic density forming a carbonium ion. The initiators react with the monomer, promoting the polymer growth, reaching a termination by ion par collapse, protons expulsion or transfer to monomer. An example of anionic polymerization is polyisobutylene production. The scheme can be seen below (Johnson *et al.*, 1994).

- Initiation

$$E^+ + M \rightarrow ME^+ \quad (1.4)$$

- Propagation

$$ME^+ + M \rightarrow MME^+ + M \cdots (M)_n E^+ \quad (1.5)$$

- Termination by ion-par collapse

$$(M)_n E^+ \rightarrow E(M)_n \quad (1.6)$$

- Termination by proton expulsion

$$(M)_n E^+ \rightarrow (M)_n + EH \quad (1.7)$$

- Termination by transfer to monomer

$$(M)_n E^+ \rightarrow (M)_n + ME \quad (1.8)$$

d) Radical polymerization

Here, a free radical is produced by the covalent bond breakdown of the initiator, where the monomer reacts whit the radical. This produces a chain reaction in which the monomer will grow into a high molecular mass. Then, the formed polymer will stop reacting by disproportionation, combination, solvent transfer, or monomer transfer. An example of radical polymerization is polyacrylic acid (PAA) production. The reaction mechanism is shown below (Johnson *et al.*, 1994).

- Initiation

$$I_n \rightarrow n\, R^* \tag{1.9}$$

$$R^* + M \rightarrow R{M_1}^* \tag{1.10}$$

- Propagation

$$M_i^* + M \rightarrow M_{i+1}^* \tag{1.11}$$

- Termination by combination

$$M_i^* + M_j^* \rightarrow P_{i+j} \tag{1.12}$$

- Termination by disproportionation

$$M_i^* + M_j^* \rightarrow P_i + P_j \tag{1.13}$$

- Termination transfer to solvent

$$M_i^* + S \rightarrow P_i + S^* \tag{1.14}$$

- Termination transfer to monomer

$$M_i^* + M \rightarrow P_i + M_1^* \tag{1.15}$$

1.3. Techniques for manufacturing polymers

There are three different techniques for manufacturing polymers, bulk, solution and dispersion, the radical polymerization could be carried using any of these techniques. Figure 1-2 shows the classification of the techniques for manufacturing and some characteristics from each everyone, in the following subsection those methods are explained.

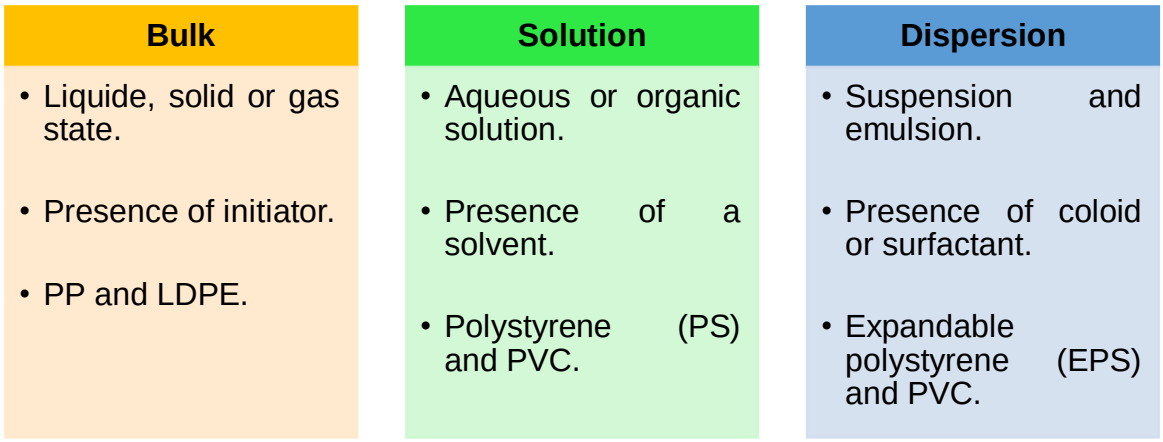

Figure 1-2: The different processes of manufacturing techniques polymerization and some characteristics, adapted from Braun *et al*, (2013).

1.3.1. Solvent polymerization (solution)

The reaction is carried out in the presence of a solvent, where the monomer and the polymer must be soluble in it, and also require agitation throughout the process. This process is used in the production of polyacrylonitrile (PAN) and polyethylene (PE). Some advantages are easy control of key performance indexes as thermal control, mass transport, handling and good molecular weight control. However, this kind of reaction increases the dispersion of molecular weights, and the final polymer is contaminated by a solvent that must subsequently be treated. Additionally, it generates polymers with a high polydispersity index, modification in thermal and chemical stability, the solvent choice must be careful (Braun *et al.*, 2013).

1.3.2. Dispersion polymerization

In the dispersion polymerization technique, the reaction is carried out in the presence of a surfactant or a protective colloid in a solvent (usually water), in which the monomer is insoluble and the catalyst could be soluble or not. This polymerization is carried out in heterogeneous conditions, in a liquid/liquid dispersion is called emulsion and, in a liquid/solid dispersion is called suspension.

In industry, it is used for the production of polyvinyl chloride (PVC) and polymethylmethacrylate (PMMA). Some advantages are the polymerization heat removal easily, no large changes in the overall viscosity in high conversions, and low particle size. Nevertheless, the presence of a surfactant hinders the separation from the final product (Braun *et al.*, 2013).

1.3.3. Bulk polymerization

Finally, in the bulk polymerization technique, the reaction is carried out with a monomer and catalyst or initiator, the monomer is soluble in polymers. This technique is employed in the production of polystyrene and low-density polyethylene. Radical polymerization also uses bulk polymerization as an industrial technique, due to the implementation of an initiator that works like the free radical as shown in the mechanism.

Some advantages are the final product is not polluted with solvent and high molecular weights are obtained. On the other hand, in this type of reaction residual unreacted monomers may remain, reaction mixtures had a high viscosity and difficulty the thermal control, which can cause the final product degradation (Braun *et al.*, 2013).

1.4. Molecular weight measurement

Due to polymers have high molecular weight, they are actually obtained with a molecular weight distribution. Molecular weight is a crucial variable in a polymerization reactor, since depending on this, the polymer has some specific properties such as: hardness, flexibility, among others. For this reason, it is necessary to monitor the molecular weight to control product quality as some properties depend on molecular size, *e.g.* for high molecular weight, the tensile strength is bigger too (Balani *et al.*, 2015). The following section diverse ways to calculate the molecular weight in polymers are depicted mentioning their importance in the process.

Molecular weight distribution refers to a set of chain length distribution. The molecular weight distribution provides relevant data to measure the molecular weight of the polymer. Due to statistical methods are required to calculate the distributions, depending on the statistic moment, the distribution may contain different distributions such as the number average molecular weight, the mass molecular weight, the average z molecular weight and the viscosity molecular weight, among others. The molecular weight distribution data is given in Table 1-2. In the table, the most important definitions are the polydispersity index and hence,

the number average molecular weight and the mass average molecular weight due to the importance of these variables in polymerization reactors.

In literature, there are different approaches to measure the molecular weight, however, the main variable used to classify a polymer is the polydispersity index (related to the polymerization grade). Also, it has been highlighted the importance of viscosity to express the molecular weight (correlation between the molecular weight and viscosity). In real applications, it is hard to measure directly the molecular weight, for this reason mathematical models are used for its estimation such as observers or Softsensors. In those approaches, a mathematical model emulates the behavior of the molecular weight in the sample through the reaction time using indirect process measurements (Hernández-Escoto, López and Alvarez, 2010). So, it is not just important the molecular weight as a variable but the way to measure molecular weight too.

Table 1-2: Definition of Molecular weights distributions adapted from Braun *et al*, (2013).

Name	Remark	Equation
Number average molecular weight	Where N_i is the number of molecules in the sample having the molecular weight M_i, and M_i is the arithmetic average of the molecule's number distribution.	$M_n = \frac{\sum N_i M_i}{\sum N_i}$ (1.16)
Mass average molecular weight	corresponds to the first moment of the mass distribution of the molecular weight.	$M_w = \frac{\sum N_i {M_i}^2}{\sum N_i M_i}$ (1.17)
Average z molecular weight	It uses the measured sedimentation equilibria in ultracentrifugation for calculation	$M_z = \frac{\sum Z_i M_i}{\sum Z_i}$ (1.18)
Viscosity average molecular weight	Where a comes from a relation between the molecular weight and the viscosity, as the Mark-Houwink-Kuhn relation	$M_v = \frac{\sum w_i {M_i}^a}{\sum w_i}$ (1.19)
Polydispersity index	It denotes the dispersion of the molecules in the polymer sample, closer to 1 the polymer presents a lower dispersion in the molecules, while the polymer present higher numbers the sample will present more dispersion. Moreover, the polydispersity index is also related to the polymerization grade. The	$PDI = \frac{M_w}{M_n}$ (1.20)

	polymerization grade is the average number of monomers repeated in the polymer chain	

1.5. State-of-the-art: control in polymerization reactors

Within the context of this research, the keywords “automatic-control-polymerization-reactors-and-control-reactor-polymer” have been used in the database Scopus®. As result, it has been found 123 papers mostly in the subject area of Chemical Engineering (22%), Engineering (23%), Chemistry (19%), material science (11%), mathematics (4%), computer science (11%), among other (10%). From those, an exhaustive literature review is performed in bulk polymerization by free radicals, where the most important papers are condensed in Table 1-3, where 14 references are for CSTR and 3 references for PFR dating from the year 1990 to 2019. This table has been constructed by reference, polymer, reactor, process operation mode, manipulated variable, controlled variable, control and optimization type, and some remarks of important aspects.

Firstly, it is worth mentioning that the relevant classification aspect is the application itself, where polystyrene is the most studied polymer in this field. Other polymers have been found as polymethyl methacrylate and polypropylene. Additionally, the polymerization most studied is the bulk polymerization by free radicals (Alvarez and Odloak, 2012; Gharaghani, Abedini and Parvazinia, 2012; Patil, Maia and Ricardez Sandoval, 2015).

From process design perspective, CSTR has implemented already automatic control (Alvarez and Odloak, 2012; Patil, Maia and Ricardez Sandoval, 2015; Qing Guo, Liu and Chen, 2015) but just a few of authors use a plug flow reactor (PFR) for the implementation (Chatzidoukas, Pistikopoulos and Kiparissides, 2009) furthermore, just one paper implemented the CSTR and PFR in series as the industrial process works (Gharaghani, Abedini and Parvazinia, 2012). Furthermore, the implementation of reactors in series for bulk polymerization processes is not frequently used presumably for the implementation of more robust mathematics (Li and Christofides, 2007). Therefore, there is an opportunity to implement different arrangement of reactors, with the idea to potentially enhance the polymerization process performance.

Regarding the controlled variables, commonly researchers select the molecular weight, the polymerization grade, the polydispersity index, a molecular weight

distribution, and even the viscosity. Besides, temperature is either used as a monitored or controlled variable. The controlled variables are an important decision since those directly connected with the control objectives. On the other hand, the conventional selection of manipulated variables are the coolant flow in the reactor's jacket, initiator flow, the solvent flow, among others (Chatzidoukas, Pistikopoulos and Kiparissides, 2009; Patil, Maia and Ricardez Sandoval, 2015). Usually, the manipulated variables are the inputs in the systems and are directly linked to the control objective. Allowing the choice of different combinations for the system control structure design.

From the controller perspective, in many cases, the implemented control is SISO feedback (e.g. P, PI, PID, PD), feedforward, or their combination (Felorzabihi, Ghadi and Dhib, 2003; Asteasuain *et al.*, 2006; Gharaghani, Abedini and Parvazinia, 2012; Patil, Maia and Ricardez Sandoval, 2015; Wang, Tan and Wu, 2019). Additionally, advanced process control application is scarce, therefore there is an opportunity to further investigate advanced control and evaluate potential process improvements.

Some articles describe the monitoring difficulties and thus investigate the implementation of observers in the system (Hernández-Escoto, López and Alvarez, 2010; Bousbia-Salah *et al.*, 2019; Wang, Tan and Wu, 2019). Those contribution highlight the importance of how to measure molecular weight and the role of implementing observers in the simulations done.

Finally, there is a couple of applications where optimizations are performed to choose the best control strategy accounting multiple parameters such as the manipulated variables and economical view (Chatzidoukas, Pistikopoulos and Kiparissides, 2009; Patil, Maia and Ricardez Sandoval, 2015). That research depicts new ways to couple optimal design and automatic control, improving the polymerization processes with a global perspective at the cost of substantial complexity increase.

As previously mentioned, bulk polymerization by free radical of styrene is still highly studied and is almost considered a benchmark for control since the kinetic parameters are easily found in the literature (Hidalgo and Brosilow, 1990; Asteasuain *et al.*, 2006; Alvarez and Odloak, 2012). Besides, this polymerization technique has had a problem controlling the viscosity and the temperature in the process. The problem is usually, solved by the implementation of automatic control, enhancing the performance of the technique, reducing the costs of the polymerization process. Additionally, changes in the molecular weight make the process easy for perturbation and analyze the response in the system.

An aspect to highlight is the majority of research are based on Hidalgo and Brosilow, (1990), because of the way the information is presented in the article. Such as the steady state variables, parameter values, assumptions in the reactor for the mass and energy balances, and the step to step of the kinetic presented in the bulk polymerization by free radical of styrene. For this research, Alvarez and Odloak, (2012) model is selected since it is a dynamic model appliable for design and control. Also, the research is based on Hidalgo and Brosilow, (1990) taking the considerations already mentioned.

Table 1-3: Common uses of polymers in different fields.

Reference	Polymer	Reactor	Manipulated Variable	Controlled Variable	Controller and optimizator	Remark
(Gazi et al., 1996)	Styrene	CSTR	-Volume fraction of solvent in the reactor. -Flow rate of the initiator. -Cooling water and monomer flow rates.	-Solvent/monomer flow rates. -Molecular weight distribution. -Reactor Temperature.	-PID controller. -Implementation of NSIM algorithm and nonparametric Monte-Carlo technique for uncertainty in the model.	-Implementation of approaches for the uncertainty in the model in some parametric values ranges.
(Felorzabihi, Ghadi and Dhib, 2003)	Styrene	CSTR	-The cooling medium temperature.	-Reactor temperature.	-Nonlinear control low based on differential geometry. -P and PI.	-This kind of control implementation shown a outperform the P and PI controllers, besides driving temperature to a new stable state condition in a shorter time and without overshoot.
(Asteasuain *et al.*, 2006)	Styrene	CSTR	-Monomer flow rate. -Initiator flow rate. -Coolant flow rate.	-Reactor temperature. -Jacket temperature. -Molecular weight.	-PI and feedforward control. -Mixed-integer dynamic optimization (MIDO). -Use of a Kalman filter.	-The use of optimization to choose the better control strategy (many control possibilities depending on the objective function). -Here use 3 different study cases, 2 polymers of different molecular weights in 3 situations.
(Guo et al., 2011)	Styrene	CSTR	-Flow rate initiator. -Flow rate coolant.	-Molecular weight. -PDI (Polydispersity index).	-Combination of feedforward and PID control.	-Use of 2 objective functions one for the transition time in operation and the consumption of the initiator.

Reference	Polymer	Reactor	Manipulated Variable	Controlled Variable	Controller and optimizator	Remark
(Gharaghani, Abedini and Parvazinia, 2012)	Styrene	CSTR and Tubular reactor	-Liquid flow rate from the return vessel. -Cooling water flow rate. -Inlet hot oil flowrate to the 1st jacket. -Inlet hot oil flow rate to the 2nd jacket. -Inlet hot oil flow rate to the 3rd jacket.	-Jacket temperature. -The reactor temperature at the exit of each section.	-Genetic algorithm for the optimization (GA), optimization. -Proportional integral derivative controller (PID) for the temperature in the CSTR. -Proportional integral control (PI) for the level in the CSTR 3 PID for the PFR.	-The state of styrene is in the bubble point in the CSTR. -The parallel use of CSTR and tubular reactor. -GA is used for optimization to maximize the final monomer conversion, to obtain the final number average molecular weight close to a common commercial grade, and finally minimization of the final polydispersity index in the product.
(Qing Guo, Liu and Chen, 2015)	Styrene	CSTR	-Flow rate initiator. -Flow rate coolant.	-Molecular weight. -PDI.	-PID and feedforward control.	-They use a solvent in the reaction and have the summation of the live polymer for the kinetic reaction. -Optimization.

Reference	Polymer	Reactor	Manipulated Variable	Controlled Variable	Controller and optimizator	Remark
(Wang, Tan and Wu, 2019)	Styrene	CSTR	-Flow rate initiator. -Flow rate monomer.	-Moment of the MWD (Molecular weight distribution).	-Active disturbance rejection controller (ADRC). -An orthogonal polynomial feedforward neural network (OPFNN) and a recurrent neural network (RNN) combined from other article.	-They compare the different control strategies for the different manipulated variables.
(Meszena and Johnson, 1999)	Styrene	CSTR, batch, tubular reactor	-N/N.	-MWD (Molecular weight distribution).	-Monitoring control.	-The use of 3 different types of reactors for the evolution of MWD with different approximations. -The flow reactor has been made in a CFD simulation. -Batch reactor and CSTR simulated solving profiles of the equations of systems and Reaction of styrene with solvent.

Reference	Polymer	Reactor	Manipulated Variable	Controlled Variable	Controller and optimizator	Remark
(Li and Christofides, 2007)	N/N	CSTR and Tubular reactor	-Concentration at the entrance of the reactor.	-Concentration in the exit of the reactor	-Linear quadratic regulator (LQR). -PI. -Optimal control.	-Two CTRS in series, makes a difference of arrangement usually seem.
(Meira and Johnson, 1981)	N/N	Tubular reactor	-Flow rate monomer. -Flow rate initiator.	-MWD.	-Novel control scheme.	-It is an experimental tubular reactor. -It is living polymerization.
(Cedex, 1982)	Styrene	Batch and Semi-Batch	-N/N.	-N/N.	-Monitoring in an experimental reactor.	-Bulk polymerization. -Has an experimental part with a batch reactor.
(Alvarez and Odloak, 2012)	Styrene	CSTR	-Flow rate initiator. -Flow rate coolant.	-Viscosity. -Reactor temperature.	-Model predictive control (MPC). -Real-time optimization.	-In the paper aboard 3 layers one with RTO, the other with the MPC and one with a target calculation, to predict the best configuration. -They have no setpoints like a fixed value, here they use a range as the setpoint.

Reference	Polymer	Reactor	Manipulated Variable	Controlled Variable	Controller and optimizator	Remark
(Nguyen, Hoang and Azlan Hussain, 2019)	Styrene	CSTR	-Flow rate initiator. -Flow rate coolant.	-Initiator concentration. -Reactor temperature.	-Passivity-based control.	-Explain the passivity theory and how it works in a MIMO. -Graphics and analysis like the in the process productive class.
(Chatzidoukas, Pistikopoulos and Kiparissides, 2009)	Olefin copolymerization	PFR	-Product withdrawal. -Cooling water feed rate. -Nitrogen feed rate. -Monomer feed rate in the make- upstream.	-Bed height. -Reactor temperature. -Reactor Pressure. -Production rate.	-PI controller. -Mixed-integer dynamic optimization (MIDO). -Mixed-integer nonlinear programming problem (MINLP).	-They use 4 sequences of changes in the polymerization grade. -They optimize wich of the control strategies is better in the reactor case. -Use of an equation for the amount off-specification polymers.
(Hernández-Escoto et al., 2009)	Homopolymer via free radical	CSTR	-Monomer feed rate. -Jacket temperature. -Output flow rate.	-Monomer concentration. -Temperature in the reactor. -Volume of reactor content.	-Proportional and integral control (PID).	-Has a diagram of the control strategy (P and ID). -Explain all the control theory, and equations for the control model.

Reference	Polymer	Reactor	Manipulated Variable	Controlled Variable	Controller and optimizator	Remark
(Hernández-Escoto, López and Alvarez, 2010)	Alkyd polymerization	Batch	-Addition of reactants. -Reactor temperature.	-Conversion of the acid functional group. -Viscosity. -Average molecular weight.	-Monitoring control.	-They use an estimator (observer) because it has had a delay in some of the sample parameters needed. -Comparison between the experimental part, whit no observer, and the observer. -Design of the observer and the consideration in the design.
(Patil, Maia and Ricardez Sandoval, 2015)	High impact polystyrene (HIPS)	CSTR	-Outlet flow rate of the reactor. -Heat flow to the system. -Monomer flow rate. -Cooling water flow rate.	-Volume of the reactor. -Product concentration. -Reactor temperature. -Monomer conversion.	-PI control. -MINLP optimization.	-They exposed 2 study cases, a non-isothermal CSTR reactor and a CSTR reactor for the HIPS polymerization. -Used optimization with cost functions for the design, schedule and control. -Mainly expose the response of multiproduct systems like the changes in the polymerization grade. -Implementation of ramp function for the grades of polymerization. -Computational cost (simulation time).

Reference	Polymer	Reactor	Manipulated Variable	Controlled Variable	Controller and optimizator	Remark
(Flores-Tlacuahuac and Biegler, 2008)	PMMA and High impact polystyrene (HIPS)	CSTR	-Initiator flow rate. -Monomer flow rate.	-Monomer conversion. -Number molecular weight.	-PI control. -Mixed-integer dynamic optimization (MIDO). -Mixed-integer nonlinear programming problem (MINLP).	-They exposed 2 study cases, CSTR reactor for PMMA polymerization and a CSTR reactor for HIPS polymerization. -In the paper used an optimization for the optimal control variables. -Used different grades for the final product, an oscillating function.

1.6. Hypothesis

- It is possible to improve the environmental impact and economic potential of a continuous process of bulk polymerization by free radicals, implementing optimal design and control structures beyond single loop control.

1.7. Objectives

1.7.1. General objective

- Develop and evaluate different control structures in a polymerization process towards improving environmental impact and economic potential, based on optimal reactor design.

1.7.2. Specific objectives

- Identify a suitable polymerization process to be implemented from a modeling perspective.
- Implement and validate the simulations for the selected polymerization model using data from the literature.
- Optimize the polymerization reactor design according to different objective functions.
- Design different control structures and implement controllers in the continuous process of bulk polymerization by free radicals.
- Evaluate the performance of the control alternatives implemented in the continuous process of bulk polymerization by free radicals.

1.8. Thesis structure

This thesis contains four chapters, one introductory chapter, two chapters for each study case development, and finally one chapter for the global conclusion and recommendations for future work.

In the introductory chapter, motivation research is presented. Later, theoretical background of basic concepts of polymer science are depicted. Additionally, state of the art of process control of styrene polymerization is performed to define the

research opportunities. Then, the thesis hypothesis is presented which lead to the research objectives.

The subsequent 2 chapters are written as scientific articles, which means each study case presents an abstract, introduction, methodology, results, conclusion, references, appendix, and nomenclature.

Chapter two is a study case selected by the state of art described in chapter one, a continuous bulk polymerization by free radical for polystyrene production in a stirred tank reactor (referred to as CSTR study case). Operation conditions are optimized using a genetic algorithm with two objective functions, namely operational cost and productivity. Subsequently, the control structure design is proposed around optimal operation conditions. Three different controllers are investigated, proportional-integral-derivative control (PID), linear-quadratic-regulator control (LQR), and linear-quadratic-Gaussian control (LQG). Finally, results from the optimal design and process control are analyzed and compared with the literature.

The third chapter focus on the continuous bulk polymerization by free radical for polystyrene production in a plug flow reactor is investigated (referred to as PFR study case). Analogously to the previous case, a genetic algorithm is used for multiobjective optimization, in order to determine the optimal operating point. Then, three control structures are designed around the optimal operation point (PID, LQR and LQG). The optimal design and the control structures proposed are assessed and compared with the literature.

In an attempt to avoid being repetitive, some information is avoided the third chapter referencing information from the second chapter.

The fourth chapter presents the thesis conclusions. and recommendations to consider in future work.

1.9. Academic contributions

1.9.1. Conference presentations

- Juan Miguel García-Mendez, Alneira Cuellar Burgos, Oscar Andrés Prado-Rubio. (2021). *Mejoras de desempeño de proceso de polimerización a través de diseño optimo y control avanzado.* 1ª Conferencia Interamericana de Ingeniería Química y Procesos y XXXI Congreso Colombiano de Ingeniería Química 2021, October 24th to 27th, Bogotá, Colombia.

- Juan Miguel García-Mendez, Alneira Cuellar Burgos, Oscar Andrés Prado-Rubio. (2021). *Diseño óptimo para la implementación de control en una polimerización de radicales libres en reactores continuos.* XLI Encuentro Nacional de la AMIDIQ, 8th to 11th, Virtual.

1.9.2. Journal papers

- Juan Miguel García-Mendez, Alneira Cuellar-Burgos, Oscar Andrés Prado-Rubio. (2023). *Optimizing process design and control development for free-radical polymerization in continuous reactors.* Status: paper under development 80%.

1.10. Nomenclature

a	Relation between the molecular weight and the viscosity.
E^+	Initiator with high electronic density.
EH	Final product of protons expulsion termination.
$E(M)_n$	Polymer size n.
I_n	Initiator in a free radical model.
M	Monomer.
${M_1}^*$	First free radical of in the free radicl model.
M_i	Arithmetic average of the molecule's number distribution.
M_i^*	Free radical of size i created in the reaction.
M_{i+1}^*	Growing radical of size i in the reaction
M_j^*	Free radical of size j created in the reaction.
M_m	Molecular weight of the monomer (styrene).
$(M)_n$	Polymer size n.
$(M)_n E^+$	Growing carbonium ion.
M_v	Viscosity average molecular weight.
M_w	Number average molecular weight in the reactor.
M_z	Average z molecular weight.
ME	Final product transfer to monomer termination.
ME^+	Carbonium ion.
N_i	Number of molecules in the sample having the molecular weight M_i.
N^-	Atom or group with a negative charge.
NM^-	Carbanion.
$N(M)_n^-$	Growing carbanion.
PDI	Polydispersity index.
P_{i+j}	Final polymer of size i plus j.
P_i	Final polymer of size i.
P_j	Final polymer of size j.
R^*	Free radical form in the initiation reaction.
S	Solvent.
S^*	Solvent radical.
w_i	Mass of all molecules i having a degree of polymerization of M_i.
Z_i	Sedimentation equilibria in an ultracentrifuge.

1.11. References

Almeida AS, Wada K, Secchi AR (2008) Simulation of styrene polymerization reactors: Kinetic and thermodynamic modeling. Brazilian J Chem Eng 25:337–349. https://doi.org/10.1590/S0104-66322008000200012

Alvarez LA, Odloak D (2012) Optimization and control of a continuous polymerization reactor. Brazilian J Chem Eng 29:807–820. https://doi.org/10.1590/S0104-66322012000400012

American Chemistry Council (2020) Ten Facts to Know about Plastics from Electronics. https://plastics.americanchemistry.com/Ten-Facts-About-Plastics-from-Electronics/

Asteasuain M, Bandoni A, Sarmoria C, Brandolin A (2006) Simultaneous process and control system design for grade transition in styrene polymerization. Chem Eng Sci 61:3362–3378. https://doi.org/10.1016/j.ces.2005.12.012

Balani K, Verma V, Agarwal A, Narayan R (2015) Physical, Thermal, and Mechanical Properties of Polymers. Biosurfaces 329–344. https://doi.org/10.1002/9781118950623.app1

Bousbia-Salah R, Florez D, Lesage F, et al (2019) Grafting of Styrene on Ground Tire Rubber Particles in a Batch Polymerization Reactor: Dynamic Real-Time Optimization. Ind Eng Chem Res 58:13622–13627. https://doi.org/10.1021/acs.iecr.9b00738

Braun D, Cherdron H, Rehahn M, et al (2013) Polymer synthesis: Theory and practice: Fundamentals, methods, experiments, fifth edition

Casatextil (2018) Dacron Unicolor. https://casatextil.co/dacron-unicolor/. Accessed 22 May 2020

Cedex N (1982) Automatic control of a reactor for bulk polymerization of styrene. 17:297–304

Chatzidoukas C, Pistikopoulos S, Kiparissides C (2009) A hierarchical optimization approach to optimal production scheduling in an industrial continuous olefin polymediation reactor. Macromol React Eng 3:36–46. https://doi.org/10.1002/mren.200800030

España, Gobierno de Marino M de MA y MR y (2007) Mejores Técnicas Disponibles de referencia europea Producción de Polímeros

Falabella (2020) Casco de bicicleta recreacional moderno para niños. https://www.falabella.com.co/falabella-co/product/4964714/Casco-de-bicicleta-recreacional-moderno-para-ninos/4964715. Accessed 22 May 2020

Felorzabihi N, Ghadi N, Dhib R (2003) Differential geometry control of a polymer

reactor. In: 2003 International Conference Physics and Control, PhysCon 2003 - Proceedings. pp 345–348

Flores-Tlacuahuac A, Biegler LT (2008) Integrated control and process design during optimal polymer grade transition operations. Comput Chem Eng 32:2823–2837. https://doi.org/10.1016/j.compchemeng.2007.12.005

Garside M (2019) Global plastic production statistics. https://www.statista.com/statistics/282732/global-production-of-plastics-since-1950/#statisticContainer

Gazi E, Ungar LH, Seider WD, Kuipers BJ (1996) Automatic analysis of Monte-Carlo simulations of dynamic chemical plants. Comput Chem Eng 20:

Gharaghani M, Abedini H, Parvazinia M (2012) Dynamic simulation and control of auto-refrigerated CSTR and tubular reactor for bulk styrene polymerization. Chem Eng Res Des 90:1540–1552. https://doi.org/10.1016/j.cherd.2012.01.019

Ghori SW, Siakeng R, Rasheed M, et al (2018) The role of advanced polymer materials in aerospace. Sustain Compos Aerosp Appl 6282038:19–34. https://doi.org/10.1016/B978-0-08-102131-6.00002-5

González Madariaga FJ (2008) EPS (expanded poliestyrene) recycled bends mixed with plaster or stucco, some applications in building industry. Inf la Construcción 60:35–43. https://doi.org/10.3989/ic.2008.v60.i509.589

Guo Q, Liu H, Chen J (2015) Optimal grade transition of the styrene polymerization process with endpoint and path constraints. Proc World Congr Intell Control Autom 2015-March:4997–5001. https://doi.org/10.1109/WCICA.2014.7053562

Guo Q, Wang H, Lin W, Yang J (2011) Optimization-based strategies for grade transition operation of a continuous styrene polymerization process

Hernández-Escoto H, Hernández-Castro S, Gabriel Segovia-Hernández J, García-Martínez A (2009) Model-Based Linear Control of Polymerization Reactors. Comput Aided Chem Eng 26:279–284. https://doi.org/10.1016/S1570-7946(09)70047-1

Hernández-Escoto H, López T, Alvarez J (2010) Estimation of alkyd reactors with discrete-delayed measurements. Chem Eng J 160:698–707. https://doi.org/10.1016/j.cej.2010.03.055

Hidalgo PM, Brosilow CB (1990) Nonlinear model predictive control of styrene polymerization at unstable operating points. Comput Chem Eng 14:481–494. https://doi.org/10.1016/0098-1354(90)87022-H

Johnson AF, McGreavy C, Laurence RL, et al (1994) Polymer reactor engineering, first. Chapman & Hali

Koltzenburg S, Maskos M, Nuyken O (2017) Polymer Chemistry, Springer

Li M, Christofides PD (2007) An input/output approach to the optimal transition control of a class of distributed chemical reactors. In: Proceedings of the American Control Conference. pp 2042–2047

Meira GR, Johnson AF (1981) Molecular weight distribution control in continuous “living” polymerizations through periodic operation of the monomer feed. Polym Eng & Sci 21:415–423. https://doi.org/10.1002/pen.760210708

Meszena ZG, Johnson AF (1999) Modelling and simulation of polymerisation processes. Comput Chem Eng 23:. https://doi.org/10.1016/S0098-1354(99)80092-1

Mundoplast (2017) Produccion mundial de plastico. https://mundoplast.com/produccion-mundial-plasticos-2017/. Accessed 15 May 2020

Nguyen TS, Hoang NH, Azlan Hussain M (2019) Feedback passivation plus tracking-error-based multivariable control for a class of free-radical polymerisation reactors. Int J Control 92:1970–1984. https://doi.org/10.1080/00207179.2017.1423393

Patil B, Maia E, Ricardez Sandoval L (2015) Integration of scheduling, design, and control of multiproduct chemical processes under uncertainty. AIChE J 61:2456–2470. https://doi.org/10.1002/aic.14833.

Plasteurope (2012) Plastics markets. https://www.plasteurope.com/news/PLASTICS_MARKETS_t221996/. Accessed 22 May 2020

PlasticEurope (2020) Plastics – the Facts 2020. Plast Mater 21 st centuryentury 16

PlasticsEurope (2009) The Compelling Facts About Plastics 2009. Plast Mater 21 st centuryentury zu finden unter www.plasticseurope.de/informations

Postobón (2020) Las botellas de PET son 100% reciclables. https://www.postobon.com/sostenibilidad/sabias-que-las-botellas-pet-son-100-reciclables. Accessed 18 May 2020

Riduco S.A. (2010) Autopartes. http://www.riduco.com/lfl/index.php?option=com_content&task=view&id=64&Itemid=125. Accessed 18 May 2020

Rojas González AF, Ríos Aranzazu LM (2018) Un nuevo modelo de cuantificación de la capacidad de pirólisis utilizando datos termogravimétricos aplicado a reprocesamiento de polímeros A new model to pyrolysis capacity quantification using thermogravimetric data for polymers reprocessed. Ing y Desarro 36:138–154

Schnurr REJ, Alboiu V, Chaudhary M, et al (2018) Reducing marine pollution from single-use plastics (SUPs): A review. Mar Pollut Bull 137:157–171. https://doi.org/10.1016/j.marpolbul.2018.10.001

Stark NM, Matuana LM (2007) Characterization of weathered wood-plastic composite surfaces using FTIR spectroscopy, contact angle, and XPS. Polym Degrad Stab 92:1883–1890. https://doi.org/10.1016/j.polymdegradstab.2007.06.017

Tejedor AS (2014) La industria de los agentes tesoactivos. https://www.eii.uva.es/organica/qoi/tema-10.php. Accessed 22 May 2020

Wang J, Tan C, Wu H (2019) Online Shape Modification of Molecular Weight Distribution Based on the Principle of Active Disturbance Rejection Controller. IEEE Access 7:53163–53171. https://doi.org/10.1109/ACCESS.2019.2912215

2. Optimal design and control of styrene polymerization in a continuous stirred-tank reactor

2.1. Abstract

This Chapter is dedicated to investigating the design and control of a continuous bulk polymerization by free radical for polystyrene production carried out in a continuous stirred-tank reactor (CSTR). For reactor design, operating conditions are optimized using two objectives function namely the operational cost and the productivity. The optimization defines the operating point for initiator flow, monomer flow, coolant flow, initiator concentration in the feed and monomer concentration in the feed. Subsequently, a control structure is designed around the optimal operating point, studying implementation of proportional-integral-derivative control (PID), linear-quadratic-regulator control (LQR), and linear-quadratic-Gaussian control (LQG). The optimal design results show how the two objective functions lead to the best-balanced operation point, in terms of lower economic evaluation and high productivity, enhancing the design. Besides, from control perspective, the three control structures are capable of controlling the system for both changes in set-points and disturbances rejection. Nevertheless, the use of advanced control shows an enhanced control action, reducing response times by a factor of 2, compared with LQR and PID controllers.

2.2. Introduction

Aligned to the objectives for sustainable future, waste management in industry has become a priority to be handled. Waste produced in the polymer industry comes from the polymerization reaction itself, generating off-specification products due to changes in process inputs or during process adaptation to the demand of different products. This implies resources, energy, and thus economic potential losses and higher environmental impact. Despite the advantages, polymerization processes

have shown some issues where an off-specification amount is produced (Q. Guo, Liu and Chen, 2015). Those generate an economical problem since in many cases it represents a considerable profit loss plus the negative environmental impact.

The real solutions to the environmental and technical problems in polymerization processes are far from being accomplished, consequently, it is necessary to investigate strategies that reduce the off-specification products since they can hardly be recovered. Optimal design complemented with process control is an attractive solution for this problem, potentially reducing costs, operation time, energy, environmental impact, the off-specification amount in the process. As consequence, there is an increasing the process performance, improving process safety and extending the life of equipment in the plant. However, the polymerization processes are nonlinear, even the kinetics and natural behavior of polymers make these kinds of processes challenging to control (Alvarez and González, 2007; Alvarez and Odloak, 2012).

Therefore, the optimal design and control can be considered more complex than other catalyzed reactions due to the robust mathematics implemented to accomplish those goals. The reason polystyrene is selected is one of the most studied polymers in the polymerization field due to its versatility to be produced in many ways. Also, the most studied way of production of polystyrene is through continuous bulk polymerization by free radicals (Alvarez and Odloak, 2012; Gharaghani, Abedini and Parvazinia, 2012; Patil, Maia and Ricardez Sandoval, 2015). Some advantages of this process are:1) The final product is not polluted with a solvent (no need for a recovery stage) and high molecular weights can be obtained (Braun *et al.*, 2013); 2) Flexibility in the process, relatively easy to analyze, including a diversity of manipulated variables for the design of control strategies; 3) The wide market of materials produced by this method, *e.g.* polystyrene (7% of global production of polymers, around 25.13 million metric tons per year) (Plasteurope, 2012; Garside, 2019). 4) Relatively simple mathematical implementation of dynamic models , which is helpful to test robust mathematics for process design and control (Johnson *et al.*, 1994; Fogler, 2006).

From the controller perspective, the implemented control strategies in literature are feedback, feedforward, a combination of both of them, using different controllers (*e.g.* P, PI, PID, PD, LQR, among others) (Felorzabihi, Ghadi and Dhib, 2003; Asteasuain *et al.*, 2006; Alvarez and González, 2007; Li and Christofides, 2007; Gharaghani, Abedini and Parvazinia, 2012; Patil, Maia and Ricardez Sandoval, 2015; Wang, Tan and Wu, 2019). The controlled variables commonly used by researchers are the molecular weight, the polymerization grade, the polydispersity index, molecular weight distribution, and even viscosity. Interestingly, some authors

present problems with the measurements of controlled variables as molecular weight, since the molecular weight is hard to monitor, thus the use of observers is proposed to circumvent this problems (Hernández-Escoto, López and Alvarez, 2010). Also, the implementation of advanced control has not been extensively investigated (Vasco De Toledo *et al.*, 2005; Alvarez and Odloak, 2012), thus, this is a fertile research area to obtain process enhancements. Where the advanced controller as the LQG controller is an interesting idea to solve the measurement problem, a controller that uses a Kalman filter (Observer). The reason the implementation of observers is advantageous is that there is no delay in the values of the controlled variables, as is the case of molecular weight.

In the current work, optimal process design and control development of a free radical polymerization of styrene in a CSTR is investigated through the implementation of multiobjective optimization and advanced automatic control. For that purpose, a model-based approach is used. The optimal design employs global optimization aiming to find the best trade-off of multiple objective functions in the Pareto front. Regarding the control, three control strategies are used, conventional Proportional-integral-derivative control (PID) as a baseline, then, Linear-quadratic-Regulator control (LQR), and Linear-quadratic-Gaussian control (LQG) are investigated. Analyzing well-established key performance indexes (settling time, rise time, time to first peak, overshoot) of each strategy for responses of each setpoint tracking and disturbance rejection for the other outputs in the system.

2.3. Methodology

The methodology is shown in Figure 2-1. As an overview, the methodology is composed by 3 main sections. First, the model of the polymerization reaction is developed with the information from literature. The model implementation is verified by confirming model prediction are consistent with reported data, and then a sensitivity analysis is performed to adjust problematic parameters and reproduce reported behavior (note: the verified parameters are not limited to kinetic parameters). Subsequently, optimal reactor design is carried out aiming to fulfill the multiobjective targets (in this case the operational cost and productivity). Then, the utopia is chosen and is used as operational point. Finally, different control structures are designed around the optimal point, different controllers are implemented. Finally, the controller performance is evaluated for setpoint tracking and disturbance rejection scenarios. In the following subsections details about each stage of the methodology are presented.

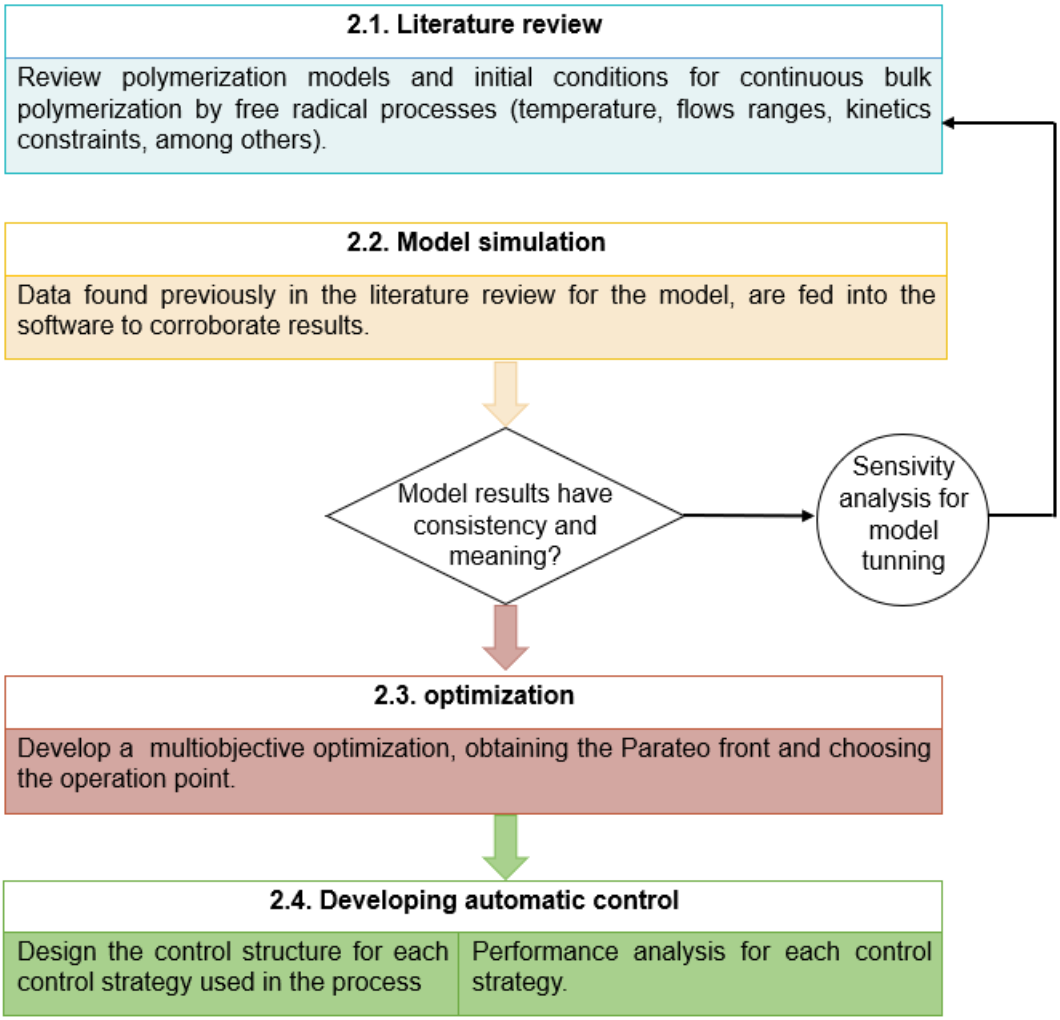

Figure 2-1: Methodology scheme.

2.3.1. Literature review

As shown in Chapter 1-state of the art condensed in Table 1-3, concludes the continuous bulk polymerization by free radical of styrene is an interesting system to evaluate the optimizing design strategy and automation influence. Alvarez and Odloak, (2012) model is selected since it shows the most detailed information about the system including parameters and kinetic model.

2.3.2. Model development

The core polymerization model is based on a continuous bulk polymerization by free radical developed by Alvarez and Odloak, (2012). However, some modifications have been introduced in the model. The model consists of 7 Ordinary differential equations (ODEs) where 2 are mass balance, 2 energy balances, 3 for the moments of molecular weight distribution. Around that model, two objective functions are proposed to calculate the process operating cost and productivity. Then, the model is solved using a a variable-step variable-order solver based on the numerical differentiation formulas from order 1 to 5 Matlab®, suitable for stiff ODEs (ode15s).

a) Continuous bulk polymerization by free radical model

From the original model proposed by Alvarez and Odloak, (2012), the main modification introduced is in the overall heat transfer coefficient reported. Further details of the coefficient change are presented and discussed below.

The reaction starts with an initiation reaction where the initiator is transformed into a radical. Then, the monomer in the solution reacts creating a chain of many monomers as shown in the propagation reaction. Finally, the reaction end with the combination of two dense chains of monomer as shown in the termination stage (could be by disproportionation or combination). The reaction mechanism for bulk polymerization by free radicals is shown below.

- Initiation

$$I_n \xrightarrow{k_d} n\, R^* \tag{2.1}$$

$$R^* + M \xrightarrow{k_i} RM_1{}^* \tag{2.2}$$

- Propagation

$$M_i^* + M \xrightarrow{k_p} M_{i+1}^* \tag{2.3}$$

- Termination by combination

$$M_i^* + M_j^* \xrightarrow{k_{tc}} P_{i+j} \tag{2.4}$$

- Termination by disproportionation

$$M_i^* + M_j^* \xrightarrow{k_{td}} P_i + P_j \tag{2.5}$$

The kinetics model takes into account the next assumptions (Alvarez and Odloak, 2012).

I. The lifetime of the polymer radical species is extremely short compared to other system time constants. Then is used the Pseudo Steady-State Hypothesis (PSSH), shown in Appendix A.
II. The monomer consumption is mainly due to propagation, this leads to the Long Chain Assumption (LCA).
III. The chain transfer reactions to monomer and to solvent are not considered.
IV. Monomer thermal initiation does not occur because this reaction is only significant at temperatures greater than 373 K. The reactor temperature considered is below this limit.
V. The overall chain termination rate constant is composed of both combination and disproportionation contributions. For styrene solution, experimental results showed that the chain termination occurs solely by combination, so the termination by disproportionation is not considered.
VI. The rate of propagation is much faster than the rate of termination, so the effect in the kinetics governed by the slow one, in the current case for the termination rate.
VII. The initiator used in the reaction is azobisisobutyronitrile (AIBN).

Developing the general mass balance for any specie in a reactor (Fogler, 2006):

$$\frac{dC_A}{dt} = \frac{F_{Ao} - F_A}{V} + r_A = \frac{Q_A C_{Af} - Q_t C_A}{V} + r_A \tag{2.8}$$

The summary of the mass balances applied to each component is shown in Appendix B. The energy balance for the reactor takes into account the next considerations (Hidalgo and Brosilow, 1990).

I. The reactor is well mixed.
II. Kinetic and potential energy changes in the system and between inlet and outlet streams are negligible.
III. The shaft work from the agitator is negligible.
IV. The mean heat capacity of the system contents is independent of composition and temperature.
V. The overall heat transfer coefficient to the reactor jacket is constant with monomer conversion.
VI. Heats of initiation and termination are negligible compared to heat of polymerization.

To be more specific the final mass balance used in the system are the balances for monomer and initiator, present below:

$$\frac{dC_I}{dt} = \frac{Q_i C_{If} - Q_t C_I}{V} - k_d C_I \tag{2.9}$$

$$\frac{dC_M}{dt} = \frac{Q_m C_{Mf} - Q_t C_M}{V} - k_p C_M C_P \tag{2.10}$$

Additionally, a general energy balance unsteady-state no isothermal CSTR reactor leads to:

$$UA(T_c - T) - \dot{W}_s + \sum_{i=1}^{n} F_{io} Cp_i (T - T_{io}) + \Delta H_{Rxn} r_A V = \sum_{i=1}^{n} N_i \, Cp_i \frac{dT}{dt} \tag{2.11}$$

The summary of the energy balance for the study case is in Appendix C. The energy balance in the reactor jacket takes into account the next considerations (Hidalgo and Brosilow, 1990).

I. The cooling water in the jacket is well mixed.
II. Kinetic and potential energy changes in the jacket and between the inlet and outlet streams are negligible.
III. The heat capacity of the jacket contents is independent of temperature.
IV. There is no shaft work.
V. The overall heat transfer coefficient is constant.
VI. The jacket is perfectly insulated from surroundings.

The final energy balance used in the system are temperature balance in the reactor and the temperature of the coolant in the jacket:

$$\frac{dT}{dt} = \frac{Q_t (T_f - T)}{V} + \frac{-\Delta H_r}{\rho C_p} k_p C_M C_P - \frac{hA}{\rho C_p V} (T - T_c) \tag{2.12}$$

$$\frac{dT_c}{dt} = \frac{Q_c (T_{cf} - T_c)}{V_c} + \frac{hA}{\rho_c C_{pc} V_c} (T - T_c) \tag{2.13}$$

The moments of molecular weight are shown below.

$$\frac{dD_0}{dt} = \left(0.5 * k_t * {C_P}^2\right) - \frac{Q_t D_0}{V} \tag{2.14}$$

$$\frac{dD_1}{dt} = \left(M_m * k_p * C_P * C_M\right) - \frac{Q_t D_1}{V} \tag{2.15}$$

$$\frac{dD_2}{dt} = \left(5 * M_m * k_p * C_P * C_M\right) + \left(\frac{5 * M_m * {k_p}^2 * {C_M}^2}{k_t}\right) - \frac{Q_t D_2}{V} \tag{2.16}$$

Where the moment zero (D_0) represents the total molar concentration of dead polymer and the first moment (D_1) represents the total molar concentration of monomer units present as a polymer (Schmidt and Ray, 1981; Ionut, 2009). Finally, the second moment (D_2) is a statistic value for the calculation of the mass average molecular weight. The molecular weight moments are used to calculate the mass average molecular weight in the reactor:

$$M_w = M_m \frac{D_2}{D_1} \tag{2.17}$$

Where M_m is the monomer molecular weight (Styrene molecular weight). Besides, it is also crucial to calculate the intrinsic viscosity and the polydispersity index. So, the intrinsic viscosity and the polydispersity index are described by the next equations:

$$\eta = 0.0012(M_w)^{0.71} \tag{2.18}$$

$$PDI = M_m \frac{D_2 D_0}{D_1^2} \tag{2.19}$$

Despite, uncertainties presented using power law expressions the intrinsic viscosity is computed as shown previously and a conversion lower than 0.5 is used to avoid high viscosity mixtures (Chen, 1994; Gazi, Seider and Ungar, 1996; Asteasuain *et al.*, 2006). As the main variable used in reactors, the conversion is also used here, described by the following equation:

$$X = \frac{C_{Mf} - C_M}{C_{Mf}} \tag{2.20}$$

When investigating the model implementation, some model output inconsistencies were found. In fact, in almost articles a different value for the overall heat transfer coefficient was used despite all have the Hidalgo and Brosilow, (1990) references as shown in Table 2-1.

Table 2-1: Overall heat transfer coefficient comparison.

	hA **value**	**units**
Hidalgo and Brosilow, (1990)	70	N/A
Alvarez and Odloak, (2012)	70	Cal/s*K
Asteasuain *et al*, (2006)	70	Cal/s*K
Gazi, Seider and Ungar, (1996)	70000	Cal/s*K
Russo and Bequette, (1998)	70	Cal/s*K

Due to the inconsistencies in the heat transfer coefficient which propagated to the simulation. The overall heat transfer in the reference is not used, instead, a new value is calculated shown in Table 2-2.

In order to carry out the simulations, the parameter values used are condensed in Table 2-2. Notice that the values of the heat transfer coefficients are constants, assuming to be temperature independent.

Table 2-2: Process parameters for the CSTR reactor, adapted from Alvarez and Odloak, (2012).

Variable	Symbol	Value	Units
Frequency factor for initiator decomposition	E_d	14897	[K]
Activation energy for initiator decomposition	A_d	5.95E+13	[1/s]
Frequency factor for propagation reaction	E_p	3557	[K]
Activation energy for propagation reaction	A_p	1.06E+07	[L/mol*s]
Frequency factor for termination reaction	E_t	843	[K]
Activation energy for termination reaction	A_t	1.25E+09	[L/mol*s]
Initiator efficiency for AIBN	f	0.6	--
Heat of polymerization	ΔH_r	-16700	[cal/mol]
Overall heat transfer coefficient	hA	300[a]	[cal/K*s]
Mean capacity of cooling jacket fluid	ρC_p	360	[cal/K*s]
Heat capacity of cooling jacket fluid	$\rho_c C_{pc}$	966.30	[cal/K*s]
Molecular weight of monomer	M_m	104.14	[g/mol]
Temperature of the reactor feed	T_f	330	[K]
Inlet temperature of cooling jacket fluid (water)	T_{cf}	295	[K]
Reactor volume	V	3000	[L]
Volume of cooling jacket fluid (water)	V_c	3312.40	[L]
Flow rate of solvent	Q_s	0.13	[L/s]

[a]See section overall heat transfer selection in results, where the value is calculated.

2.3.3. Determination of optimal design

Global optimization is used to determine the optimal design employing the build-in function “gamultiobj”. This method finds the Pareto front of multiple fitness functions using a genetic optimization algorithm. Despite the optimizer chosen is a global optimizer, the Pareto found could be local or global. Additionally, the “gamultiobj” is convenient since it can handle process constraints defined values of conversion and mass average molecular weight.

b) Cost and productivity objective functions

In many cases, the operation point for polymerization processes is reported in the literature due to extensive research in this area. Although the information found in literature, interestingly some recent case studies perform optimizations to find the operation point (Asteasuain *et al.*, 2006; Alvarez and Odloak, 2012; Patil, Maia and Ricardez Sandoval, 2015). For this reason, in the present work, it has been decided to implement an optimization for the operation point selection, using two objective functions. One function is based on an economic evaluation and the other function is based on the productivity of the final product.

The economic evaluation is based on Asteasuain *et al*, (2006), taking the operation cost for styrene production presented by this author, which is condensed in Equation 2.23 (Asteasuain *et al.*, 2006):

$$CO = 343.16\,V^{0.529} + t_R\left(0.5\left(1.32 * 10^{-4} * Q_C + 0.011 * C_{If}\right) + 2 * 10^{-3} Q_M C_{Mf} M_m\right) \quad (2.23)$$

Where t_R is the total time of reaction, and in this case, the reactor volume remains constant. The productivity is also calculated by the definition of productivity in a reactor, which represents the production of the final product in this case dead polymer amount (D_0). Despite the exit of the reactor the mix of the death polymer and living polymer, the calculation just considers the death polymer since it is the final product at least in terms of the mass balances.

$$PR = D_0 * 3600 * \frac{Q_t}{V} \quad (2.24)$$

$$PR_{total} = \left(\sum D_0\right) * 3600 * \frac{Q_t}{V} \quad (2.25)$$

$$PR_{ss} = D_0|_{last} * 3600 * \frac{Q_t}{V} \quad (2.26)$$

PR_{total} is the productivity in all the time elapse the reaction and PR_{ss} is the productivity in the steady state.

The objective functions are the operational cost and the productivity at the steady-state (Equation 2.23 and Equation 2.26). For the CSTR case study, there are 2 constraints: a) for the reactor conversion and b) for the mass average molecular weight in the final product, as shown in Table 2-3.

The conversion constraint is implemented because CSTR reactors with higher conversion achieve the system is too viscous to mix. This is a technical difficulty since there is a point where stirring becomes energetically unfeasible, and the mixture must be transferred to another process to complete the polymerization. Where the gel effect must be taken into account (Hamielec, Hodgins and Tebbens, 1967; Wallis, Ritter and Andre, 1975; Chen, 1994; Gazi *et al.*, 1996; Asteasuain *et al.*, 2006). In literature, the conversion values proposed here as a constraint together with the low temperatures used here (herein temperature is considered low) reach values between 50,000-90,000 g/mol (Wallis, Ritter and Andre, 1975; Alvarez and Odloak, 2012). While for higher temperatures, the molecular weights found are between 15,000-45,000 g/mol (Asteasuain *et al.*, 2006; Flores-Tlacuahuac and Biegler, 2008; Guo *et al.*, 2011). So the mass average molecular weight constraint is defined due to the range between 70000 g/mol and 80000 g/mol is a target for industrial polystyrene and near as found in the literature.

Table 2-3: CSTR conversion and mass average molecular weight constraints for the optimization.

Optimization constraints	
0.3<X<0.4	70000 g/mol <M_w<80000 g/mol

The optimization outputs are the initiator flow, monomer flow, cooling fluid flow, initiator concentration, and monomer concentration in the feed (*i.e.* Q_i, Q_m, Q_c, C_{If}, C_{mf}). Due to the high density of values obtained by the optimization, the optimal search zone was restricted, choosing values resembling the values of the operation point reported in the literature (Gazi, Seider and Ungar, 1996; Russo and Bequette, 1998; Asteasuain *et al.*, 2006; Flores-Tlacuahuac and Biegler, 2008; Alvarez and Odloak, 2012; Gharaghani, Abedini and Parvazinia, 2012; Patil, Maia and Ricardez Sandoval, 2015). The values obtained by the refined optimization are used to create a Pareto front, then the first derivate criterium is used to select the Utopia point in the front, setting the operation point for the process. The first derivate criterium employs the numerical derivate of the function that represents the set data. Then, where the differentiated function value is sufficiently cero is the point used as the Utopia point (Alcocer García, 2018).

Preliminary simulations showed that the process cost and productivity did not present directly and antagonist behavior due to the fact first objective function (productivity) is maximized and the second objective function (operational cost) is minimized in the optimization (see Figure 2-2). For this reason, one axis is inverted to obtain the antagonist behavior, in this case, the axis changed is the cost in the Pareto front leading cost vs 1/productivity thus continuing the first derivate criterium with normality.

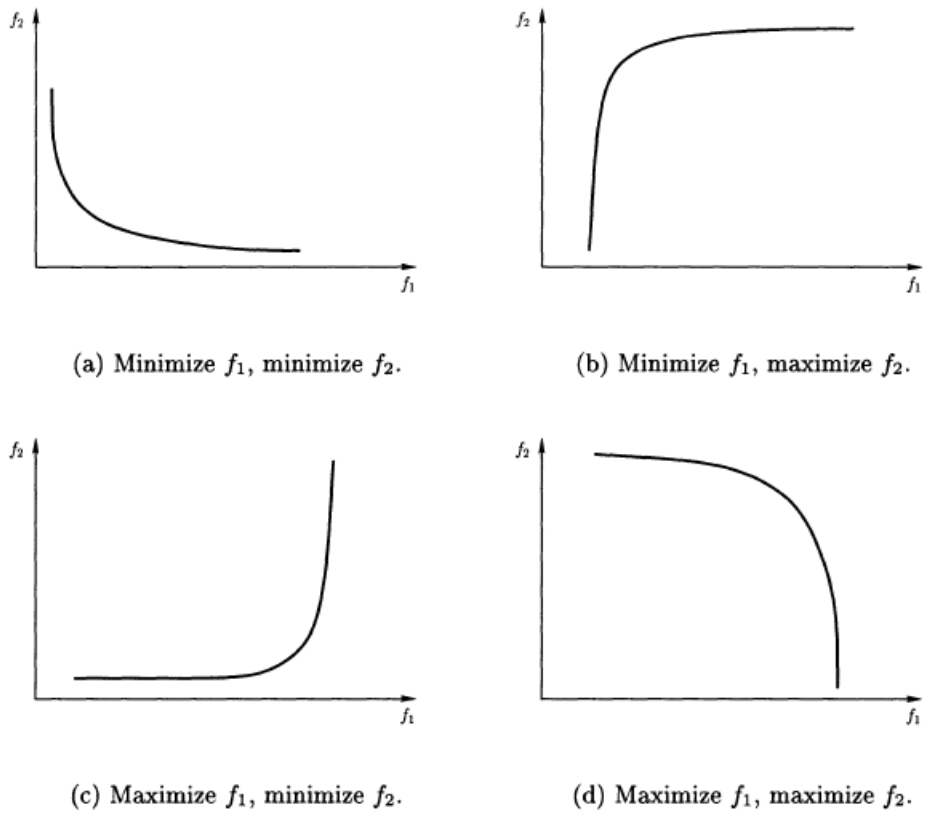

Figure 2-2: Common shapes of tradeoff surface considering two objectives function (Collete and Siarry, 2003).

2.3.4. Control structure design

The control structure design is summarized in a series of steps that must be analyzed when the control will be implemented in any process. Figure 2-3 describes briefly these steps for the control structure design (Seborg and Edgar, 2003).

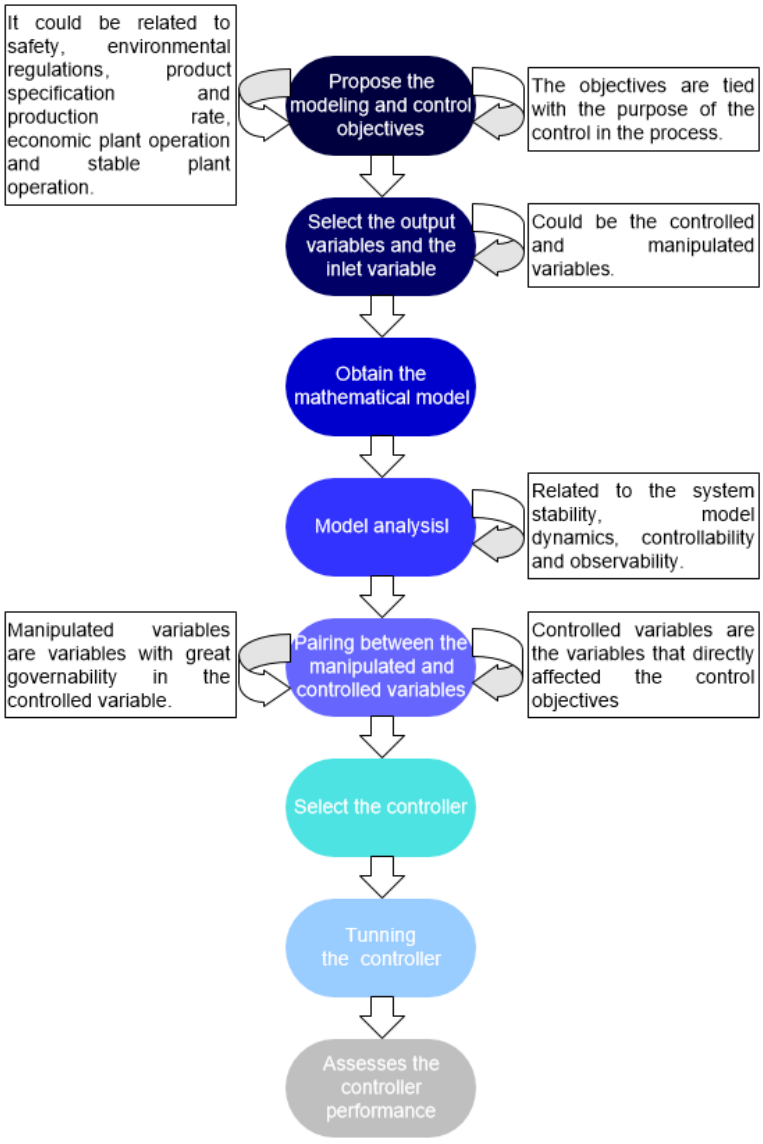

Figure 2-3: Control structure design steps, adapted from Seborg and Edgar, (2003).

c) Control objectives

- The main objective is to reduce the off-specification material in the process, based on the transition time for changes in the specification for the product (*i.e.* settling time).

- Controlling the quality of the products, keeping the conversion, temperature, and the mass average molecular weight in the process.

d) Mathematical model

The mathematical model is already shown in the Model development section.

e) Model analysis

To achieve the model analysis the system is linearized using the Matlab® command “linmod”, which determine continuous-time linear state-space model around the operating point by numerical approximation (the Utopia point selected in the optimization).

- **Stability**

  The system stability is determined by the eigenvalues of the matrix A obtained by linearizing the system to a state space representation, where the eigenvalues are the roots of the characteristic equation. The general stability criterion establishes that all the roots of the characteristic equation are negative or have negative real parts (Seborg and Edgar, 2003).

- **Controllability**

  Controllability is a system characteristic that allows determining the ability of input variables to move the states of a system in a finite time, generally represented by a state-space model. Before designing a control structure, the controllability of the system must be determined, starting from the state-space representation and determining the controllability matrix (Seborg and Edgar, 2003).

- **Observability**

  Observability is a complementary structural characteristic of a state representation of a system, or the system itself, which indicates the ability to estimate the historical values of a state based on knowledge of the system's input and output variables (Seborg and Edgar, 2003),. This is particularly important to design the state estimator (Observer).

- **Pairing variables**

  Taking into account the degrees of freedom analysis is exposed in the at the beginning, it was selected 5 potential manipulated variables (optimized variables: Q_i, Q_m, Q_c, C_{If}, C_{Mf}, variables obtained from the reactor design) and 4 controlled variables (C_M, T, D_1, D_2). The pairing strategy between the manipulated and controlled variables in a single input-single output approach (SISO) is performed using the Relative Gain

Array (RGA) methodology. The values in the RGA matrix indicate that the manipulated variables with the value nearest to 1 is the best option to execute the control action in the desired variable, thus the appropriate pairing. Figure 2-4 represents the manipulated and controlled variables in the system with the final RGA methodology.

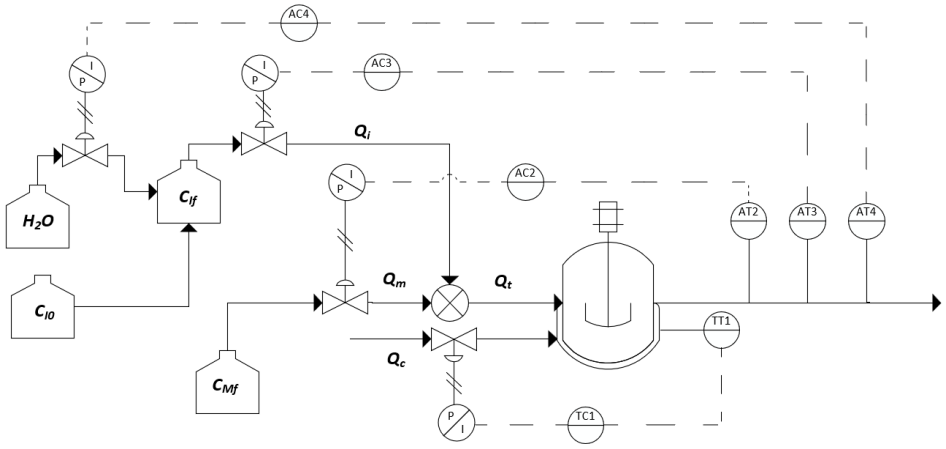

Figure 2-4: P&ID of the controlled CSTR, Intrumentation for the monomer concentration, the temperature in the reactor, the first moment of the molecular distribution and the second moment of the molecular distribution. (Note: this is the schematic representation to control the first moment of the molecular distribution moment through diluting or concentrating the input stream to the reactor of initiator).

The RGA methodology is employed for the PID controller because the LQR and LQG use a multivariable control method, where the control action corresponds to a coordinated response.

f) Controllers

The following section is summarized information of the feedback controllers used, PID, LQR, and LQG. For the present study case, preliminary investigation showed a better performance between PI and PID controllers even with noise, reason PID is implemented in the system. The implementation is carried out by a Matlab-based graphical programming environment for modeling, Simulink®.

The controller's performance is evaluated using different key performance indexes: the settling time ($\boldsymbol{t_s}$), rise time ($\boldsymbol{t_r}$), time to first peak ($\boldsymbol{t_p}$) and overshoots ($\boldsymbol{O_S}$) (Seborg and Edgar, 2003), taking into account that the major control objective is to reduce the settling time. The system response is assessed by setpoint tracking and disturbance rejection tests. Notice that setpoint changes are implemented as ramp inputs, due to numerical problems related to stiffness

when implementing the step disturbance in the system. Besides, both control strategies have noise implementation in the inputs and outputs signals.

- **Proportional-integral-derivative control (PID)**

  It is the combination of the proportional, integral, and derivative control, several variations of PID control are used in practice (Seborg and Edgar, 2003). The parallel implementation used with derivative filter, where the derivative action can be combined with proportional and integral action by having each of the modes operate in parallel (Figure 2-5). The PID control transfer function is:

$$\frac{P'(s)}{E(s)} = K_c \left[1 + \frac{1}{\tau_I s} + \frac{\tau_D s}{\alpha\tau_D s + 1}\right] \tag{2.27}$$

  The structure is implemented in Simulink®. The controller tuning method used is the Internal Model Control (IMC), The IMC method is used to allow model uncertainty and tradeoffs between performance and robustness to be considered in a more systematic fashion (Seborg and Edgar, 2003). More information about the tuning is in Appendix D.

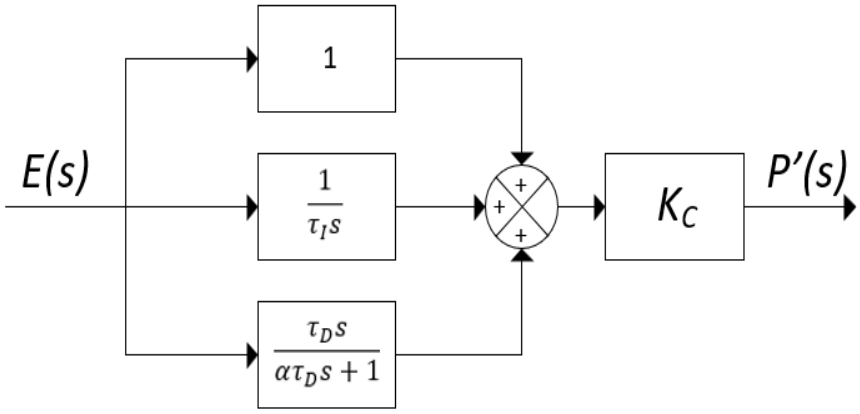

Figure 2-5: Block diagram of parallel PID controller, Adapted from Seborg and Edgar, (2003).

- **Linear-quadratic-regulator control (LQR)**

  A full state feedback controller comes from optimal control theory. This regulator is usually used for the implementation of linear-quadratic-

Gaussian control (LQG) as an early step in the construction of LQG (Skogestad and Postlethwaite, 2001). As the name suggests, LQR is a regulator (control disturbances in the system but not set-point tracking). To allows the controller to perform setpoint tracking, an integral action is included., resulting in the implementation shown in Figure 2-6. The LQR control action is determined by the solution of the optimization defined by the objective function which balances the system performance andthe controller effort. Details about the LQR are depicted in Appendix E. Now the objective function or cost function to minimize in the controller is (Mathworks, 2021):

$$J = \int_0^\infty (x^T Q x + u^T R u + 2x^T N_L u) dt \tag{2.28}$$

Where Q and R are weights that represent the actuator performance and actuator effort, respectively. In summary, Q penalize bad performance, R penalize actuator effort, and N_L penalize cross products of the input and the state, usually, the last variable is set to cero. The controller action is determined by its gain (K). This gain is computed as a function of the linearized model assisted by the solution of the stationary Riccati equation.

$$A^T SA - S - (A^T SB + N_L)(B^T SB + R)^{-1}(B^T SA + N_L^T) + Q = 0 \tag{2.29}$$

This calculation of K is done using the following equation.

$$K = (B^T SB + R)^{-1}(B^T SA + N_L^T) \tag{2.30}$$

To solve the problem, the matrices Q and R must be defined. Conventionally, those are tuned manually to achieve the desired response in the system (trial and error) (Mathworks, 2019). In the present case, Q and R are defined as diagonal matrices with the normalization of the states and inputs in the system as:

$$Q_{ii} = \frac{1}{{x_i}^2} \tag{2.31}$$

$$R_{jj} = \frac{1}{{u_j}^2} \tag{2.32}$$

Those values were set as the tuning parameter in the LQR and LQG control, due to the good behavior of the values on the control loop.

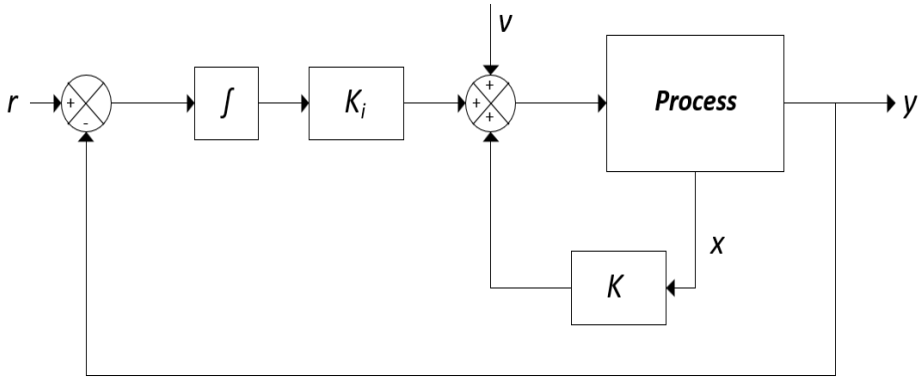

Figure 2-6: Block diagram of general LQR with integral action, Adapted from Seborg and Edgar, (2003).

- ## Linear-Quadratic-Gaussian control (LQG)

The LQG is the combination of an LQR and a Kalman filter. Kalman filter is an optimal estimation algorithm used for state estimation that can only be measured indirectly or not measured at all. Besides, it is also used as a signal filter to mitigate white noise (Skogestad and Postlethwaite, 2001; Mathworks, 2017).

The Kalman filter here is used to calculate the response of unmeasured variables using physically measurable variables, *e.g.* the case of the mass average molecular weight (measurable) and the moments of molecular weight distribution (physically unmeasurable). Additionally, the Kalman filter removes the implemented noise in the inputs and outputs in the system. The filter used is implemented in Simulink®, estimating the states of continuous-time linear system which is represented by:

$$\hat{x}(k+1) = A\hat{x}(k) + Bu(k) + L(k)(y(k) - C\hat{x}(k)) \tag{2.33}$$

Where $L(k)$ represents the optimal gain for the Kalman filter in the instant of time k. The optimal gain that minimizes the mean squared error was derived by Kalman at the 60', leading to:

$$L(k) = P(k-1)C^T(CP(k-1)C^T + R_w)^{-1} \tag{2.34}$$

More information about the Kalman filter is in Appendix F. The parameters for tunning are the process noise covariance (R_v) and the measurement noise covariance (R_w), that correposnds to the inputs and outputs in the system, respectively. These parameters must be tuned manually to achieve the desired response in the system same as the gain

for the regulator. The block diagram of the LQG with integral action is used, as seen in Figure 2-7.

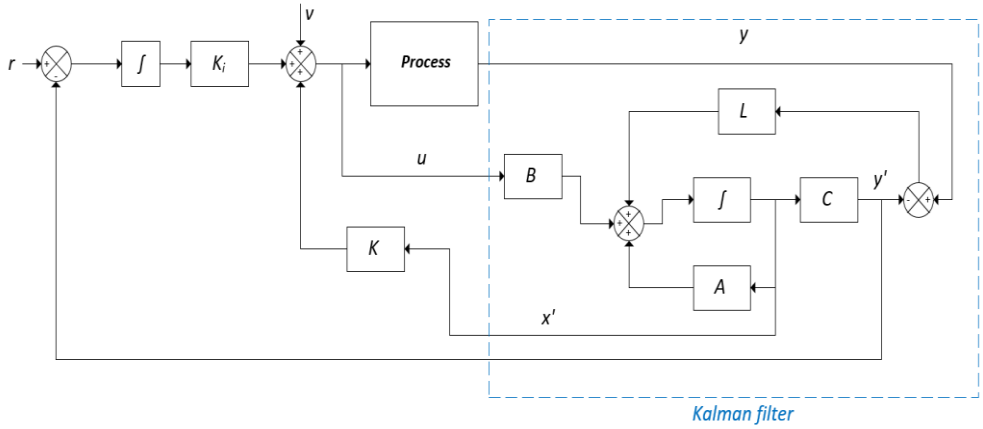

Figure 2-7: Block diagram of LQG controller with integral action, adapted Skogestad and Postlethwaite, (2001).

2.4. Results

Section 2.4.1 shows the calculous of the overall heat transfer coefficient and why the coefficients in literature are discarded. Section 2.4.2 shows the determination of the reactor optimal design and a discussion of the results obtained and obtained in the literature. Section 2.4.3 shows the model analysis and control structure design, together with the tunning for the three control structures. Section 2.4.4 shows the results obtained by the control structures, ending with a discussion of the results obtained in the current job and the literature.

2.4.1. Overall heat transfer coefficient selection

To overcome the inconsistent problem of the heat transfer coefficient problem mentioned in the Model development section, the reactor stability index (RSI) is used through a sensitivity analysis (Luyben, 2007). This ratio is defined by:

$$RSI = \frac{\Delta T\ design}{\Delta T\ max} = \frac{T - T_c}{T - T_{Cf}} \tag{2.21}$$

$$T = Reactor\ temperature$$

$$T_c = Jacket\ temperature$$

$$T_{cf} = Cooling\ fluid\ temperature\ at\ the\ entrance$$

Using the data of the model proposed by Hidalgo and Brosilow, (1990), at 0.4 hours (24 min):

$$RSI = \frac{T - T_c}{T - T_{Cf}} = \frac{336.5068 - 296.3075}{336.5068 - 295} = 0.9787 \qquad (2.22)$$

This means that from 100% of the available temperature difference, has been used the 97.87% of the Δtemperature. Therefore, the ignition-extinction curve is simulated at different heat transfer coefficients to fulfill the condition. Figure 2-8 shows the values of different heat transfer coefficients, with values higher than 250 Cal/s*K the system is stable. As result, the overall heat transfer coefficient is changed by a value of 300 Cal/s*K, to ensure the process is stable (in this case is a stable-unstable point see Figure 2-8).

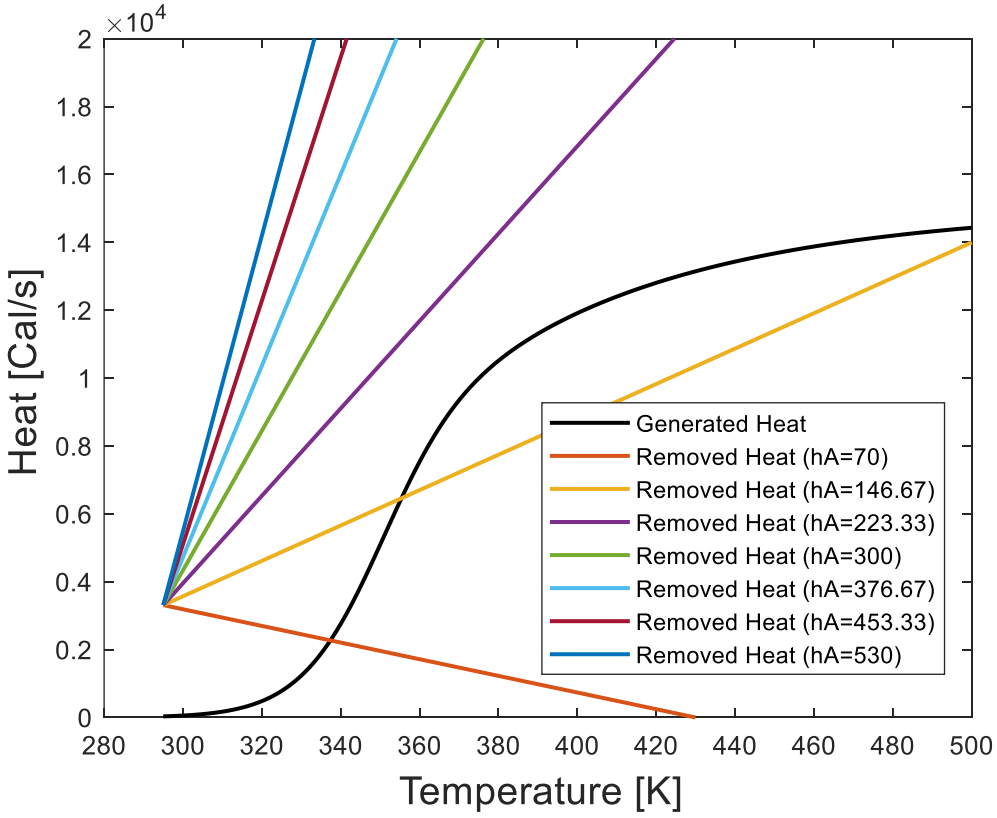

Figure 2-8: Ignition-extinction curve, with different values for the overall heat transfer coefficient (hA) in the CSTR system.

2.4.2. Optimal process design

From the results of the optimization, a Pareto front is obtained depicting the antagonistic behavior of the objective functions as shown in Figure 2-9. Where the abscissa coordinate is productivity in the process and the ordinate coordinate is the inverse of the operational cost.

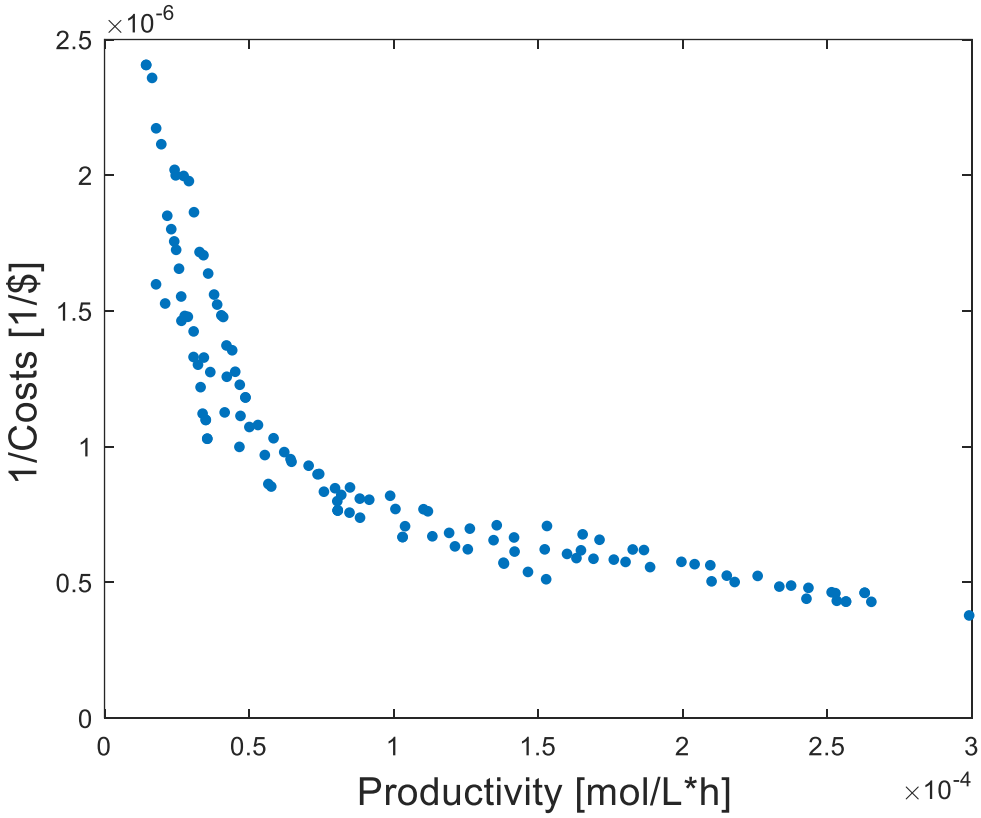

Figure 2-9: Pareto front with antagonist behavior, $Cost^{-1}$ vs productivity.

As best trade off, the Utopia point is found implementing the first derivative criteria, where the function represented by the data obtained in the optimization is numerically differentiated and plotted. Figure 2-10 represents the obtained function.

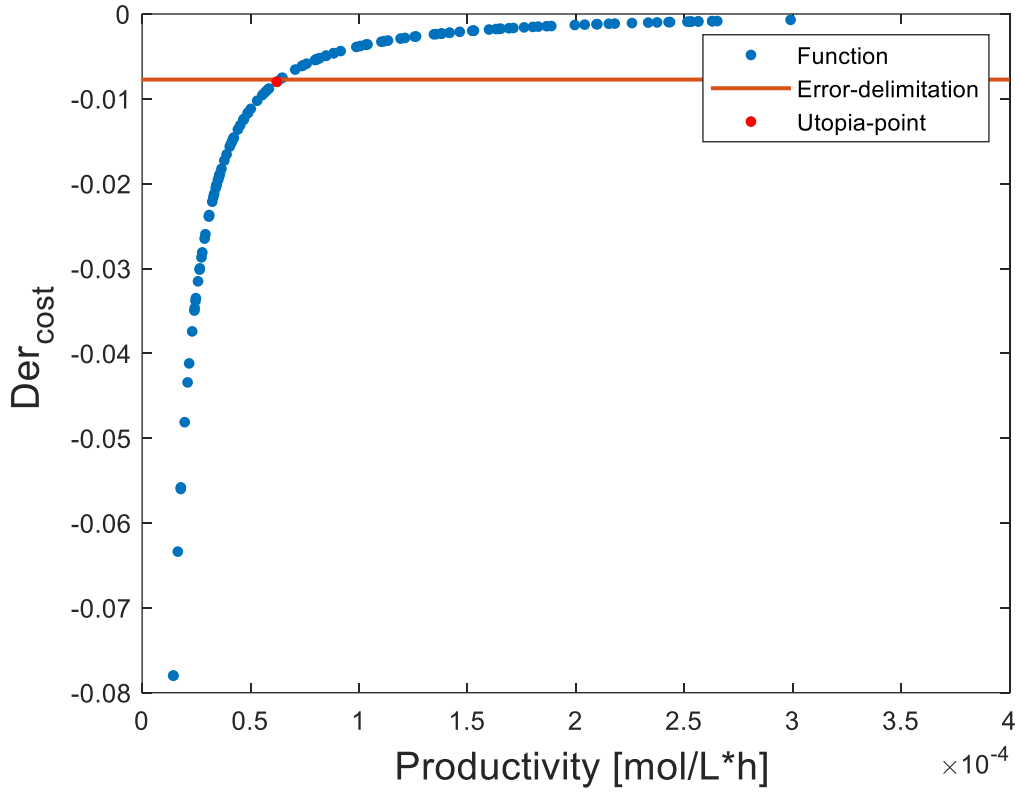

Figure 2-10: First derivate criterium graphic for CSTR study case, cost^{-1} differentiated vs productivity. Delimitation error is the band of 10% of the change in the differentiated function.

Now, the orange line in Figure 2-10 is the band of 10% of the change in the derivative of the function. The extinct criterium is to select a value when the derivate is cero, however here the values do not reach the exact value of cero. The reason why the value of the band is 10%, instead of reaching the value cero, is chosen the value when the derivate almost does not change after that value being then a reasonable selection. Then the Utopia point is represented by the red point whose coordinates are 6.21E-05 mol/L*h of productivity and -7.99E-03 L*h/mol*USD of cost^{-1} differentiated (corresponding to operational cost values of 521932.83 USD/year and productivity values of 6.21e-05 mol/L*h). Table 2-4 represents the values of operation variables in the process corresponding to the selected Utopia point. The obtained design corresponds to the operation point for the implementation and evaluation of control structure.

Interestingly, the extreme points of the optimization front correspond to the constraints, for low productivity values, the mass average molecular weight values obtained are near to 70000 g/mol and for high productivity values, the conversion values obtained are near 0.4. Thus, suggesting the approach used for the selection of the optimal point is adequate considering that the values obtained are not the

same values of the constraints. If the optimal values were closer to the constraint, the optimal value must be in another region of the search zone bounded by the constraint.

Table 2-4: Optimal parameters for the CSTR reactor.

Variable	Symbol	Value	Units
Flow rate of initiator	Q_i	0.15	[L/s]
Flow rate of monomer	Q_m	0.47	[L/s]
Flow rate of cooling jacket fluid	Q_c	0.32	[L/s]
Concentration of initiator in feed	C_{If}	0.51	[mol/L]
Concentration of monomer in feed	C_{Mf}	4.35	[mol/L]
Operational cost with optimal point	CO	521932.83	[USD/year]
Productivity at the steady-state	PR_{ss}	6.21E-05	[mol/L*h]
Polydispersity index	PDI	1.51	--
Mass average molecular weight	M_w	72436.24	[g/mol]
Reactor conversion	X	0.38	--

In some cases in the literature, trajectories are optimized together with steady-state variables, easing the change of set point for the manipulated variables (Asteasuain *et al.*, 2006; Guo *et al.*, 2011; Alvarez and Odloak, 2012; Q. Guo, Liu and Chen, 2015). Here, the scheduling is not implemented, thus the comparison is only done by the steady-stated values obtained at the optimal point.

Similarities are shared with the optimization done by Asteasuain *et al*, (2006) the number of design variables optimized for the steady-state are 7 (conversion, temperature, feed process temperature, jacket temperature, cooling flow, initiator flow, and volume) a higher number of variables used in the present optimization (5 variables: the initiator flow, monomer flow, cooling fluid flow, initiator concentration, and monomer concentration in the feed). Comparing the values of steady-state, values of conversion and cooling flow are similar Asteasuain *et al*, (2006) found values of 0.33-0.37 for conversion and cooling flow of 0.079-0.138 L/s depending on the grade transition for. Herein, values of 0.38 of conversion (around 2.7%-15% difference) and 0.32 L/s (around 132%-305% difference) for the optimal point obtained. Meanwhile, the initiator flow results are considerably different, around 2 orders of magnitude. Analyzing the simulations, differences are found for Asteasuain *et al*, (2006) system as the initiator flow, with values of 2.51E-3 to 3.48E-3 L/s depending on the grade transition. The initiator flow obtained here is 0.15 L/s, with differences over the 100% error for both values. A possible explanation for the abrupt change of the flows can be explained by the difference in the volumes since these affect all the balances in the reactor. Notwithstanding the change in the overall heat transfer coefficient reported in Table 2-1, could also contribute to the

differences. This is due to this parameter influence the energy balance, affecting the values obtained for temperature and therefore the values of kinetic parameters. Also, have to take into account that for this case the comparison might not be fair since different variables are optimized. For Asteasuain *et al*, (2006), the objective function is the transition route of polymerization while herein the objective function are the operational cost and productivity). Then, it is reasonable to obtain different values for the steady-state that can be reached. Other parameter values are not taken into account due are not being part of the optimization variables, in the case of Asteasuain *et al*, (2006) temperature, feed process temperature, jacket temperature and volume are not optimized here. Since the variables used here as manipulated variables were the result of the bibliographic review, these same manipulated variables are used for the optimal design of the system.

Comparing the values obtained here, with Alvarez and Odloak, (2012), many of the parameters presented are comparable with at least the same magnitude order (i.e. flow rate monomer, flow rate of cooling jacket fluid, concentration of initiator in feed, and concentration of monomer in feed). Although the model used here is based on Alvarez and Odloak, (2012) some variables values are changed since the operation variables are modified by the operational point reached in the optimization. One example is the flow rate initiator value, which is one order of magnitude larger than the obtained here, generating differences above 1000%. Also, the monomer flow rate presented values of 0.105 L/s for Alvarez and Odloak, (2012) while the flow obtained here is 0.47L/s (347.6% difference). Comparing the flow rate of cooling jacket fluid, the value obtained by Alvarez and Odloak, (2012) is 0.131 L/s and the value obtained here is 0.32 L/s (144.28% difference). Although the high values differences are evidenced in the last-mentioned variables, the monomer flow rate and flow rate of cooling jacket fluid values obtained are almost 3 or 4 times higher than the values reported. Worth mentioning, comparing the values of concentration of initiator and monomer in the feed, differences are not higher than 50% (13.38% and 50%, respectively).

Due to the current system being based on Alvarez and Odloak, (2012), the biggest change made for this case is the overall heat transfer coefficient, further reinforcing that the reaction parameter changes drastically the values obtained in the optimal design. As a final aspect, notice that there is a difference in the objective functions used in each case for the optimization, which also affect the values of the optimal design. For Alvarez and Odloak, (2012) the objective function is the production rate and herein the objective functions are the operational cost and productivity. It can also be speculated that the molecular weight does not have a major impact on the optimization since they present very close or similar values for each case. The molecular weight constriction used here (values between 70000-80000 g/mol) while in Alvarez and Odloak, (2012) used values between 75000-95000 g/mol.

Also, some differences were found for the molecular weight, in literature set values are between 30000-50000 g/mol whereas in the present work is set around 70000-80000 g/mol (values defined for styrene in the market) (Asteasuain *et al.*, 2006; Guo *et al.*, 2011; Patil, Maia and Ricardez Sandoval, 2015). These changes depend on the source consulted since each author can propose different ranges of molecular weights for optimization.

From computational perspective, the optimization computational time in literature is between 2.5 h to 16 h. In this research, computation times were obtained between 1.75 h to 10 h. The equipment used in the literature is a Pentium IV 2.8GHz, DECstation 5000, Pentium 4 2.66 GHz, Core i7-3770 340 GHz 8 RAM, 2GHz 4GB (Gazi, Seider and Ungar, 1996; Asteasuain *et al.*, 2006; Chatzidoukas, Pistikopoulos and Kiparissides, 2009; Flores-Tlacuahuac and Grossmann, 2010; Patil, Maia and Ricardez Sandoval, 2015). While herein the equipment used are Intel core i7-8750H 2.2 GHz 16384MB RAM and Intel core i7-7700 3.6GHz 8MB RAM. Comparing equipment with similar specifications, in this case, CPUs with Intel Core i7 present similarities in the response times for optimization. However, the computational time may be affected by the different objective functions used and software. As relevant aspect, in some of the references the polymer used is different from styrene as the methyl methacrylate (MMA) or some variations of the styrene as the high impact polystyrene (HIPS). With changes in the polymer used, also kinetics, considerations, variables range, could change used too. Even changes in the system as the production of polystyrene in another thermodynamic state (bubble point) could change easily the whole system, getting some differences found compared with literature (Chatzidoukas, Pistikopoulos and Kiparissides, 2009; Gharaghani, Abedini and Parvazinia, 2012; Patil, Maia and Ricardez Sandoval, 2015).

The optimal point obtained reached herein is 6.21E-05 mol/L*h of productivity and -7.99E-03 L*h/mol*USD of cost^{-1} differentiated. Representing the best balance in terms of the highest productivity and the lowest operational cost compared with the other points obtained in the optimization. Besides, the fulfillment of the constraints proposed, with conversion values of 0.377 and molecular weight values of 72436.24 g/mol.

2.4.3. Control structure design

The following sections shows the verification of the stability of the system, controllability, and observability. Besides show the structure and tunning results for the PID, LQR, and LQG in that order.

g) Model analysis

As a crucial role in the control structure stability, controllability and observability always must be verified in every system. Therefore, the stability is corroborated by the values of eigenvalues for the A matrix shown in Table 2-5. The system controllability and observability are verified by the rank of both matrices must be the same rank of matrix A (full rank) shown in Table 2-6.

Table 2-5: Eigenvalues of matrix A, from the state space representation, system poles.

Eigenvalues
-2.50E-04
-2.50E-04
-2.50E-04
-5.60E-04
-1.21E-04
-2.53E-04
-2.50E-04

Table 2-6: CSTR ranks of controllability, observability, and A matrices.

$Rank_{controlability}$	**$Rank_{observabilty}$**	**$Rank_{A}$**
7	7	7

As seen in Table 2-5 the stability is corroborated with all the eigenvalues has a negative real part. In Table 2-6, the controllability, and observability of the current system are verified indicating that all matrices are full rank. Now the control structure design is performed.

h) PID control structure

Preliminary results for the RGA pairing are shown in Table 2-7. The values for the monomer concentration in the feed are very low compared with other values of inputs, for that reason that input is removed from the control structure.

Table 2-7: CSTR RGA methodology results with 5 inputs, the first line represents the inputs and the first column the outputs.

	Q_i	Q_m	Q_c	C_{If}	C_{Mf}
C_M	-0.22	1.06	0.02	-0.02	0.16
T	0.18	0.35	0.53	-0.06	-0.01
D_1	0.04	0.00	-0.11	0.98	0.09
D_2	0.98	-0.43	0.56	-0.02	-0.10

Then, from 5 manipulated variables only 4 could be used. Thus, at this stage it is decided to use 4 manipulated variables: Initiator flow, monomer flow, cooling fluid flow and the Initiator concentration in the feed (Q_i, Q_m, Q_c, C_{If}). The results for the variables pairing are listed in Table 2-8, according to the RGA methodology.

Table 2-8: CSTR RGA matrix results with 4 inputs, the first line represents the inputs and the first column the outputs.

	Q_i	Q_m	Q_c	C_{If}
C_M	-0.12	1.12	0.02	-0.02
T	0.21	0.33	0.53	-0.07
D_1	0.00	0.00	-0.11	1.12
D_2	0.91	-0.44	0.56	-0.03

- The appropriate pairing for single-input single-output system controllers (SISO) is “to manipulate” the monomer inlet flow to control the monomer concentration, to manipulate the cooling fluid flow to control the temperature in the reactor, to manipulate the initiator concentration in the feed to control the first moment of the molecular distribution and, to manipulate the initiator flow to control the second moment of the molecular distribution (red values in Table 2-8). As a remark, some of the optimization problems in the literature presented some nonlinearities easing the choice for the manipulated variables through the optimization of these variables (Asteasuain *et al.*, 2006; Flores-Tlacuahuac and Biegler, 2008). Interestingly, the RGA methodology used herein worked satisfactorily even with the model linearization.

Using the linearized model and IMC methodology for the PID controller tuning, considering PID controller operates in parallel the parameters for the PID controllers are shown in Table 2-9.

Table 2-9: CSTR tuning parameters for the PID controller.

	P	I	D	N
C_M controller	3.54E+02	9.59E-02	5.19E+02	3.41
T controller	-4.60E-01	-5.03E-05	-1.05E+03	2.19E-03
D_1 controller	1.74	2.09E-04	3.62E+03	2.40E-03
D_2 controller	-3.71E-04	-6.18E-08	-1.16E-01	1.60E-02

The final implementation of PID control in Simulink® is shown in Figure 2-11. As a general aspect for all controllers, white noise was implemented in the inputs and outputs, also the use of "goto" block to represent the feedback in the control loops in Simulink®. The deviation standard is shown in Table 2-10 for the outputs and Table 2-11 for the inputs in the system.

Table 2-10: CSTR outputs deviation standard.

	OUTPUTS DEVIATION STANDARD			
Controller	C_M	T	D_1	D_2
PID	1.55E-06	1.13E-03	2.23E-04	1.99E-01
LQR	1.17E-04	7.34E-03	6.06E-04	2.83E-01
LQG	1.72E-08	3.66E-06	2.14E-07	1.53E-04

Table 2-11: CSTR inputs deviation standard.

	INPUTS DEVIATION STANDARD			
Controller	Q_m	Q_c	C_{If}	Q_i
PID	1.52E-03	4.36E-03	5.82E-03	4.47E-04
LQR	1.36E-02	4.47E-02	2.29E-01	2.51E-03
LQG	3.57E-05	3.54E-05	3.55E-04	1.12E-04

Besides, a sub-system is implemented for the estimation of the conversion and the mass average molecular weight based on the system states (required by controllers PID and LQR). Besides, saturators are included to ensure appropriate values for the inputs *e.g.* negative input values in the control loop.

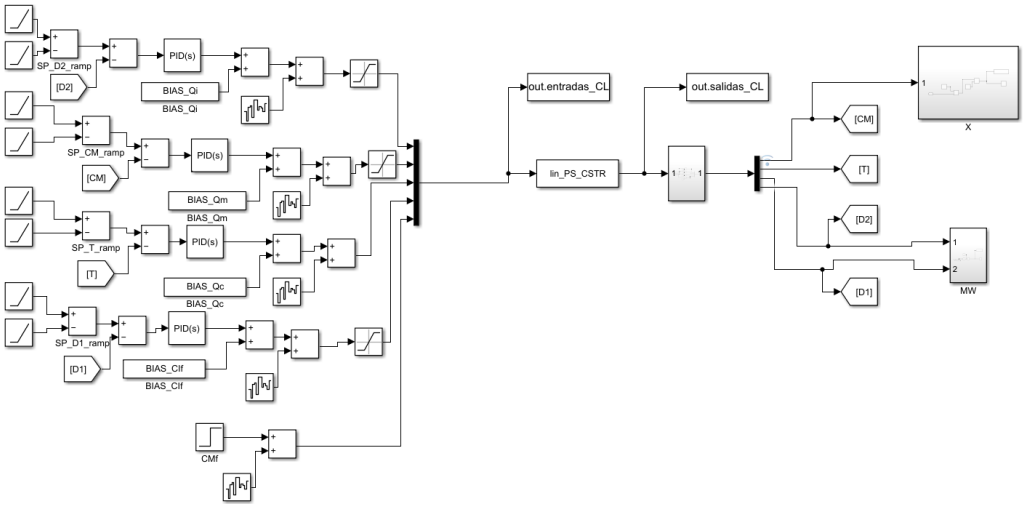

Figure 2-11: CSTR PID control structure implementation in Simulink®. Notice that the 'goto' block is used to simplify the closed loops implemented.

i) LQR control

As previously said in the tunning of LQG control, Q and R are normalized as shown in Equation 2.31 and Equation 2.32. The final implementation of LQR control in Simulink® is shown in Figure 2-12 and the values for the tuning of Q and R are listed in Table 2-12.

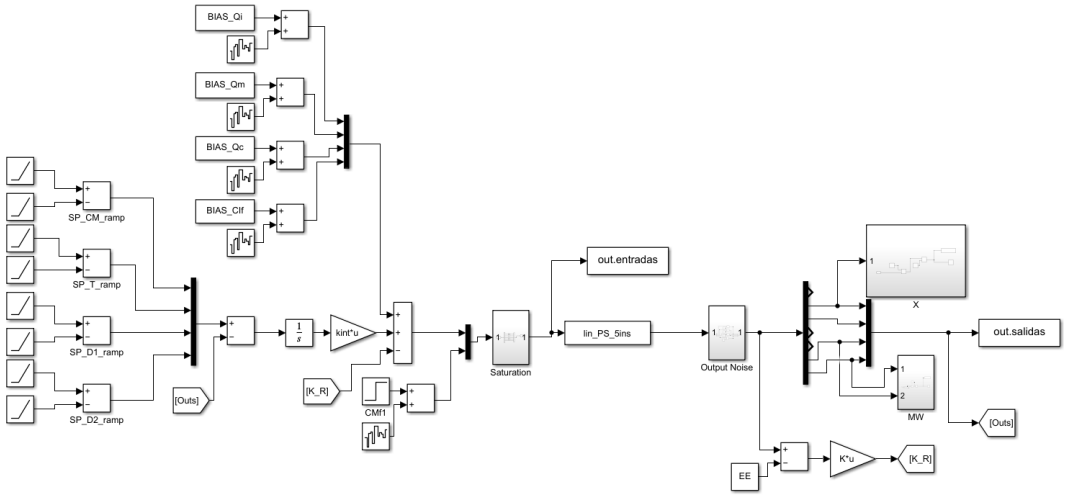

Figure 2-12: CSTR Simulink® diagram for LQR controller with integral action. Notice that the 'goto' block is used to simplify the closed loops implemented.

j) LQG control

As the LQG control is an extension of the LQR control the tunning is the same for both controllers. The final implementation of LQG control in Simulink® is shown in Figure 2-13 and values for the tuning of the Q, R, and the Kalman filter are shown in Table 2-12.

Table 2-12: CSTR tuning parameters for the LQR and LQG controller (Note: these are the values of diagonal of each matrix listed).

LQG tuning		Kalman filter tuning	
Q	R	R_v	R_w
94.36	44.43	1.00E-20	1
0.14	4.48	1.00E-20	1
9.87E-06	9.48	1.00E-20	1
1.07E-05	3.76	1.00E-20	-
2.10E+08	-	1.00E-20	-
0.09	-	1.00E-20	-
1.89E-07	-	1.00E-20	-

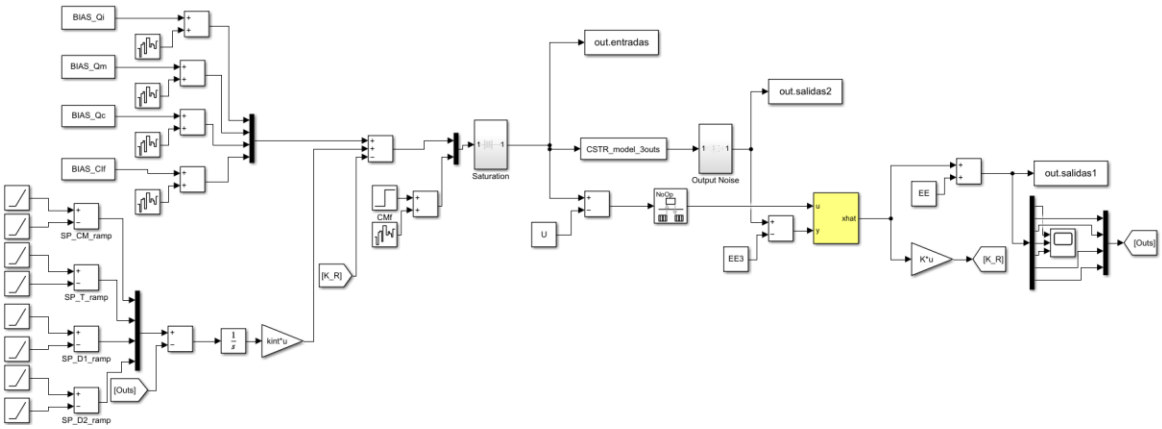

Figure 2-13: CSTR Simulink® diagram for LQG controller. Notice that the 'goto' block is used to simplify the closed loops implemented. The highlighted block is the Kalman filter implemented for state estimation.

A remark must be done, taking into account that the system implemented for the LQG controller has 3 outputs, conversion, temperature, and mass average molecular (for the Kalman filter implementation as an observer). While PID and LQR have 4 outputs, thus, the white noise used in the outputs for the LQR controller is different from the other two control configurations.

2.4.4. Controllers' performance evaluation

For all control strategies evaluation, a setpoint change of 2% is introduced. Notice that with larger values, the system presents numerical error due to limitations with the mathematical method used in Simulink®, despite the numerical method was adjusted by iterating values of relative tolerance, absolute tolerance, and evaluating different numerical methods used.

For practical effects, the present section shows one of the representative figures and tables obtained for changes in the setpoint for C_M. Further results are depicted in the CSTR supplementary material section. Moreover, for a better understanding of the control action in the manipulated and controlled variables, figures without the noise implementation are shown in Figure 2-15, Figure 2-19, Figure 2-20, and Figure 2-21.

As a general observation (see Figure 2-14, Figure 2-16, Figure 2-17, Figure 2-18), the response of LQG controller effectively suppresses the noise implemented in the systems. The noise present in the response for C_M is because the value of noise removed is much bigger than the response obtained. Despite this, the system is evaluated with that value of noise to be fair with the other changes in setpoint (where the LQG controller suppresses the noise).

Whereas the PID and LQR controllers present noise in all the signals, LQG controller does not. Then, it is evident that the implementation of the Kalman filter estimates non measurable states from a set of measurable state while filtering the noise out. For a better appreciation of changes in setpoint and performance indexes (t_s, t_r, t_p, O_S) for the setpoint tracking and disturbances rejection tests are presented in Table 2-13, Table 2-14, Table 2-15 and Table 2-16.

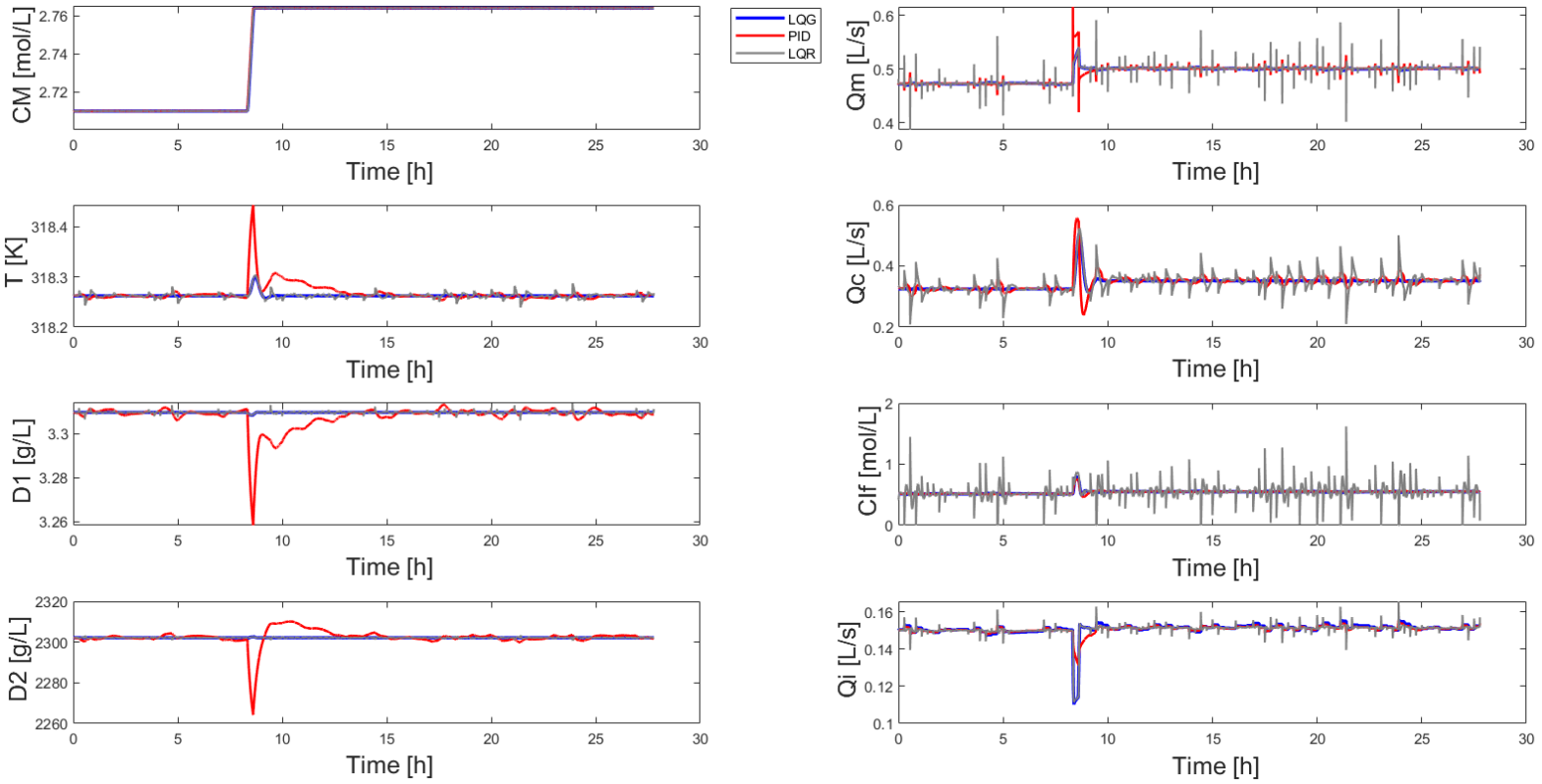

Figure 2-14: CSTR system Response for setpoint change in C_M (2% above original setpoint) with noise implementation.

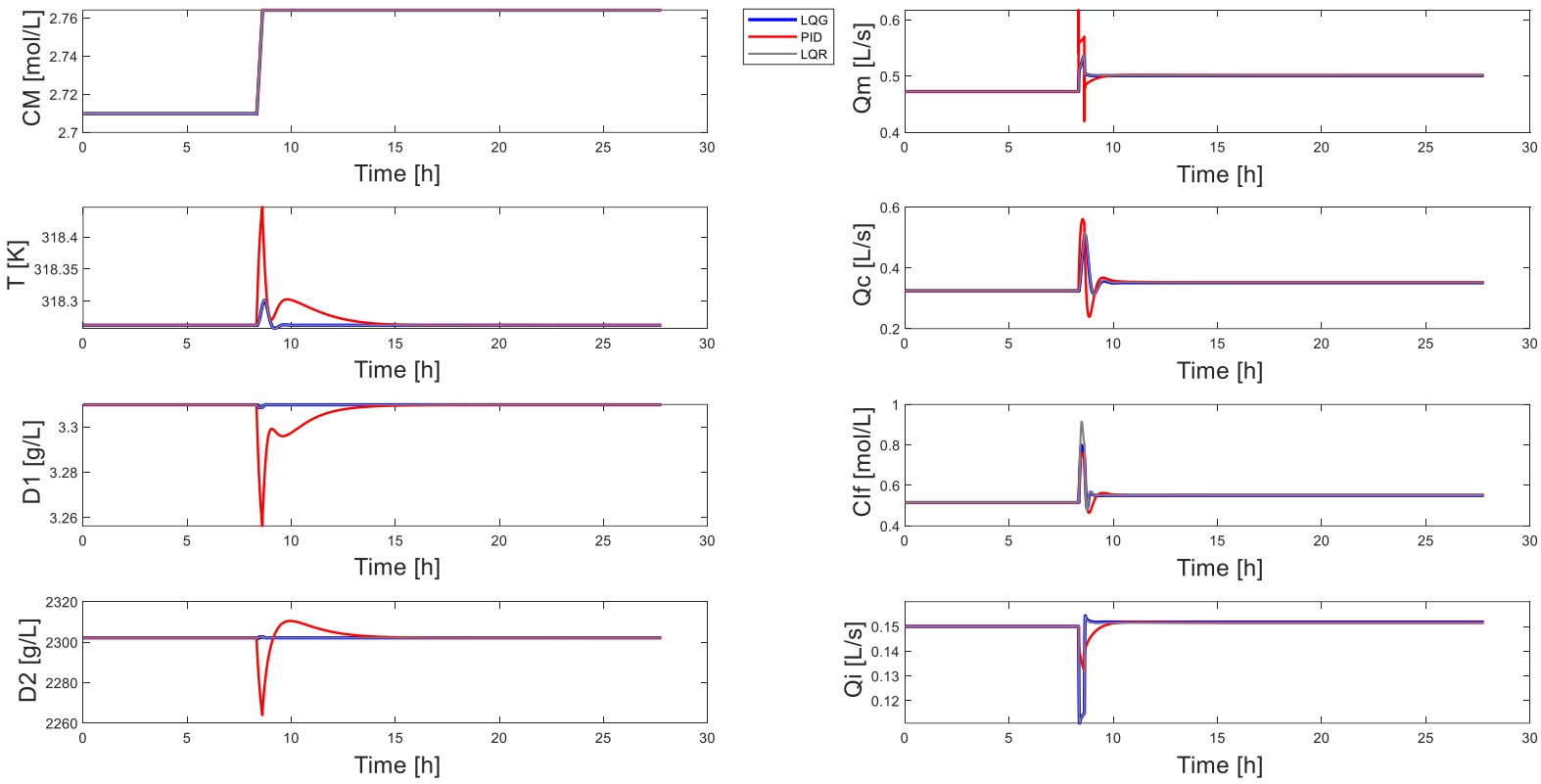

Figure 2-15: CSTR system Response for setpoint change in C_M (2% above original setpoint) without noise implementation.

Table 2-13: CSTR Performance indexes for setpoint change of C_M.

Set point change	C_M (2.71-2.76 mol/L)		
Controller	**PID**	**LQR**	**LQG**
Rise time C_M [h]	0.28	0.30	0.30
Rise time T [h]	6.98	0.72	0.72
Rise time D_1 [h]	8.10	0.41	0.43
Rise time D_2 [h]	0.81	0.08	0.08
Time to first peak C_M [h]	0.28	0.32	0.32
Time to first peak T [h]	0.28	0.40	0.37
Time to first peak D_1 [h]	0.28	0.19	0.21
Time to first peak D_2 [h]	0.28	0.04	0.03
Settling time C_M [h]	0.34	0.38	0.43
Settling time T [h]	6.98	2.13	1.30
Settling time D_1 [h]	8.10	0.92	0.58
Settling time D_2 [h]	7.54	1.08	0.57
Overshoot	1.29E-03	2.85E-03	2.22E-03

Evaluating the performance indexes, the values of settling time are lower for the LQG control in almost all cases (5-13 times lower than the PID controller and 1-1.07 times lower than the LQR). An exception is the case of set point changes in the monomer concentration, where the PID control is 26% faster. Also, in the case of set point changes realized in the temperature where the LQR control is 1.06 times faster than LQG. However, in general the response for disturbances is quicker with the LQG control than the PID control. Suggesting a better general response for LQG controllers.

Particularly, the PID controllers do not present overshoot at least for two of the setpoint changes (set point changes for D_1 and D_2). Easily verified in Table 14, and Table 15, where red values of settling time, rise time, time to first peak, are the same values. Meanwhile, LQR and LQG controllers presented overshoot in all responses. The results indicate that the PID controller does not exceed the set point targeted, while LQG and LQR controller do. As a consequence, more effort in the manipulated variables is required to return to the desired set point. Generally, the values of time to first peak and rise time are almost set at the same time. Some cases for disturbance rejections present a high difference between the time to first peak and rise time, showing the controller effort to handle the same value for the disturbed variable. This phenomenon is more frequent in PID, at least in LQR and LQG the difference is considerably smaller.

In summary, the LQG control can reach setpoint changes almost 2 times faster than the PID and LQR control. Besides the response for disturbance by setpoint can reach 5-14 times faster stabilization with the LQG control than the PID and LQR control (those depending on the setpoint disturbance and the analyzed variable).

Comparing the results with the literature, here the number of manipulated variables used is larger, a total of 4 (Q_i, Q_m, Q_c, C_{If}), this doesn't necessarily mean a better control, it means there this control structure is managing more control objectives. In literature, researchers used more simplistic approaches with one or two manipulated variables (Hidalgo and Brosilow, 1990; Alvarez and Odloak, 2012; Nguyen, Hoang and Azlan Hussain, 2019; Wang *et al.*, 2019). No information was found about the implementation of LQG controller or Kalman filter to calculate non-measured variables physically by the system for styrene polymerization in CSTR, then the presented results are novel. Some previous studies present the implementation of Gaussian or white noise in the system (Viel, Busvelle and Gauthier, 1995; Na and Rhee, 2000) and perform a Kalman filter with a different approach than the employed here (Viel, Busvelle and Gauthier, 1995).

Previous research has investigated model predictive control (MPC), where the settling time is almost the same for changes in the setpoint, approximately 4.5 hours to reach the set point response (Hidalgo and Brosilow, 1990; Gazi *et al.*, 1996) while here, PID and LQG implementation takes around 4 hours. Alvarez and Odloak, (2012) takes around 20-50 hours, larger times to stabilize the response, almost 5 times the value results exposed here. In other cases, the settling time for setpoint changes is around 4.5 and 8 hours, and the settling time for the manipulated variables are around 2.5 and 5 hours (Viel, Busvelle and Gauthier, 1995; Gazi *et al.*, 1996; Na and Rhee, 2000; Guo *et al.*, 2011). Similar responses for the results presented here nevertheless, in this work those times were lower at least with the LQG controller. Although lower times have been found (0.3 hours) in Nguyen, Hoang and Azlan Hussain, (2019) but must be considered the differences between the parameters design used by the author. For example, the volume used is 3 times lower than the value used here, producing different scenarios with completely different systems, conditions, and parameters. Making the comparison with other previous studies quite difficult, due to many of the systems have been changed in some design parameters for the reactor, including kinetic parameters, consideration for the mass and energy balances, controllers, among others.

2.5. Conclusions

From the model perspective, despite the system presenting some uncertainties, the CSTR system is set in such a way that the assumptions and constraints ensure adequate industrial behavior for this kind of polymerization system.

Here in, the styrene polymerization case has been investigated from multi-objective optimal design and control assessment for a CSTR. The optimization approach used with two objective functions is an interesting approach, due to the lack of information for the economic evaluation is compensated with the ideal production capacity in the plant helping to find the optimal point. Weighing into both technical evaluations (economical and productivity evaluation), selecting the operating point more fairly, enhancing the design. Where the selected optimal point corresponds to a cost value of 521932.83 USD/year and a productivity value of 6.21e-05 mol/L*h. Representing the best balance between the lowest operating cost and the highest productivity in the system proposed.

The variables selected as manipulable grant controllability and the measured variables grant observability in the system proposed, key indicators in any control structure design.

RGA methodology has been shown to be a simple and powerful tool to design a control structure. Ensuring a good association between the manipulated and the controlled variables. For this case, the pairing is using the monomer inlet flow to control the monomer concentration, the cooling fluid flow to control the temperature in the reactor, the initiator concentration in the feed to control the first moment of the molecular distribution and, the initiator flow to control the second moment of the molecular distribution.

From the controllers' performance perspective, the best controller is the LQG with lower response times achieving times 5-13 times faster than the PID controller and 1-1.07 times faster than the LQR, and the controllers found in the literature, improving the environmental impact and economic potential in polymerization systems. Also, the LQG controller can suppress the noise in the plant and even has a response in terms of variables that cannot be physically measured but also are important in the system (*e.g.* molecular weight moments). Nevertheless, PID and LQR controllers provide a good response as well for set point tracking and disturbance in the system. Exposing the advantage of using control in the polymerization process, even with not the best results for the previously named controllers, in some cases present similar values in performance indexes to the LQG controller.

2.6. Nomenclature

A	A matrix from the state-space (states matrix).
A_d	Activation energy for initiator decomposition.
A_p	Activation energy for propagation reaction.
A_t	Activation energy for termination reaction.
A^T	Matrix A transposed.
B	B matrix from the state-space (inputs matrix).
B^T	Matrix B transposed.
C	C matrix from the state-space (outputs matrix).
C_A	Concentration of the limiting reagent A.
C_{Af}	Concentration of the limiting reagent A in the feed.
C_I	Concentratrion of the initiator.
C_{If}	Concentration of initiator in the feed.
C_M	Concentratrion of the monomer.
C_{Mf}	Concentration of monomer in the feed.
C_{M^*}	Concentration of monomer intermediate in a free radical model.
C_P	Concentration of monomer intermediate.
Cp_i	Heat capacity for the i reagent.
C_{R^*}	Concentration of initiator intermediate.
D	Parameter D of the PID controller.
D_0	Cero moment of molecular weight.
D_1	First moment of molecular weight.
D_2	Second moment of molecular weight.
E_d	Frequency factor for initiator decomposition.
E_i	Rate of energy from the reagent i in the system.
E_{in}	Rate of energy added to the system.
E_{out}	Rate of energy leaving the system.
E_p	Frequency factor for propagation reaction.
E_t	Frequency factor for termination reaction.
f	Initiator efficiency for AIBN.
F_A	Molar flow of the limiting reagent A.
F_{Ao}	Molar flow of the limiting reagent A.
F_i	Molar flow rate of the reagent i in the system.
F_{in}	Molar flow into the system.
F_{io}	Initial molar flow rate of the reagent i in the system.
F_{Io}	Molar flow of the initiator.
F_I	Molar flow of the initiator in the feed.
F_{Mo}	Molar flow of the monomer.
F_M	Molar flow of the monomer in the feed.
F_{out}	Molar flow out of the system.
g	Gravity.
$G_c(s)$	Transfer function.
hA	Overall heat transfer coefficient.

H	Lagrange function or Hamiltonian.
H_i	Enthalpy of the reagent i in the system.
$H_i°$	Enthalpy of formation of the reagent i in the system at the reference temperature.
I	Parameter I of the PID controller.
I_d	Identity matrix from the error covariance matrix.
I_n	Initiator in a free radical model.
k	Instant of time for the correction and prediction for the Kalman filter.
k_d	Rate constant for decomposition reaction.
k_f	Gain in the identification parameters for the transfer function for the order reduction.
k_i	Rate constant for initiation reaction.
k_j	Rate constant for reaction i in the system.
k_p	Rate constant for propagation reaction.
k_t	Rate constant for termination reaction.
k_{tc}	Rate constant for termination reaction by combination.
k_{td}	Rate constant for termination reaction by disproportionation.
K	Gain of LQR controller.
K_c	Gain for the transfer function describes the PID controller.
K_i	Gain for the integral action in the LQR and LQG controllers.
$L(k)$	Optimal gain for the Kalman filter in the instant of time k.
M	Monomer in the free radical model.
${M_1}^*$	First free radical of in the free radical model.
M_i^*	Free radical of size i created in the reaction.
M_{i+1}^*	Growing radical of size i in the reaction
M_j^*	Free radical of size j created in the reaction.
M_m	Molecular weight of the monomer (styrene).
M_w	Mass average molecular weight in the reactor.
n	Moles number of free radicals obtained in the initiation.
N	Parameter N of the PID controller.
N_A	Moles number of the limiting reagent A in the system.
N_i	Moles number of the i specie in the system.
N_L	Matrix that penalizes cross products of the input and the state in the LQR controller.
N^T	Transponse matrix of N.
O_S	Overshoot.
P	Parameter P of the PID controller.
PDI	Polydispersity index.
P_{i+j}	Final polymer of size i plus j.
P_i	Final polymer of size i.
P_j	Final polymer of size j.
$P(k)$	Error covariance matrix at time k.
PR	Productivity.
PR_{ss}	Productivity in the steady-state.
PR_{total}	Total productivity in the operation.

P_s	Total press in the system.
Q	Weight that represents actuator performance in the LQR controller.
$\dot{Q}$	Rate of flow of heat to the system from the surroundings
Q_A	Flow of the limiting reagent A.
Q_c	Flow rate of cooling jacket fluid.
$\dot{Q}_{Cond}$	Rate of conduction flow heat.
$\dot{Q}_{Conv}$	Rate of convection flow heat.
$\dot{Q}_{Elec}$	Rate of electric flow heat.
Q_i	Flow rate of initiator.
Q_{ii}	Normalization of states in the system.
Q_m	Flow rate of monomer.
$\dot{Q}_{Rad}$	Rate of radiation flow heat.
Q_s	Flow rate of solvent.
Q_t	Sum of all flows inning the reactor.
r_A	Reaction rate for the limiting reagent A.
R	Weight that represents actuator effort in the LQR controller.
R^*	Free radical form in the initiation reaction.
R^2	Coefficient of determination.
R^{-1}	Inverse matrix of R.
R_{jj}	Normalization of inputs in the system.
R_v	Process noise covariance.
R_w	Measurement noise covariance.
s	Dependent variable in the frequency domain.
S	Solution of Riccati equation.
T	Reactor temperature.
t_R	Total time of reaction.
T_f	Temperature of the reactor feed.
T_{cf}	Inlet temperature of cooling jacket fluid.
T_c	Cooling jacket fluid temperature.
t_s	Settling time.
t_r	Rise time.
t_p	Time to first peak.
Tr	Reference temperature.
t	Time.
T_{io}	Initial temperature of the i component in the system.
u	Imputs in the system.
u_j	Imput in the j position.
UA	Total overall heat transfer coefficient in the system.
U_i	Internal energy of the i component.
v	Process disturbance.
ν_i	Stoichiometry coefficient of the i component in the system.
V	Reactor volume.
V_c	Volume of cooling jacket fluid.
$\tilde{V}_i$	Molar volume of the i component.

w	Measurement noise.
$\dot{W}$	Rate of work done by the system on the surroundings.
$\dot{W}_s$	Shaft work.
X	Reactor conversion.
x	Matrix of states in the system.
$\dot{x}$	State vector.
$x(k)$	States in the instant of time k.
$\hat{x}(k)$	Estimate of the states in the Kalman filter.
x_i	State in the i position.
x^T	Transpose of the matrix x.
$\dot{y}$	Output vector.
$y(k)$	Output vector in the instant of time k.
Z_i	Difference of the value of the reference position concerning the final position of the object.

2.6.1. Greek letters

α	Constant for the derivative filter in a PID controller.
ΔH_{Rxn}	Enthalphy of reaction.
ΔH_r	Heat of polymerization.
ΔT	The difference of temperatures between two measuring points.
θ	Dead time in a transfer function.
λ	The equivalent to Lagrange multiplier in optimization problems.
ρC_p	Mean heat capacity of reactor fluid.
$\rho_c C_{pc}$	Heat capacity of cooling jacket fluid.
τ	Time constant in a transfer function.
τ_I	Integral tuning parameter.
τ_D	Derivative tuning parameter.

2.7. References

Alcocer García H (2018) Optimización multi-objetivo enfocada en la integración del diseño y control en secuencias intensificadas para la purificación de ácido levulínico

Alvarez J, González P (2007) Constructive control of continuous polymer reactors. J Process Control 17:463–476. https://doi.org/10.1016/j.jprocont.2006.09.007

Alvarez LA, Odloak D (2012) Optimization and control of a continuous polymerization reactor. Brazilian J Chem Eng 29:807–820. https://doi.org/10.1590/S0104-66322012000400012

Asteasuain M, Bandoni A, Sarmoria C, Brandolin A (2006) Simultaneous process and control system design for grade transition in styrene polymerization. Chem Eng Sci 61:3362–3378. https://doi.org/10.1016/j.ces.2005.12.012

Braun D, Cherdron H, Rehahn M, et al (2013) Polymer synthesis: Theory and practice: Fundamentals, methods, experiments, fifth edition

Chatzidoukas C, Pistikopoulos S, Kiparissides C (2009) A hierarchical optimization approach to optimal production scheduling in an industrial continuous olefin polymediation reactor. Macromol React Eng 3:36–46. https://doi.org/10.1002/mren.200800030

Chen CC (1994) A continuous bulk polymerization process for crystal polystyrene. Polym Plast Technol Eng 33:55–81. https://doi.org/10.1080/03602559408010731

Collete Y, Siarry P (2003) Multiobjective Optimization: Principles and Case Studies. Springer, New York

Felorzabihi N, Ghadi N, Dhib R (2003) Differential geometry control of a polymer reactor. In: 2003 International Conference Physics and Control, PhysCon 2003 - Proceedings. pp 345–348

Flores-Tlacuahuac A, Biegler LT (2008) Integrated control and process design during optimal polymer grade transition operations. Comput Chem Eng 32:2823–2837. https://doi.org/10.1016/j.compchemeng.2007.12.005

Flores-Tlacuahuac A, Grossmann IE (2010) Simultaneous Cyclic Scheduling and Control of Tubular Reactors: Single Production Lines. Ind Eng Chem Res 49:11453–11463. https://doi.org/10.1021/ie1008629

Fogler HS (2006) Elements of Chenzicn 1 Reaction Engineering

Garside M (2019) Global plastic production statistics. https://www.statista.com/statistics/282732/global-production-of-plastics-since-

1950/#statisticContainer

Gazi E, Seider WD, Ungar LH (1996a) Verification of controllers in the presence of uncertainty: Application to styrene polymerization. Ind Eng Chem Res 35:2277–2287. https://doi.org/10.1021/ie9504361

Gazi E, Ungar LH, Seider WD, Kuipers BJ (1996b) Automatic analysis of Monte-Carlo simulations of dynamic chemical plants. Comput Chem Eng 20:

Gharaghani M, Abedini H, Parvazinia M (2012) Dynamic simulation and control of auto-refrigerated CSTR and tubular reactor for bulk styrene polymerization. Chem Eng Res Des 90:1540–1552. https://doi.org/10.1016/j.cherd.2012.01.019

Guo Q, Liu H, Chen J (2015) Optimal grade transition of the styrene polymerization process with endpoint and path constraints. In: Proceedings of the World Congress on Intelligent Control and Automation (WCICA). pp 4997–5001

Guo Q, Wang H, Lin W, Yang J (2011) Optimization-based strategies for grade transition operation of a continuous styrene polymerization process

Hamielec AE, Hodgins JW, Tebbens K (1967) Polymer Reactors and Molecular Weight Distribution: Part II. Free Radical Polymerization in a Batch Reactor. AIChe 13:1087–1091. https://doi.org/doi/abs/10.1002/aic.690130610

Hernández-Escoto H, López T, Alvarez J (2010) Estimation of alkyd reactors with discrete-delayed measurements. Chem Eng J 160:698–707. https://doi.org/10.1016/j.cej.2010.03.055

Hidalgo PM, Brosilow CB (1990) Nonlinear model predictive control of styrene polymerization at unstable operating points. Comput Chem Eng 14:481–494. https://doi.org/10.1016/0098-1354(90)87022-H

Ionut B (2009) Modeling and optimization of tubular polymerization reactors

Johnson AF, McGreavy C, Laurence RL, et al (1994) Polymer reactor engineering, first. Chapman & Hali

Li M, Christofides PD (2007) An input/output approach to the optimal transition control of a class of distributed chemical reactors. In: Proceedings of the American Control Conference. pp 2042–2047

Luyben WL (2007) Chemical reactor design and control. John Wiley & Sons, Inc.

Mathworks (2021) lqrd. https://www.mathworks.com/help/control/ref/lqrd.html

Mathworks (2019) State Space, Part 4: What Is LQR Control? In: Videos and wevinars. https://www.mathworks.com/videos/state-space-part-4-what-is-lqr-control-1551955957637.html

Mathworks (2017) Understanding Kalman Filters. https://www.youtube.com/watch?v=mwn8xhgNpFY&ab_channel=MATLAB. Accessed 23 Feb 2022

Na SS, Rhee HK (2000) Polynomial ARMA model identification for a continuous styrene polymerization reactor using on-line measurements of polymer properties. J Appl Polym Sci 76:1889–1901. https://doi.org/10.1002/(SICI)1097-4628(20000624)76:13<1889::AID-APP6>3.0.CO;2-Y

Nguyen TS, Hoang NH, Azlan Hussain M (2019) Feedback passivation plus tracking-error-based multivariable control for a class of free-radical polymerisation reactors. Int J Control 92:1970–1984. https://doi.org/10.1080/00207179.2017.1423393

Patil B, Maia E, Ricardez Sandoval L (2015) Integration of scheduling, design, and control of multiproduct chemical processes under uncertainty. AIChE J 61:2456–2470. https://doi.org/10.1002/aic.14833.

Plasteurope (2012) Plastics markets. https://www.plasteurope.com/news/PLASTICS_MARKETS_t221996/. Accessed 22 May 2020

Russo LP, Bequette BW (1998) Operability of chemical reactors: Multiplicity behavior of a jacketed styrene polymerization reactor. Chem Eng Sci 53:27–45. https://doi.org/10.1016/S0009-2509(97)00281-9

Schmidt AD, Ray WH (1981) The dynamic behavior of continuous polymerization reactors-I. Isothermal solution polymerization in a CSTR. Chem Eng Sci 36:1401–1410. https://doi.org/10.1016/0009-2509(81)80174-1

Seborg DE, Edgar TF (2003) Process Dynamics and Control, second. Jhon Wiley and Sons, Inc.

Skogestad S, Postlethwaite I (2001) Multivariable feedback control Analysis and design, second edi

Vasco De Toledo EC, Martini RF, Maciel MRW, Maciel Filho R (2005) Process intensification for high operational performance target: Autorefrigerated CSTR polymerization reactor. Comput Chem Eng 29:1447–1455. https://doi.org/10.1016/j.compchemeng.2005.02.017

Viel F, Busvelle E, Gauthier JP (1995) Stability of polymerization reactors using I/O linearization and a high-gain observer. Automatica 31:971–984. https://doi.org/10.1016/0005-1098(95)00009-L

Wallis JPA, Ritter RA, Andre H (1975) Continuous production of polystyrene in a tubular reactor: Part II. AIChE J 21:691–698. https://doi.org/10.1002/aic.690210408

Wang J, Tan C, Wu H (2019a) Online Shape Modification of Molecular Weight Distribution Based on the Principle of Active Disturbance Rejection Controller. IEEE Access 7:53163–53171. https://doi.org/10.1109/ACCESS.2019.2912215

Wang Y, Ostace GS, Majewski RA, Biegler LT (2019b) Optimal grade transitions in a gas-phase polymerization fluidized bed reactor. In: IFAC-PapersOnLine. pp 448–453

2.8. CSTR supplementary material

The following section contains the supplementary material as the Figures (with and without noise) and tables for values of the control performance for the system with changes in the setpoints for T, D_1 and D_2.

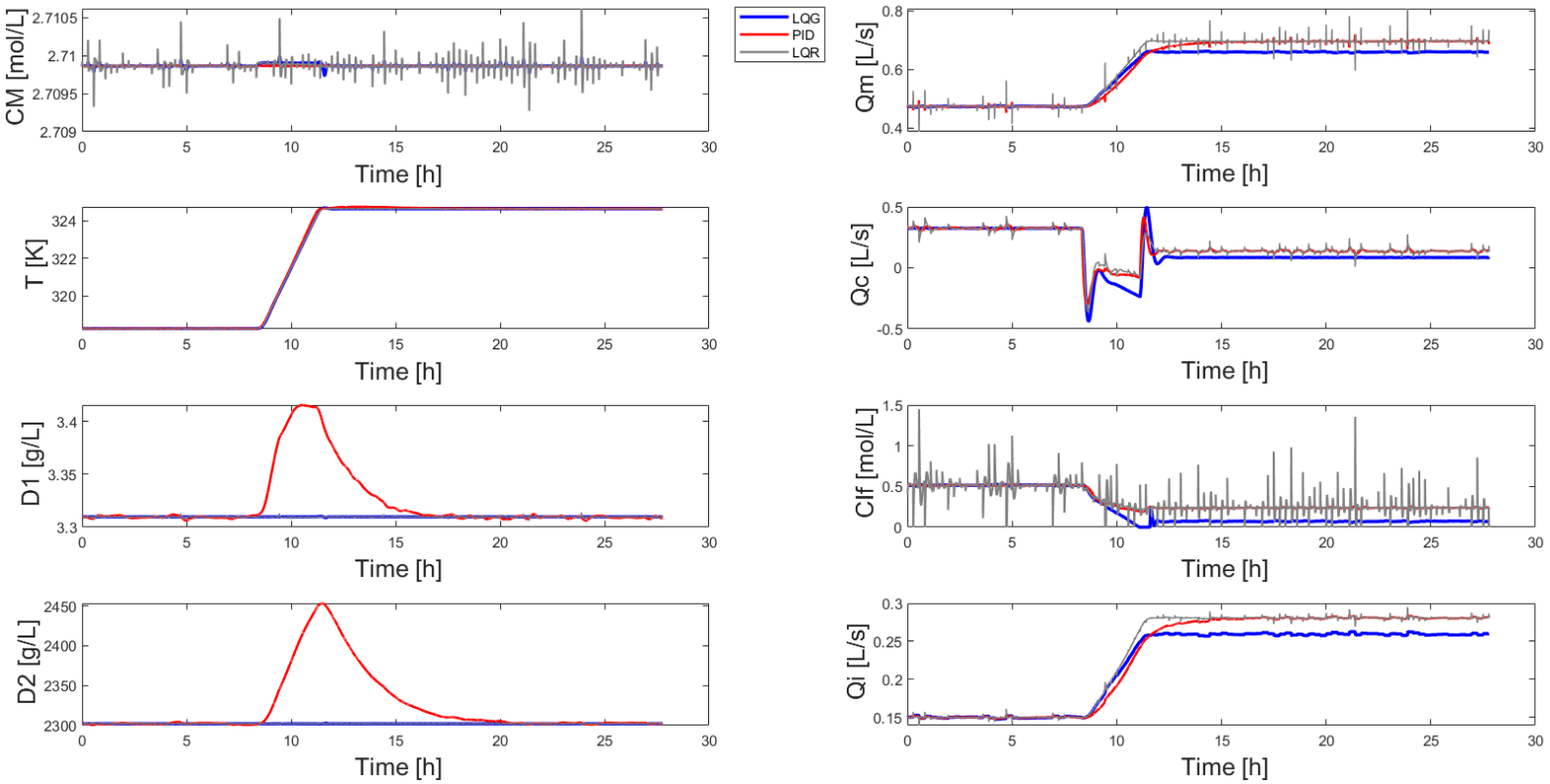

Figure 2-16: CSTR system Response for setpoint change in T (2% above original setpoint) with noise implementation.

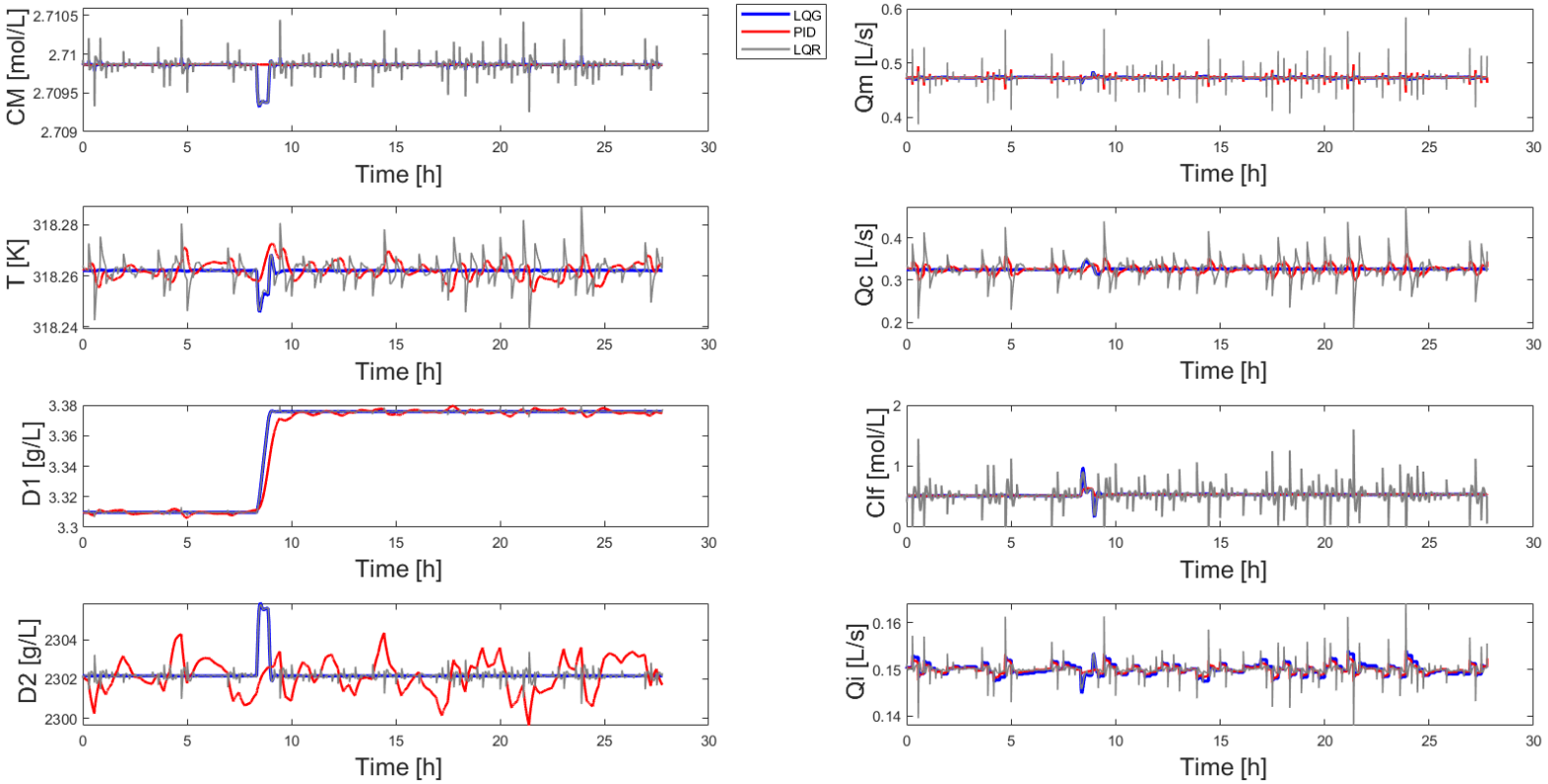

Figure 2-17: CSTR system Response for setpoint change for $\boldsymbol{D_1}$ (2% above original setpoint) with noise implementation.

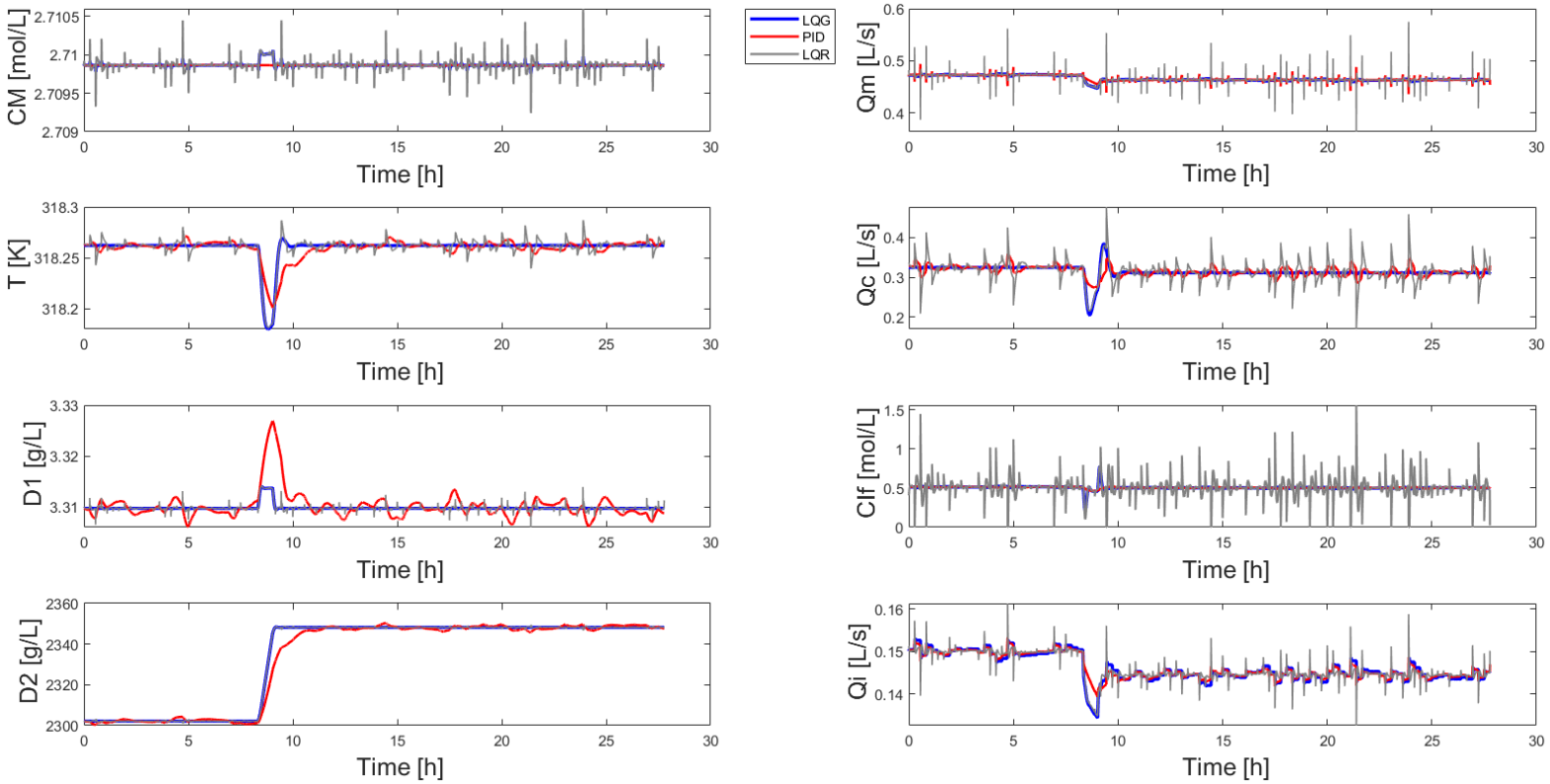

Figure 2-18: CSTR system Response for setpoint change for $\boldsymbol{D_2}$ (2% above original setpoint) with noise implementation.

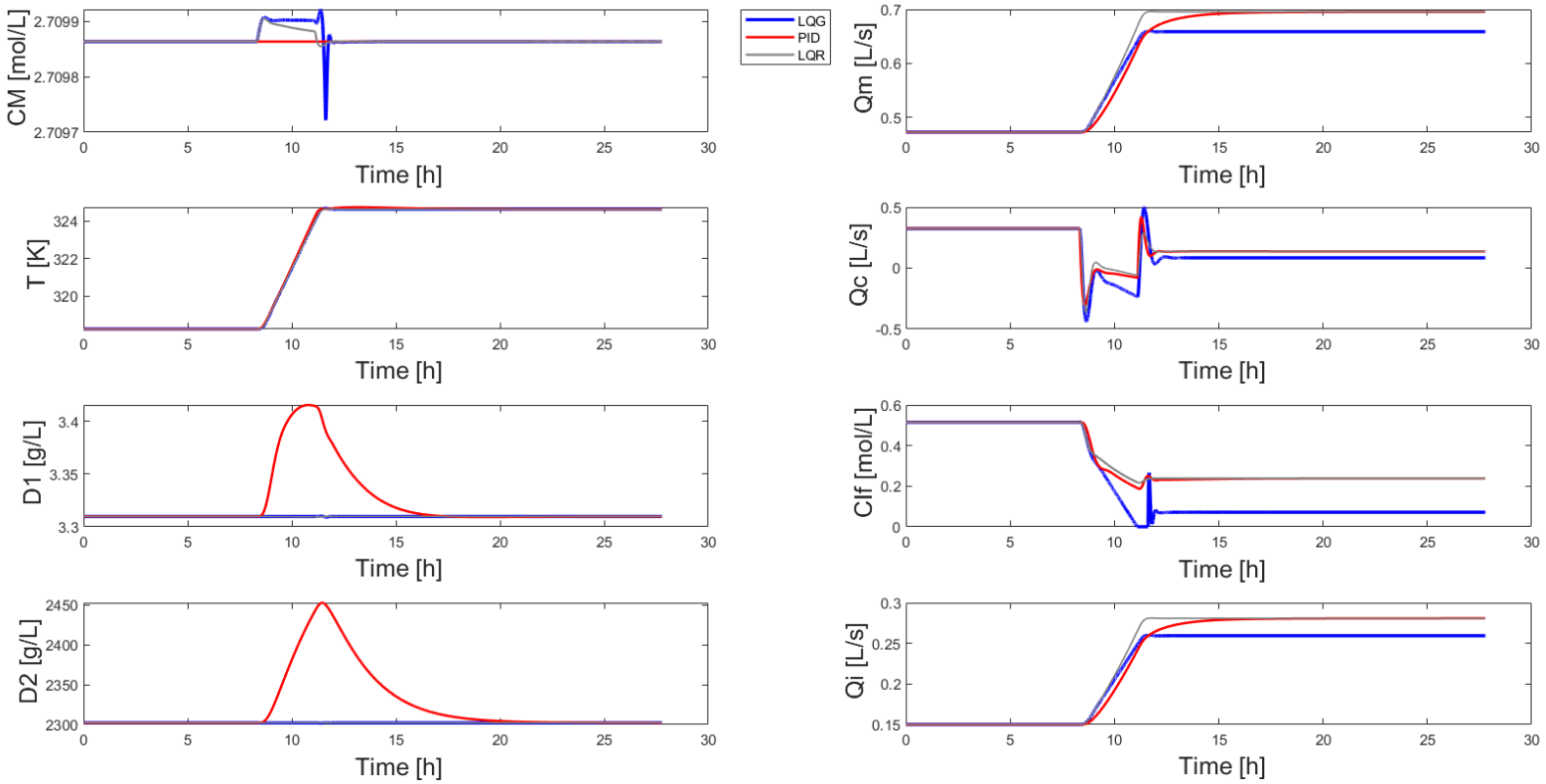

Figure 2-19: CSTR system Response for setpoint change in $\boldsymbol{T}$ (2% above original setpoint) without noise implementation.

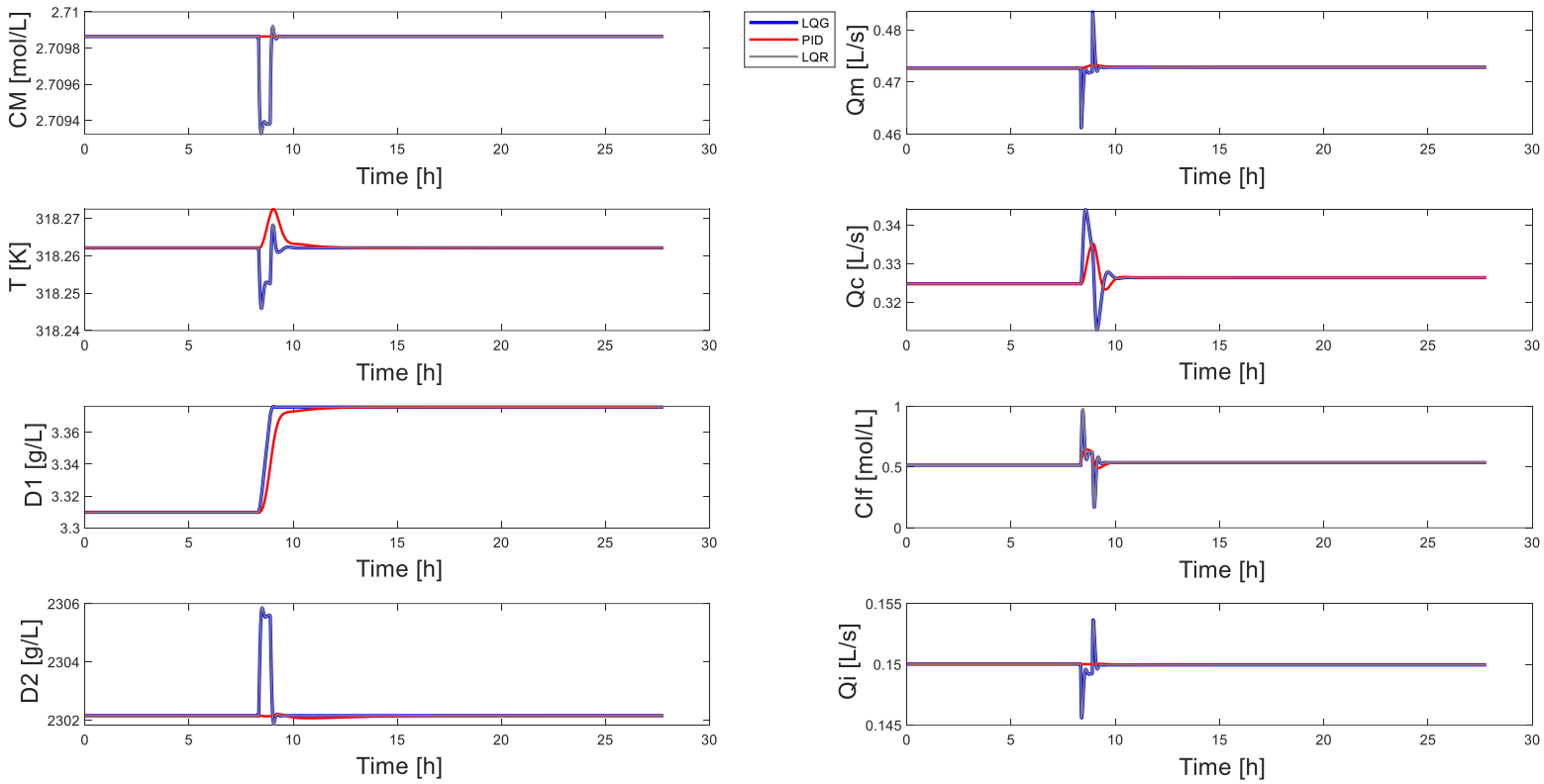

Figure 2-20: CSTR system Response for setpoint change for $\boldsymbol{D_1}$ (2% above original setpoint) without noise implementation.

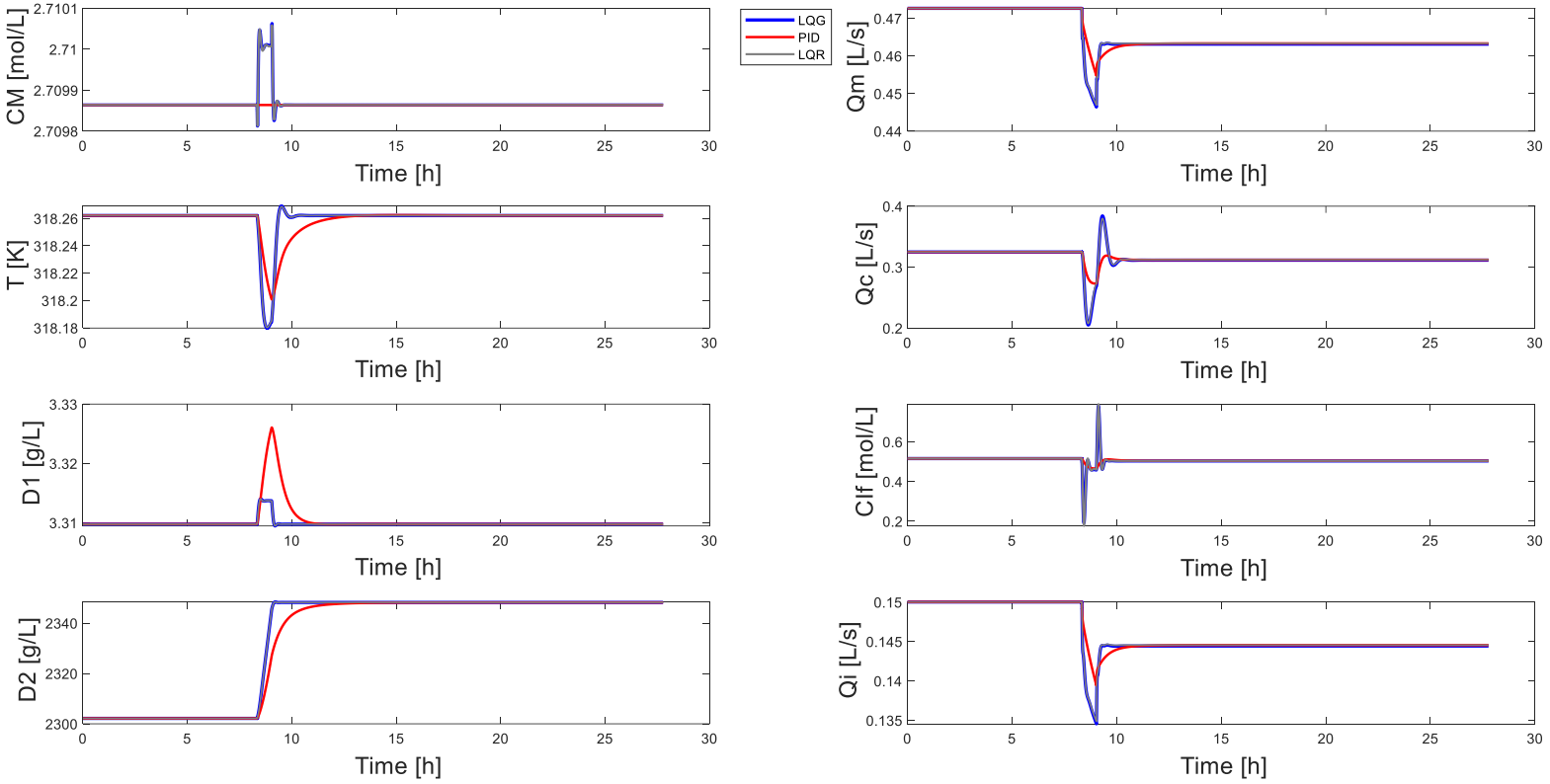

Figure 2-21: CSTR system Response for setpoint change for $\boldsymbol{D_2}$ (2% above original setpoint) with noise implementation.

Table 2-14: CSTR performace indexes for setpoint change of T.

Set point change	T (318.26-324.63 K)		
Controller	**PID**	**LQR**	**LQG**
Rise time C_M [h]	7.50	2.88	3.19
Rise time T [h]	9.14	3.22	3.15
Rise time D_1 [h]	10.66	3.50	2.83
Rise time D_2 [h]	13.43	2.12	3.23
Time to first peak C_M [h]	2.78	0.30	3.30
Time to first peak T [h]	9.14	3.44	3.27
Time to first peak D_1 [h]	2.47	2.78	3.34
Time to first peak D_2 [h]	3.15	0.41	3.34
Settling time C_M [h]	8.73	3.92	3.61
Settling time T [h]	9.14	3.58	3.81
Settling time D_1 [h]	10.66	4.18	3.90
Settling time D_2 [h]	13.43	4.09	3.74
Overshoot	1.49E-02	2.83E-03	8.66E-03

Table 2-15: CSTR performace indexes for setpoint change of D_1.

Set point change	D_1 (3.31-3.38 g/L)		
Controller	**PID**	**LQR**	**LQG**
Rise time C_M [h]	0.64	0.63	0.64
Rise time T [h]	4.87	0.62	0.62
Rise time D_1 [h]	4.38	0.68	0.68
Rise time D_2 [h]	0.67	0.68	0.68
Time to first peak C_M [h]	0.28	0.13	0.13
Time to first peak T [h]	0.72	0.15	0.14
Time to first peak D_1 [h]	4.38	0.74	0.73
Time to first peak D_2 [h]	2.44	0.18	0.18
Settling time C_M [h]	2.10	1.22	1.04
Settling time T [h]	4.87	2.07	1.51
Settling time D_1 [h]	4.38	1.01	1.01
Settling time D_2 [h]	10.24	1.24	1.08
Overshoot	-	8.17E-03	6.66E-03

Table 2-16: CSTR performace indexes for setpoint change of D_2.

Set point change	D_2 (2302.15-2348.20 g/L)		
Controller	**PID**	**LQR**	**LQG**
Rise time C_M [h]	0.69	0.04	0.04
Rise time T [h]	5.07	1.04	1.04
Rise time D_1 [h]	2.83	1.19	0.82
Rise time D_2 [h]	5.43	0.82	0.81
Time to first peak C_M [h]	0.00	0.72	0.72
Time to first peak T [h]	0.70	0.48	0.49
Time to first peak D_1 [h]	0.70	0.17	0.17
Time to first peak D_2 [h]	5.43	0.87	0.87
Settling time C_M [h]	1.37	1.34	1.28
Settling time T [h]	5.07	2.15	1.91
Settling time D_1 [h]	2.83	1.38	1.21
Settling time D_2 [h]	5.43	1.13	1.05
Overshoot	-	3.70E-03	5.66E-02

2.9. Appendix

The following section presents some important information to complement the information presented in the document, including more data about the model used, the tunning for the PID, derivation of PID and LQR controller.

A. Kinetics

The reaction mechanism is shown below.

- Initiation

$$I_n \xrightarrow{k_d} n\, R^* \tag{2.35}$$

$$R^* + M \xrightarrow{k_i} RM_1{}^* \tag{2.36}$$

- Propagation

$$M_i^* + M \xrightarrow{k_p} M_{i+1}^* \tag{2.37}$$

- Termination by combination

$$M_i^* + M_j^* \xrightarrow{k_{tc}} P_{i+j} \tag{2.38}$$

- Termination by disproportionation

$$M_i^* + M_j^* \xrightarrow{k_{td}} P_i + P_j \tag{2.39}$$

Deriving the kinetic from the mechanism for the Initiator, this reactive specie appears just in one reaction, leading to:

$$\frac{dC_I}{dt} = -2fk_dC_I \tag{2.40}$$

The intermediate in the reaction for initiation appears in 2 reactions, just like that:

$$\frac{dC_{R^*}}{dt} = 2fk_dC_I - k_iC_{R^*}C_M \tag{2.41}$$

The monomer appears in 2 reactions so the reaction will be:

$$\frac{dC_M}{dt} = k_iC_{R^*}C_M - k_pC_{M^*}C_M \tag{2.42}$$

The monomer intermediate profile is:

$$\frac{dC_{M^*}}{dt} = k_pC_{R^*}C_M - C_{M^*}^2k_t \tag{2.43}$$

Assuming a Pseudo Steady-State Hypothesis (PSSH) to suppress the intermediate reactive spicie in the reaction, is assumed the net velocity is very fast, so the differential of velocity is approximate cero, so Equation 2.41 is transformed to:

$$2fk_dC_I = k_iC_{R^*}C_M \tag{2.44}$$

Clearing remains:

$$C_{R^*} = \frac{2fk_dC_I}{k_iC_M} \tag{2.45}$$

If we do the same in Equation 2.43 leads:

$$k_pC_{R^*}C_M = C_{M^*}^2k_t \tag{2.46}$$

$$C_{M^*} = \left(\frac{k_iC_{R^*}C_M}{k_t}\right)^{1/2} \tag{2.47}$$

So the monomer intermediate concentration is:

$$C_{M^*} = \left(\frac{2fk_dC_I}{k_t}\right)^{1/2} = C_P \tag{2.48}$$

Furthermore, the Reaction rate constants present an Arrhenius behavior as shown:

$$k_j = A_j \exp\left(\frac{-E_j}{T}\right), \quad j = d, p, t \tag{2.49}$$

$$d: Initiator\ decompotition\ reaction$$

$$p: Propagation\ reaction$$

$$t: Termination\ reaction$$

Besides the termination reaction for the styrene occurs solely by combination, so the effects from disproportionation. As seen below:

$$k_t = k_{tc} \tag{2.50}$$

B. Mass balances

General mass balance:

$$In - Out = Accu - Gen \tag{2.51}$$

$$F_{Ao} - F_A = \frac{dN_A}{dt} - r_A V \tag{2.52}$$

For the 2 species entering the reactor (initiator and monomer):

$$\frac{dC_I}{dt} = \frac{F_{Io} - F_I}{V} + r_I \tag{2.53}$$

$$\frac{dC_M}{dt} = \frac{F_{Mo} - F_M}{V} + r_M \tag{2.54}$$

Replacing the molar flow for concentration:

$$\frac{dC_I}{dt} = \frac{Q_i C_{If} - Q_t C_I}{V} - k_d C_I \tag{2.55}$$

$$\frac{dC_M}{dt} = \frac{Q_m C_{Mf} - Q_t C_M}{V} - k_p C_M C_P \tag{2.56}$$

Where Q_t is the sum of all flows inning the reactor:

$$Q_t = Q_i + Q_s + Q_m \tag{2.57}$$

C. Energy balance

General energy balance Unsteady-State nonisothermal reactor:

$$\begin{aligned} &Rate\ of\ accumation\ of\ energy\ within\ the\ system \\ &= Rate\ of\ flow\ of\ heat\ to\ the\ system\ from\ the\ surroundings \\ &- Rate\ of\ work\ done\ by\ the\ system\ on\ the\ surroundings \\ &+ rate\ of\ energy\ added\ to\ the\ system\ by\ mass\ flow\ into\ the\ system \\ &+ rate\ of\ energy\ leaving\ the\ system\ by\ mass\ flow\ out\ of\ the\ system \end{aligned}$$

$$\frac{dE_{sist}}{dt} = \dot{Q} - \dot{W} + F_{in}E_{in} - F_{out}E_{out} \tag{2.58}$$

$$\frac{dE_{sist}}{dt} = \dot{Q} - \dot{W} + \sum_{i=1}^{n} F_i E_i|_{in} - \sum_{i=1}^{n} F_i E_i|_{out} \quad (2.59)$$

$$\dot{W} = \dot{W}_s - \sum_{i=1}^{n} F_i \tilde{V}_i P_s|_{in} + \sum_{i=1}^{n} F_i \tilde{V}_i P_s|_{out} \quad (2.60)$$

Replacing:

$$\frac{dE_{sist}}{dt} = \dot{Q} - \dot{W}_s + \sum_{i=1}^{n} F_i \tilde{V}_i P_s|_{in} - \sum_{i=1}^{n} F_i \tilde{V}_i P_s|_{out} \sum_{i=1}^{n} F_i E_i|_{in} - \sum_{i=1}^{n} F_i E_i|_{out} \quad (2.61)$$

$$\frac{dE_{sist}}{dt} = \dot{Q} - \dot{W}_s + \sum_{i=1}^{n} F_i (\tilde{V}_i P_s + E_i)|_{in} - \sum_{i=1}^{n} F_i \tilde{V}_i P_s + E_i)|_{out} \quad (2.62)$$

$$E_i = U_i + \frac{{u_i}^2}{2} + gZ_i + others \quad (2.63)$$

$$E_i = U_i + \frac{{u_i}^2}{2} + gZ_i + others \quad (2.64)$$

$$H_i = U_i + P_s \tilde{V}_i \quad (2.65)$$

$$H_i = E_i + P_s \tilde{V}_i \quad (2.66)$$

Replacing:

$$\frac{dE_{sist}}{dt} = \dot{Q} - \dot{W}_s + \sum_{i=1}^{n} F_i H_i|_{in} - \sum_{i=1}^{n} F_i H_i|_{out} \quad (2.67)$$

$$E_{sist} = \sum_{i=1}^{n} N_i E_i = \sum_{i=1}^{n} N_i U_i = \sum_{i=1}^{n} N_i H_i - P_s V \tag{2.68}$$

Derivating:

$$\frac{d}{dt}\left(\sum_{i=1}^{n} N_i H_i - P_s V\right) = \sum_{i=1}^{n} \frac{d}{dt}(N_i H_i) \tag{2.69}$$

$$\sum_{i=1}^{n} \left(\frac{dN_i}{dt} H_i + \frac{dH_i}{dt} N_i\right) \tag{2.70}$$

$$H_i = H_i° + \int_{Tr}^{T} Cp_i \, dT \tag{2.71}$$

Derivating:

$$\frac{dH_i}{dt} = Cp_i \frac{dT}{dt} \tag{2.72}$$

Replacing:

$$\dot{Q} - \dot{W}_s + \sum_{i=1}^{n} F_i H_i|_{in} - \sum_{i=1}^{n} F_i H_i|_{out} = \sum_{i=1}^{n} N_i \, Cp_i \frac{dT}{dt} + \sum_{i=1}^{n} H_i \frac{dN_i}{dt} \tag{2.73}$$

$$\frac{dN_i}{dt} = -\nu_i r_A V + F_{io} - F_i \tag{2.74}$$

$$\dot{Q} - \dot{W}_s + \sum_{i=1}^{n} F_{io} H_{io} - \sum_{i=1}^{n} F_i H_i = \sum_{i=1}^{n} N_i \, Cp_i \frac{dT}{dt} + \sum_{i=1}^{n} H_i(-\nu_i r_A V) + \sum_{i=1}^{n} H_i(F_{io} - F_i) \tag{2.75}$$

$$\dot{Q} - \dot{W}_s + \sum_{i=1}^{n} F_{io}(H_{io} - H_i) + \Delta H_{Rxn} r_A V = \sum_{i=1}^{n} N_i \, Cp_i \frac{dT}{dt} \tag{2.76}$$

$$\dot{Q} = \dot{Q}_{Elec} + \dot{Q}_{Cond} + \dot{Q}_{Conv} + \dot{Q}_{Rad} = \dot{Q}_{Conv} = UA(T_c - T) \tag{2.77}$$

Leading:

$$UA(T_c - T) - \dot{W}_s + \sum_{i=1}^{n} F_{io} Cp_i (T - T_{io}) + \Delta H_{Rxn} r_A V = \sum_{i=1}^{n} N_i \, Cp_i \frac{dT}{dt} \tag{2.78}$$

Reorganizing the last equation for the temperature in the reactor:

$$\frac{dT}{dt} = \frac{Q_t(T_f - T)}{V} + \frac{-\Delta H_r}{\rho C_p} k_p C_M C_P - \frac{hA}{\rho C_p V}(T - T_c) \tag{2.79}$$

For the temperature in the reactor jacket same reorganizing:

$$\frac{dT_c}{dt} = \frac{Q_c(T_{cf} - T_c)}{V_c} + \frac{hA}{\rho_c C_{pc} V_c}(T - T_c) \tag{2.80}$$

D. PID tuning

The internal model control (IMC) method is used for the tunning in the PID controller and using the Curve Fitting toolbox from Matlab® for parameters identification. The tuning is developed from the perspective of a good balance between set point tracking and disturbance rejection.

Now usually, the parameters identification makes a disturbance 10% above and under the value of the manipulated variable and analyzes the system response. For the current study case, the magnitude of the disturbance is done by a specter of disturbances, 10% above and under, 20% above, and 50% above and under the value of the manipulated variables, the summary of the identification parameters are listed in Table 2-17, Table 2-18, Table 2-19 and Table 2-20. The results of each disturbance for the current manipulated variable are compared by the value of the no linearized model (model using S-Function), the root-mean-square error (RMSE) is used for the comparison. As seen in Table 2-21 the RMSE lower is the best option, for all cases, the best value of RMSE for the 4 manipulated variables is the disturbance 10% above the original value (red values in the table).

Table 2-17: CSTR identification parameters from different disturbances of Q_m.

CONTROLLING C_M					
Q_m distrubance	**+10%**	**+20%**	**+50%**	**-10%**	**-50%**
System classification	First-order plus deadtime				
Set data	$k_f * Amplitude * \left(1 - e^{-\left(\frac{x-\theta}{\tau}\right)}\right) * Heaviside(x-\theta)$				
Amplitude	0.05	0.09	0.24	-0.05	-0.24
k_f	2.02	1.91	1.64	2.29	3.12
τ	3691.00	3487.00	2992.00	4182.00	5708.00
θ	2.94	2.83	2.35	2.97	1.22
Adjuted R^2	1.00	1.00	1.00	1.00	1.00

Table 2-18: CSTR identification parameters from different disturbances of Q_c.

CONTROLLING T					
Q_c distrubance	**+10%**	**+20%**	**+50%**	**-10%**	**-50%**
System classification	Second-order critically damped				
Set data	$k_f * Amplitude * \left(1 - \left(\left(\frac{x}{\tau} + 1\right) * e^{-\left(\frac{x-\theta}{\tau}\right)}\right)\right) * Heaviside(x)$				
Amplitude	0.03	0.06	0.16	-0.03	-0.16
k_f	-13.04	-12.22	-10.27	-15.08	-22.06
τ	4572.00	4353.00	3835.00	5113.00	6957.00
Adjuted R^2	0.99	0.99	0.99	0.99	0.99

Table 2-19: CSTR identification parameters from different disturbances of C_{If}.

CONTROLLING D_1					
C_{If} distrubance	**+10%**	**+20%**	**+50%**	**-10%**	**-50%**
System classification	Second-order critically damped				
Set data	$k_f * Amplitude * \left(1 - \left(\left(\frac{x}{\tau} + 1\right) * e^{-\left(\frac{x-\theta}{\tau}\right)}\right)\right) * Heaviside(x)$				
Amplitude	0.05	0.10	0.26	-0.05	-0.26
k_f	3.45	3.39	3.23	3.59	4.00
τ	4161.00	4151.00	4129.00	4189.00	4296.00
Adjuted R^2	1.00	0.99	0.99	1.00	1.00

Table 2-20: CSTR identification parameters from different disturbances of Q_i.

CONTROLLING D_2					
Q_i distrubance	**+10%**	**+20%**	**+50%**	**-10%**	**-50%**
System classification	First-order plus deadtime				
Set data	$k_f * Amplitude * \left(1 - e^{-\left(\frac{x-\theta}{\tau}\right)}\right) * Heaviside(x-\theta)$				
Amplitude	0.02	0.03	0.08	-0.02	-0.08
k_f	-7280.00	-7055.00	-6444.00	-7765.00	-8889.00
τ	5677.00	5565.00	5248.00	5911.00	6413.00
θ	660.60	633.70	560.70	719.00	855.30
Adjuted R^2	0.99	0.99	0.99	0.99	0.99

Table 2-21: RMSE between the linear and the no linear model, with different changes in setpoint inputs.

RMSE					
Distrubance	**+10%**	**+20%**	**+50%**	**-10%**	**-50%**
C_M	3.06E-05	4.60E-05	1.03E-04	3.36E-05	1.07E-04
T	3.53E-02	6.48E-02	1.28E-01	4.29E-02	3.61E-01
D_1	1.47E-02	2.89E-02	6.85E-02	1.54E-02	8.78E-02
D_2	0.90	1.71	3.66	1.01	6.35

With the identification parameters, the tunning is done. The IMC method is used according to Seborg and Edgar, (2003). Taking into account PID controller operates in parallel the transfer function equation is:

$$G_c(s) = K_c\left(1 + \frac{1}{\tau_I s} + \frac{\tau_D s}{\alpha\tau_D s + 1}\right) \tag{2.81}$$

Operating:

$$G_c(s) = \left(K_c + \frac{K_c}{\tau_I s} + \frac{K_c\tau_D s}{\alpha\tau_D s + 1}\right) \tag{2.82}$$

Factorize:

$$G_c(s) = \left(K_c + \frac{K_c}{\tau_I s} + \frac{\frac{K_c\tau_D s}{\alpha\tau_D s + 1}}{1 + \frac{1}{\alpha\tau_D s}}\right) \tag{2.83}$$

Where the Simulink® form for the PID parallel transfer function is:

$$G_c(s) = \left(P + \frac{I}{s} + D\frac{N}{1 + N\frac{1}{s}} \right) \tag{2.84}$$

Comparing Equation 2.83 and Equation 2.84 the expression for P, I, D, and N in terms of Equation 2.84 variables are:

$$P = K_c \tag{2.85}$$

$$I = \frac{K_c}{\tau_I} \tag{2.86}$$

$$D = K_c \tau_D \tag{2.87}$$

$$N = \frac{1}{\alpha\ \tau_D} \tag{2.88}$$

The value of the parameter α used here is 0.2, value obtained by trial and error (Seborg and Edgar, 2003). And the values for P, I, D, N are shown in Table 2-9.

E. LQR derivation

With a system defined as:

$$\dot{x} = Ax + Bu \tag{2.89}$$

$$\dot{y} = Cx \tag{2.90}$$

To control the system written in terms of the state feedback law.

$$u = -Kx \tag{2.91}$$

Using optimal control, minimizing the desired state and the effort of the input in the system, the objective function is set as follows.

$$J = \int_0^\infty (states - inputs)dt \tag{2.92}$$

The objective function is also set as:

$$J = \int_0^\infty (states^2 - inputs^2)dt \tag{2.93}$$

Now to determine the squared states is the vector multiplication of the states as follow:

$$x^2 = [x_1 \ x_2 \ \cdots \ x_n] \begin{bmatrix} x_1 \\ x_2 \\ \vdots \\ x_n \end{bmatrix} = x^T x \tag{2.94}$$

In the same way for the inputs:

$$u^2 = [u_1 \ u_2 \ \cdots \ u_n] \begin{bmatrix} u_1 \\ u_2 \\ \vdots \\ u_n \end{bmatrix} = u^T u \tag{2.95}$$

Now replacing the objective function leads:

$$J = \int_0^\infty (x^T Q x - u^T R u)dt \tag{2.96}$$

Appearing the variables Q and R weighting factors, where priories the reachability of the states or the effort in the inputs to achieve the proper control actions. Now the problem is determine the input signal which takes the system to the zero-state in an optimal manner, minimizing the deterministic objective given by Equation 2.93. Using Lagrange multipliers to solve the optimization problem:

$$H = x^T Q x + u^T R u + \lambda(Ax + Bu) \tag{2.97}$$

Derivating:

$$\frac{dH}{d\lambda} = H\lambda = Ax + Bx = \dot{x} \tag{2.98}$$

$$-\frac{dH}{dx} = -Hx = -Qx - A^T\lambda = \dot{\lambda} \tag{2.99}$$

$$\frac{dH}{du} = Hu = Ru + B^T\lambda = 0 \tag{2.100}$$

Leading the following system:

$$\dot{x} = Ax + Bu \tag{2.101}$$

$$\dot{\lambda} = -Qx - A^T\lambda \tag{2.102}$$

$$0 = Ru + B^T\lambda \tag{2.103}$$

Where Equation 2.101 is the estate equation, Equation 2.102 is the co-state equation, and Equation 2.103 is the stationary equation. Using Equation 2.103 clearing remains:

$$u = -R^{-1}B^T\lambda \tag{2.104}$$

With:

$$\lambda = Sx \tag{2.105}$$

Replacing in Equation 2.104:

$$u = (-R^{-1}B^TS)x \tag{2.106}$$

Using Equation 2.91 remains:

$$K = -R^{-1}B^TS \tag{2.107}$$

And replacing Equation 2.107 in Equation 2.101 lead:

$$\dot{x} = Ax + B(-R^{-1}B^TSx) \tag{2.108}$$

Replacing Equation 2.105 and Equation 2.108 in Equation 2.102 lead:

$$S\dot{x} = SAx - SBR^{-1}B^TSx = Qx - A^TSx \tag{2.109}$$

Rearranging:

$$SAx - SBR^{-1}B^TSx + Qx + A^TSx = 0 \tag{2.110}$$

$$(SA - SBR^{-1}B^TS + Q + A^TS)x = 0 \tag{2.111}$$

$$SA - SBR^{-1}B^TS + Q + A^TS = 0 \tag{2.112}$$

Where the value of S solves all the equations on the system leading to the value of K for the controller. This equation is also called the Riccati equation (Skogestad and Postlethwaite, 2001).

F. Kalman filter

The filter Kalman has two sections, prediction and correction (time update and measurement update). The prediction corresponds to external factors (noise) that could affect the value of the states in the system at a current time, the correction where the external factors affect the measure by the sensors in the system.

Now to predict and correct for a given system at an instant of time k is described as follows.

$$x(k+1) = Ax(k) + Bu(k) + Fv(k) \tag{2.114}$$

$$y(k) = Cx(k) + w(k) \tag{2.115}$$

Where v and w are Gaussian white noise, represented as a covariance matrix as follows:

$$R_w = E(w(k)w(k)^T) \tag{2.116}$$

$$R_v = E(v(k)v(k)^T) \tag{2.117}$$

Where R_w is the covariance matrix for measurement noise w and R_v the covariance matrix for process disturbance v. The actual goal is to minimize the mean square error, also called the error covariance matrix at time k, described by the next equation:

$$P(k) = E(e(k)e(k)^T) = E((x(k) - \hat{x}(k))(x(k) - \hat{x}(k))^T) \tag{2.118}$$

The discrete linear dynamic estimator is used to find an estimate $\hat{x}(k)$, that minimizes the mean square error thus:

$$\hat{x}(k+1) = A\hat{x}(k) + Bu(k) + L(k)(y(k) - C\hat{x}(k)) \tag{2.119}$$

The optimal gain that minimizes the mean squared error was derived by Kalman at the 60', leading:

$$L(k) = P(k-1)C^T(CP(k-1)C^T + R_w)^{-1} \tag{2.120}$$

3. Optimal design and control in a styrene polymerization in continuous plug flow reactor

3.1. Abstract

This chapter studies the control and optimization for continuous bulk polymerization by free radical for polystyrene production developed in a plug flow reactor (PFR), as a way to improve the results obtained in the CSTR. Using two objectives function in a Pareto front, the operational cost for the production and the productivity, the optimization defines the operating point in values of volume, initiator concentration in the feed, and monomer concentration in the feed. Then applying the operation point the automatic control is implemented, using three control structures, proportional-integral-derivative control (PID), linear-quadratic-regulator control (LQR), and linear-quadratic-Gaussian control (LQG). The optimal design results show how the two objective functions lead to a balanced optimal operation point, in terms of lower cost and high productivity. Besides, results indicate the three control structures can control the system with changes in set-points and disturbance rejection. Nevertheless, the use of advanced control (LQR and LQG) shows an improvement of the closed loop response, exhibiting dynamics 3 times faster than the conventional controller (*i.e.*, PID). The LQG controller is chosen as the best controller over LQR due to employing of the Kalman filter can achieve state estimation from measured states to unmeasured states. Also, the use of the first moment of molecular weight as a controlled variable is novel in continuous bulk polymerization by free radical for polystyrene, due to no information was not found in the literature.

3.2. Introduction

Polymers are materials characterized by being formed by macromolecules, which means molecules of high molecular weight constituted by smaller molecular units (monomer) reaching molecular weights between 1000-1000000 g/mol. Due to their high molecular weights, polymers are highly commercial, bearing applications in

the automobile, energy, textile, electrical, and food industry (Koltzenburg, Maskos and Nuyken, 2017).

Polymerization reactions are far from simple in their physical characteristics and unusual chemical steps compared to small molecular reactions, in addition, to the use of different techniques and methods to produce a polymer (Xu et al., 2017). Polymers are very sensitive to changes and disturbances in the system, making them prone to generating off-specification products. Interestingly, analyzing the studies carried out for polymers off-specification, polystyrene always appears as the polymer used in plenty of research. The common research employed technique and method to produce polystyrene is bulk polymerization by free radical, where the most used reactors to carry out the reaction are continuous stirred tank reactors (CSTR) and tubular reactors (PFR) (Chen, 1994). Both of them present advantages and disadvantages, however, due to operational problems with productivity in the systems, a battery of CSTR must be set to solve the problem. Alternatively, it has been shown that a PFR can produce the same or higher productivity than the CSTR battery, improving operational costs in the plant (Flores-Tlacuahuac and Grossmann, 2010). Even so, PFR dynamic simulations are more complex due to the nature mass and energy balances for this kind of reactor, making challenging the implementation of mathematical models as PDE's.

Seeing the polymerization processes are systems that present uncertainty and disturbances, carrying problems such as a decrease in the process performance, increase energy consumption, and an increased amount of off-specification product. Specifically, the last one is a current problem in the literature due to the big environmental problem caused by these off-specification products. Emphasizes the importance to apply automatic control, to reduce costs, operation time, energy, environmental impact, quantity off-specification amount in the process, and increase performance in the process, among others.

Mainly in PFR reactors, regulatory control strategy used is, to set the temperature in the system, manipulating cooling or heat flows in the jackets of the reactor (Gharaghani, Abedini and Parvazinia, 2012; Padideh, Mohammad and Hossein, 2013). This is noticeable by the fact problems with the heat transfer across the tube, so controlling temperature implies an important role in this kind of operation (Wallis, Ritter and Andre, 1975). No information was found about the use of the moments of molecular weight in the system as a controlled variable. As was expected often controllers used are PI and PID, which are the basics controllers, but not less effective to control the system. This is a great opportunity to implement complex controllers to compare the response with traditional control structures.

In the current work, optimal process design and control development of a free radical polymerization of styrene in a PFR is investigated through the implementation of multiobjective optimization and advanced automatic control strategies. For that purpose, a model-based approach is used to investigate potential operation improvements. The optimal design employs global optimization, based on genetic algorithm (GA) nonetheless the optimization finds the best trade-off of multiple objective functions in the Pareto front. Regarding the control, three control strategies are used, Proportional-integral-derivative control (PID), Linear-quadratic-Regulator control (LQR), and Linear-quadratic-Gaussian control (LQG). Analyzing diverse performance indexes (settling time, rise time, time to first peak, overshoot) of each strategy for responses of each setpoint tracking and disturbance rejection for the other outputs in the system.

3.3. Methodology

Considering that the current study case is an analogy from the first study case (taking the model presented in Chapter 2, changing the reactor employed). Most of the methodology section is the same as the first study case, with at least the same process. The present section describes the changes done for the implementation of a PFR reactor and which section is used the same methodology as Chapter 2. The methodology summary is shown in Figure 2-1. In this case, the same steps are followed to achieve the results.

3.3.1. Literature review

As seen in previous sections of the thesis, the literature review information obtained is condensed in Chapter 1 Literature review along with Table 1-3. It was concluded that the best system to use in the implementation of automatic control is the bulk polymerization by free radical of polystyrene. This reacting system is still highly studied and can be considered as a benchmark for control since the kinetic parameters are easily found in the literature. It decided to use the same parameter values presented by Alvarez and Odloak, (2012) and employ the mass balances for a PFR reactor presented by Flores-Tlacuahuac and Grossmann, (2010). Notice that further model details increase the complexity of the numerical implementation, which can generate even further numerical problems than the evidenced in the last Chapter. Therefore, a relatively simple reactor implementation is considered sufficient to demonstrate the benefit of optimal design and advanced control implementation.

3.3.2. Model development

The reactor model used is based on Padideh, Mohammad and Hossein, (2013). Where it is proposed a tubular reactor for thermal bulk post-polymerization of styrene. Where is assumed that static mixers are installed inside the reactor and plug flow patterns in the reactor. The balances in the reactor are presented as follows:

$$\rho \frac{\partial \omega_m}{\partial t} = -\rho V_z \frac{\partial \omega_m}{\partial z} - R_p \tag{3.1}$$

$$c_p \rho \frac{\partial T_1}{\partial t} = -c_p V_z \frac{\partial T_1}{\partial z} - R_p \Delta H + \frac{Q}{\pi R^2} \tag{3.2}$$

$$Q = h_i \left(2\pi R_1 L_j\right)(T_w - T_1) = U_o (2\pi R_o L_j)(T_j - T) \tag{3.3}$$

$$V_j c_{p,j} \rho_j \frac{dT_j}{dt} = F_j c_{p,j} \left(T_{j,in} - T_j\right) - Q \tag{3.4}$$

From the reactor presented by Padideh, Mohammad and Hossein, (2013), some considerations were taken for the final system used in this thesis. Further considerations used herein are:

I. Then, it is decided to propose an isothermal system due to this type of reactor presents a high dimensionality and highly nonlinear behavior. *e.g.* systems that present reactions with terms of multiple steady states and oscillatory behavior, the size of the increase in the Taylor approximation in the use of numerical methods, among others. (Chapra and Canale, 2007; Flores-Tlacuahuac and Grossmann, 2010). Motivation is to avoid numerical issues in the implementation of the advanced controllers based on the experience of the previous case study.
II. The reactor work in isothermal operation, assuming a huge amount of cooling fluid to preserve the same temperature inlet the reactor. Therefore the temperature is assumed as constant.
III. The reactor is set by an area/length ratio of 0.1, trying to conserve the same properties provided by Hidalgo and Brosilow, (1990).

IV. Due to the mass balances are partial differential equations (PDE), the finite difference method (FDM) of first order is used to solve the problem through the method of lines, more information in Appendix H (Chapra and Canale, 2007).
V. The cost function for the current study case (PFR) is modified in such a way the cost function is the same in the CSTR study case, more information is in the Optimal operation point section below.
VI. The model is assuming that the concentration variation is just axial and no diffusion along the axial spatial coordinate.
VII. The model uses the same kinetic present by Hidalgo and Brosilow, (1990), the same kinetic used in Chapter 2.
VIII. Negligible gel effect in the reaction.
IX. To simplify the numerical implementation and troubleshooting, the model is taken as one PFR with the representative size of a three PFR battery. Figure 3-1 is the diagram of the final model.

The model consists of 5 partial differential equations (PDEs) where 2 are mass balance, 3 for the moments of molecular weight distribution, and two functions are set for the process cost and the productivity. To solve the PDEs, the FDM in the method of lines is used. 50 nodes are employed, then the PDEs are transformed into 250 ODEs. Around that model, two objective functions are proposed to calculate for the process operating cost and productivity. The system of ODE's is solved using a nonstiff method explicit Runge-Kutta (2,3) pair of Bogacki and Shampine ODE's in Matlab® (ode23).

a) Continuous bulk polymerization by free radical model

The reaction model is the same used in Chapter 2, including the reaction mechanism, and the consideration for the kinetic model. Now developing the general mass balance for any specie in a reactor (Fogler, 2006):

$$In - Out = Accu - Gen \tag{3.5}$$

$$F_A|_V - F_A|_{V+\Delta V} = \frac{dN_A}{dt} - r_A \Delta V \tag{3.6}$$

Leading the general mass balance for a PFR reactor as follow.

$$-\frac{\partial F_A}{\partial V} + (r_A) = \frac{\partial C_A}{\partial t} \tag{3.7}$$

The summary of the mass balances applied to each component is shown in Appendix G. More specifically the final mass balances used in the system are the balances for monomer and initiator, present below:

$$-\nu\frac{\partial C_I}{\partial Z}+(r_I)=\frac{\partial C_I}{\partial t} \tag{3.8}$$

$$-\nu\frac{\partial C_M}{\partial Z}+(r_M)=\frac{\partial C_M}{\partial t} \tag{3.9}$$

According to the model proposed by Padideh, Mohammad and Hossein, (2013), the moments of the molecular weight can obtained based on the information of the system of Chapter 2 (based on Alvarez and Odloak, (2012)). The equations to determine the moments of molecular weight are shown below.

$$\frac{\partial D_0}{\partial t}=\left(0.5*k_t*{C_P}^2\right)-\nu\frac{\partial D_0}{\partial x} \tag{3.10}$$

$$\frac{\partial D_1}{\partial t}=\left(M_m*k_p*C_P*C_M\right)-\nu\frac{\partial D_1}{\partial x} \tag{3.11}$$

$$\frac{\partial D_2}{\partial t}=\left(5*M_m*k_p*C_P*C_M\right)+\left(\frac{5*M_m*{k_p}^2*{C_M}^2}{k_t}\right)-\nu\frac{\partial D_2}{\partial x} \tag{3.12}$$

The calculation of mass average molecular weight in the reactor, intrinsic viscosity, the polydispersity index and the conversion are calculated in the same way in the last chapter (represented by Equation 2.17, Equation 2.18 and Equation 2.19 correspondingly). The parameters used in the simulation are listed in Table 3-1.

Table 3-1: Process parameters for the PFR reactor.

Variable	Symbol	Value	Units
Frequency factor for initiator decomposition	E_d	14897	[K]
Activation energy for initiator decomposition	A_d	5.95E+13	[1/s]
Frequency factor for propagation reaction	E_p	3557	[K]
Activation energy for propagation reaction	A_p	1.06E+07	[L/mol*s]
Frequency factor for termination reaction	E_t	843	[K]
Activation energy for termination reaction	A_t	1.25E+09	[L/mol*s]
Temperature of the reactor feed	T	330	[K]
Initiator efficiency for AIBN	f	0.60	--
Flow rate of initiator	Q_i	0.03	[L/s]
Flow rate of solvent	Q_s	0.13	[L/s]
Flow rate of monomer	Q_m	0.13	[L/s]
Molecular weight of monomer	M_m	104.14	[g/mol]

3.3.3. Determination of optimal design

To get the optimal operation point is used the same methodology in the CSTR study case, the function “gamultiobj” is used, with some changes in the constraints of conversion and mass average molecular weight. The changes are discussed in the following section.

b) Cost and productivity optimization

The economic evaluation is based on the economic evaluation used in Chapter 2, using an analogy from the core polymerization model. As well as the cost function of the CSTR study case, the cost function for the PFR study case must be fair for comparison. So, the same structure of the cost function is used for both reactors, hence the cost function itself is modified. To achieve that goal a ratio is calculated as follows:

$$Capital\ Cost\ CSTR\ [\$] = 176400 * {D_r}^{1.066} * L^{0.802} \quad (3.13)$$

$$Capital\ Cost\ PFR\ [\$] = 35000 * {D_r}^{1.066} * L^{0.802} \quad (3.14)$$

Both cost functions were taken from Luyben, (2007), and they are employed since here is presented a capital cost for both cases (CSTR and PFR). The difference between the expressions is the coefficient that multiplies the dependent variables, in this case, the diameter and the length of the reactor. Also proving the cost values of the CSTR reactors are higher than the PFR reactors in comparison. Then a ratio is calculated as follows:

$$Relation\ cost\ CSTR/PFR = \frac{176400}{35000} = 5.04 \quad (3.15)$$

The relation is used to calculate the change of a cost function with the same structure as the CSTR study case (based on Asteasuain *et al*, (2006)) for the PFR study case as follows:

$$Cost\ CSTR = 343.16 * V^{0.529} \quad (3.16)$$

$$Cost\ PFR = \frac{343.16}{5.04} * V^{0.529} = 69.09 * V^{0.529} \quad (3.17)$$

So, the final cost function used in the optimization is shown below.

$$CO = 69.09\ (3\,V)^{0.529} + t_R\left(0.5\left(0.011 * C_{If}\right) + 2 * 10^{-3}\ Q_M C_{Mf} M_m\right) \quad (3.18)$$

Productivity remains the same way, represented by Equation 2.26. The objective functions are the operational cost and the productivity at the steady-state (Equation 3.18 and Equation 2.26). For the PFR case study, there are 2 constraints: a) for the reactor conversion and b) for the mass average molecular weight in the final product, as shown in Table 3-2.

Table 3-2: PFR conversion and mass average molecular weight constraints for the optimization.

Optimization constraints	
0.5<X<0.7	70000 g/mol <M_w<80000 g/mol

Due to the low conversions obtained in PFR reactors as principal reactor systems due to rheological problems (Wallis, Ritter and Andre, 1975; Chen, 1994). It is decided not to take these effects into account in the system. To have a better understanding of how the reactor behaves without this type of restriction, so high conversion could be attained. Regarding the molecular weight constraint, it is used the same range between 70000 g/mol and 80000 g/mol as was exposed in the CSTR case, target for industrial polystyrene and near as found in the literature.

The optimization outputs are the initiator concentration in the feed, monomer concentration in the feed, and the reactor volume (*i.e.* C_{If}, C_{mf}, V). The optimal search zone was restricted, choosing values resembling values of Alvarez and Odloak, (2012). Also, the first derivate criterium is used to achieve the Utopia point in the Pareto (Alcocer García, 2018). As in Chapter 2, the first derivate criterium is used in a normal way, where the derivate did not reach the value of cero, so the optimal point is selected by a zone that represents low variation values for the differentiated function.

3.3.4. Control structure design

As early discuss many of the sections from the control structure design are the same as presented in Figure 2-3, almost all section has few changes compared with the same sections in the previous Chapter.

c) Control objectives

- The main objective is focused on controlling the quality of the products, keeping the conversion and the mass average molecular weight in the process

- Reduce the off-specification amount in the process.

d) Mathematical model

The mathematical model is already shown in the Model development section.

e) Model análisis

The command “linmod” in Matlab® is also used to linearize the system. The changes implemented for the current Chapter are listed below.

- **Stability**

The stability is determined by the eigenvalues of the matrix A obtained by linearizing the system to a state space representation.

- **Controllability**

Due to the spare system of equation, the controllability is calculated employing a staircase form for the controllability matrix (Also known as Kalman decomposition). Where the system can be decomposed into a standard form helping to clear the controllable components in the system.

- **Observability**

Analogously to the controllability, the staircase form is employed to calculate the observability matrix.

- **Pairing variables**

As a clarification, the system presented 250 outputs, 50 ODEs for each state in the system when the first ODE corresponds to the first node and the fiftieth is the last node of the state. However, when the control is applied the main importance is focused on the final response in the system, so the control loop is used directly in the last node.

So as the main objectives are linked to the conversion and mass average molecular weight, these are transformations of the states as seen in Equation 2.17 and Equation 2.20. Thus are directly related to the monomer concentration, the first and second moment of the molecular weight.

In order to use the variables optimized, the pairing variables employed are the initiator concentration in the feed and the monomer concentration in the feed (C_{If}, C_{Mf}) and the controlled variables set the monomer concentration and the first moment of the molecular weight (C_M, D_1). The values within the RGA matrix indicate that the manipulated variable with the value nearest to 1 is the best option to execute the control action in the desired variable. Figure 3-1 represents the manipulated and controlled variables in the system.

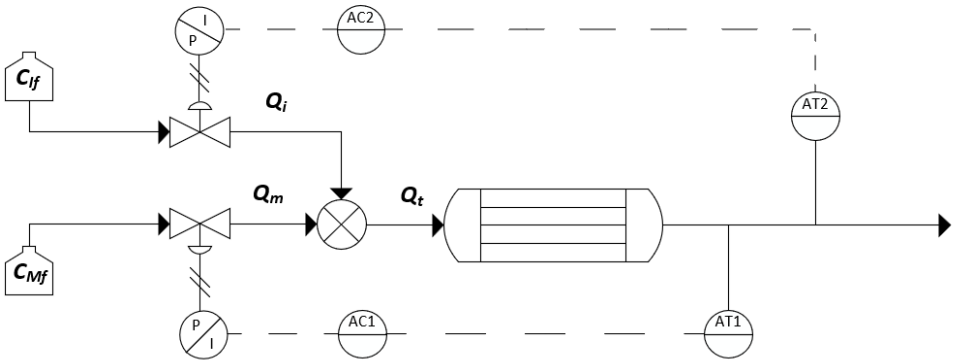

Figure 3-1: P&ID of the controlled PFR, instrumentation for the monomer concentration and the first moment of the molecular weight.

- ## Controllers

Taking into account that the controllers are the same that in the previous study case (PID, LQR, and LQG) and also are implemented in the same software (Simulink®), the following section is focused on the tunning of every controller and the explanation of each controller in the Control structure design section in the last Chapter. Also, the controller's performance is evaluated using different key performance indexes: the settling time ($\boldsymbol{t_s}$), rise time ($\boldsymbol{t_r}$), time to first peak ($\boldsymbol{t_p}$) and overshoots ($\boldsymbol{O_s}$) (Seborg and Edgar, 2003).

- ## Proportional-integral-derivative control (PID)

For the PID controller tuning, the inhouse PID tuning tool from the block in Simulink® is used (PID Tuner App). In the app, the designer manually adjusts design criteria in two design modes. Tuning the PID gains to achieve a good balance between the performance and robustness of the PID controller response. The algorithm chooses a crossover frequency (loop bandwidth) based on the plant dynamics, and designs for a target phase margin of 60°. When you interactively change the response time, bandwidth, transient response, or phase margin using the PID Tuner interface, the algorithm computes new PID gains (The MathWorks Inc., 2013).

- ## Linear-quadratic-regulator control (LQR)

As was discussed by the thesis the tunning of LQR controller the matrix $\boldsymbol{Q}$ and $\boldsymbol{R}$ must be changed manually to achieve the desired result. For the PFR study case is used the normalization of the states and inputs in the system (Equation 2.41 and Equation 2.42) at least for the $\boldsymbol{Q}$ matrix, the $\boldsymbol{R}$ matrix was tunned by iteration changing the values of the diagonal matrix manually.

- **Linear-quadratic-Gaussian control (LQG)**

  The LQR is usually seen as the previous step to design the LQG controller. Thus the same methodology for the LQR tuning is applied to tune the LQG controller (using normalization for the matrix $\boldsymbol{Q}$ and iteration tuning for the matrix $\boldsymbol{R}$).

3.4. Results

Section 3.4.1 shows the solution of the reactor optimal design and a discussion of the results obtained for the PFR study case and the literature. Section 3.4.2 shows the model analysis and control structure design, with the tunning for the three control structures. Section 3.4.3 shows the results obtained by the control structures, ending with a discussion of the results obtained and the literature.

3.4.1. Optimal process design

From the results of the optimization, a Pareto front is obtained representing the antagonistic behavior of the objective functions as shown in Figure 3-2. Abscissa coordinate is productivity in the process and the ordinate coordinate is the inverse of the operational cost.

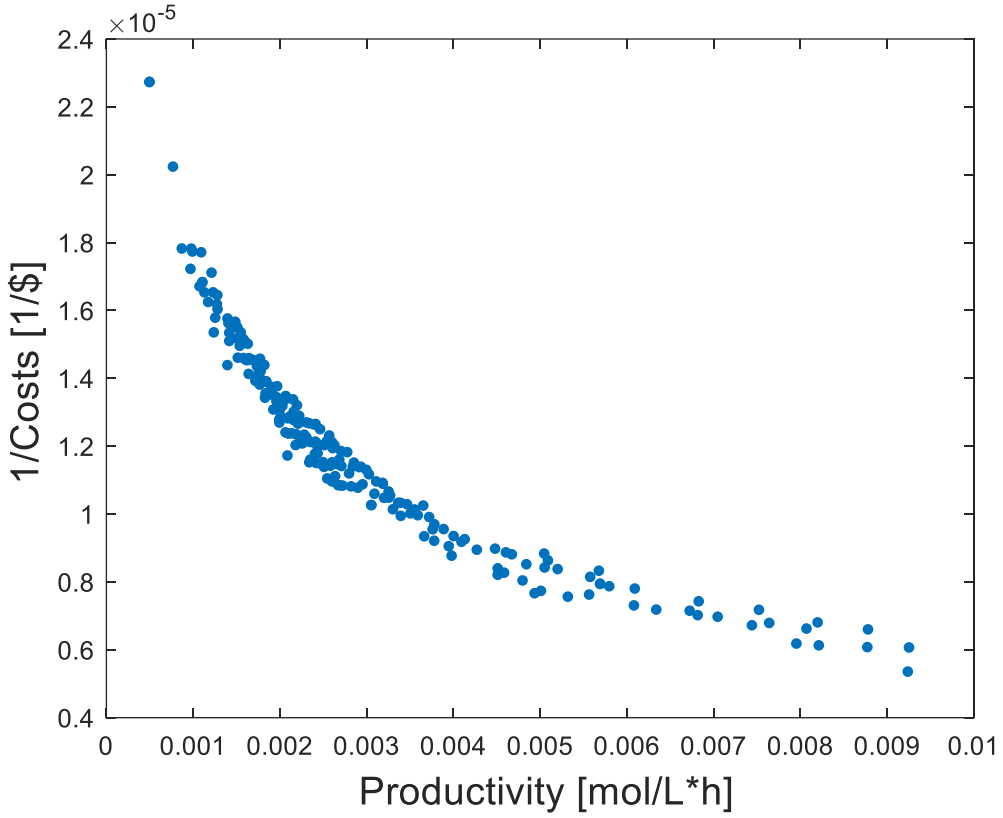

Figure 3-2: Pareto front with antagonist behavior, $Cost^{-1}$ vs productivity.

The Utopia point is found implementing the first derivative criteria, where the function represented by the data obtained in the optimization is numerically differentiated and plotted. Figure 3-3 represents the obtained function.

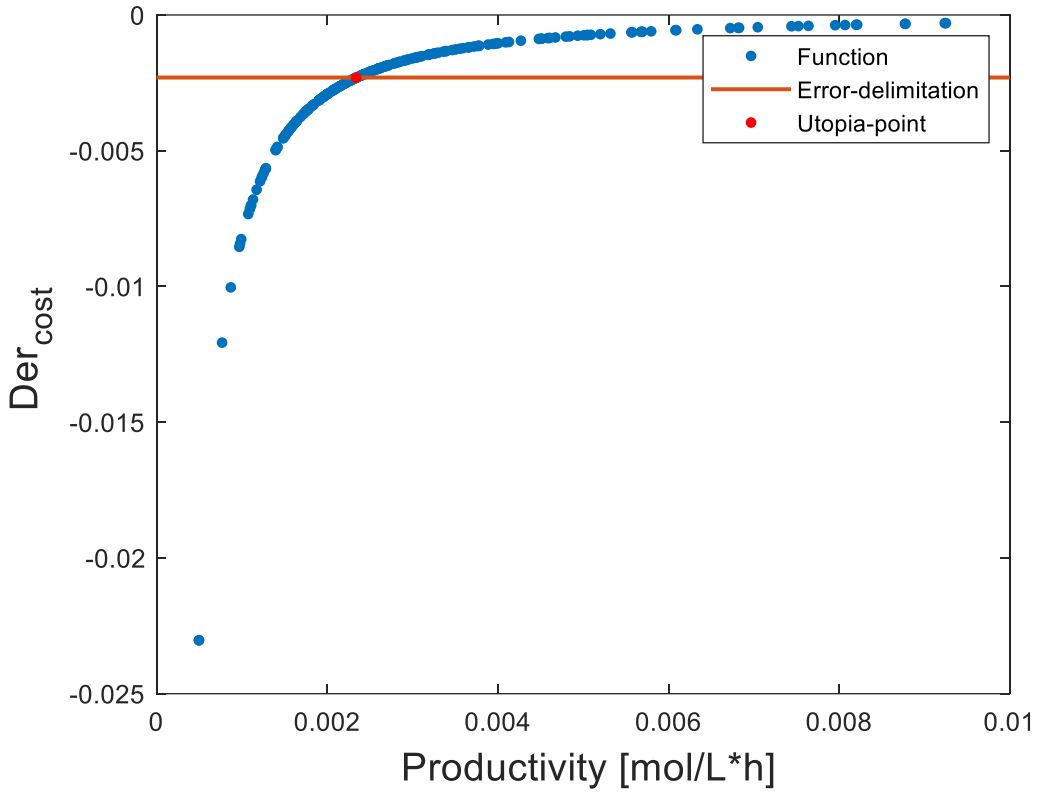

Figure 3-3: First derivate criterium graphic for the PFR system, $cost^{-1}$ differentiated vs productivity. Delimitation error is the band of 10% of the change in the differentiated function.

Now the orange line in Figure 3-3 is the band of 10% of the change in the derivative of the function. Then, the Utopia point is represented by the red point whose coordinates are 2.34E-03 mol/L*h of productivity and -2.31E-03 L*h/mol*USD of $cost^{-1}$ differentiated (corresponding to operational cost values of 86171.80 USD/year and productivity values of 0.0024 mol/L*h). Table 3-3 represents the values of operation variables in the process corresponding to the selected Utopia point. Now with these values, the operation point is set for the implementation and evaluation of control structure.

Comparing results with the previous study case in Chapter 2, operational cost is reduced for the PFR study case, reaching values 6 times lower than the cost obtained in the CSTR study case. In the same way, results for productivity in the PFR reactor reach values almost 40 times bigger compared with the CSTR reactor. This could be explained by the change in the conversion constraint for the optimization, achieving high values of conversion thus productivity high values are obtained. The biggest change is the isothermal restriction, because the omission of the cooling flow presented in the economic objective function.

The parameters obtained in the optimization for the PFR are also compared with respect to the CSTR, where it is observed that very similar values are obtained for both cases. If the value of the volume of one single PFR (3156.73) is compared with that of Alvarez and Odloak, (2012) (3000L), there is only of 5.2% difference. However the real comparison must be with a 3 times larger reactor, obtaining differences of 215% with the full reactor large. Comparing values of the concentrations in the food of the PFR (0.77 L/mol of initiator and 17.75 L/mol of monomer) with Alvarez and Odloak, (2012) (0.588 L/mol of initiator and 8.681 L/mol of monomer). A difference of 31% is obtained for the initiator and 93% for the monomer. However, it must be taken into account that it has almost the same order of magnitude for both cases. This change can be explained by the size of the proposed reactor which it is almost 3 times larger, due to the objective functions in the optimization are the operational cost and the productivity but not the reactor volume.

Table 3-3: Optimal parameter for the PFR reactor.

Variable	Symbol	Value	Units
Reactor volume	V	3156.73	[L]
Total rector volume	V_T	9470.19	[L]
Concentration of initiator in feed	C_{If}	0.77	[mol/L]
Concentration of monomer in feed	C_{Mf}	16.75	[mol/L]
Operational cost with optimal point	CO	86171.80	[$]
Productivity at the steady-state	PR_{ss}	0.0024	[mol/L*h]
Polydispersity index	PDI	1.61	--
Mass average molecular weight	M_w	70869.58	[g/mol]
Reactor conversion	X	0.61	--

The number of design variables used here are 3, meanwhile, the highest in literature is 4 (Temperatures in the jacket for each reactor, with a total of 1 CSTR and 3 PFR in series) (Gharaghani, Abedini and Parvazinia, 2012). However, the present thesis is focused on optimizing variables directly related to the mass balances in the polymerization process employing a different approach from the literature. Although some of the optimized variables here were already used in CSTR reactors, as has been the case of Asteasuain *et al*, (2006), analyzed in the previous Chapter.

Computational effort for the optimization in literature is between 0.92 h to 12.08 h, while herein takes a time between 0.12 h to 0.36 h (Flores-Tlacuahuac and Grossmann, 2010; Gharaghani, Abedini and Parvazinia, 2012). In Flores-

Tlacuahuac and Grossmann, 2010, the equipment used is a 2GHz 4GB computer. While herein the equipment used are Intel core i7-8750H 2.2 GHz 16384MB RAM and Intel core i7-7700 3.6GHz 8MB RAM. The large differences are mainly due to the model complexity (i.e., assumptions and reaction mechanism which lead to more complex PDE's), in some cases, the polymer used is different from polystyrene, modifying key parameters in reactors like kinetic in the system. Note that the dimensions of the reactor are also different, but it must be taken into account that this model does not represent a reaction of polystyrene by free radicals (Flores-Tlacuahuac and Grossmann, 2010).

Conversion values found in literature are between 0.33-0.9 are very similar to the values found herein laying between 0.5-0.7 (Wallis, Ritter and Andre, 1975; Gharaghani, Abedini and Parvazinia, 2012). Obtaining differences between 32%-76.47%. This could be explained by taking into account that the gel effect was omitted for conversions greater than 0.35 and also by the fact that the energy balances were omitted.

The mass average molecular weights in the literature, are set values between 50000-300000 g/mol, whereas in the present work are set at 70000-80000 g/mol. (Wallis, Ritter and Andre, 1975; Flores-Tlacuahuac and Grossmann, 2010; Gharaghani, Abedini and Parvazinia, 2012). These changes depend on the source consulted since each author can propose different ranges of molecular weights for optimization.

The optimal point obtained reached herein is 2.34E-03 mol/L*h of productivity and -2.31E-03 L*h/mol*USD of cost^{-1} differentiated. Representing the best balance in terms of the highest productivity and the lowest operational cost compared with the other points obtained in the optimization. Besides the fulfillment of the constraints proposed, with conversion values of 0.61 and molecular weight values of 70869.58 g/mol.

3.4.2. Control structure design

The following sections shows the verification of the stability of the system, controllability, and observability. Besides present the structure and tunning results for the PID, LQR, and LQG correspondingly.

f) Model analysis

The stability in the system is verified with the values of eigenvalues in the system, due to the Large number of states in the system (~250) full results are not show here. Nevertheless, the values were verified and all eigenvalues

present a real part negative, meaning that the optimal point is stable. Regarding controllability and observability are verified by the rank of both matrices must be the same rank of matrix A shown in Table 3-4.

Table 3-4: Eigenvalues of matrix A, from the state space representation, system poles.

$\mathbf{Rank_{controlability}}$	$\mathbf{Rank_{observabilty}}$	$\mathbf{Rank_{A}}$
250	250	250

Indicating full rank, thus the stability, controllability, and observability, of the current system are verified, and now the control structure design is performed.

g) PID control

The results for the variables pairing are listed in Table 3-5.

Table 3-5: RGA methodology results for the PFR study case.

	C_{If}	C_{Mf}
C_M	-6.15	7.15
D_1	7.15	-6.15

- The appropriate pairing for SISO controllers is “to manipulate” the monomer concentration in the feed to control the monomer concentration and to manipulate the initiator concentration in the feed to control the first moment of the molecular distribution, (red values).

The parameters for the automated PID tunning are shown in Table 3-6.

Table 3-6: PFR tuning parameters for the PID controller.

	P	I	D	N
C_M **controller**	0.56	1.34E-05	-39615.06	1.16E-05
D_1 **controller**	1.82E-03	1.30E-08	-10.99	3.93E-05

The final implementation of PID control in Simulink® is shown in Figure 3-4. There is a numerical problem the solution of the ODE's the S-function in Matlab®, producing and spreading noise in the responses in the system (henceforth called integration noise). In an attempt to mitigate the integration noise, low-pass filter is implemented prior the PID and LQR controllers. On the other hand, the implementation of low-pass filter in LQG is redundant due to the presence of the Kalman filter.

The controllers have the implementation of white noise in the inputs, and some of the outputs emulating noisy signals in the sensors (henceforth called measurements noise). Besides, a sub-system is employed to the conversion and the mass average molecular weight (for controller PID and LQR), where the transformation with the corresponding states is done. Also, the use of "goto" block to represent the feedback in the control loops in Simulink®.

A way to show the impact of the integration noise presented in the response, Table 3-7 contains the standard deviation for the closed loop signal with no perturbation to quantify the amount of the noise in the signal belonging to integration noise and measurements noise. Preliminary results shows, without the implantation of measurements noise, that the response always carries a quantity of noise (integration noise). This means that there is always a significant noise in the system's responses by default.

Table 3-7: Standard deviation for the closed loop signal with no perturbation and no use of filters.

	DEVIATION STANDARD	
	C_M Response	**D_1 Response**
PID system without measurements noise	1.58E-04	1.60E-02
PID system with measurements noise	4.85E-04	6.18E-02
LQR system without measurements noise	1.01E-03	1.05E-01
LQR system with measurements noise	2.26E-06	1.09E-03
LQG system without measurements noise	1.27E-04	7.20E-03
LQG system with measurements noise	4.86E-03	4.97

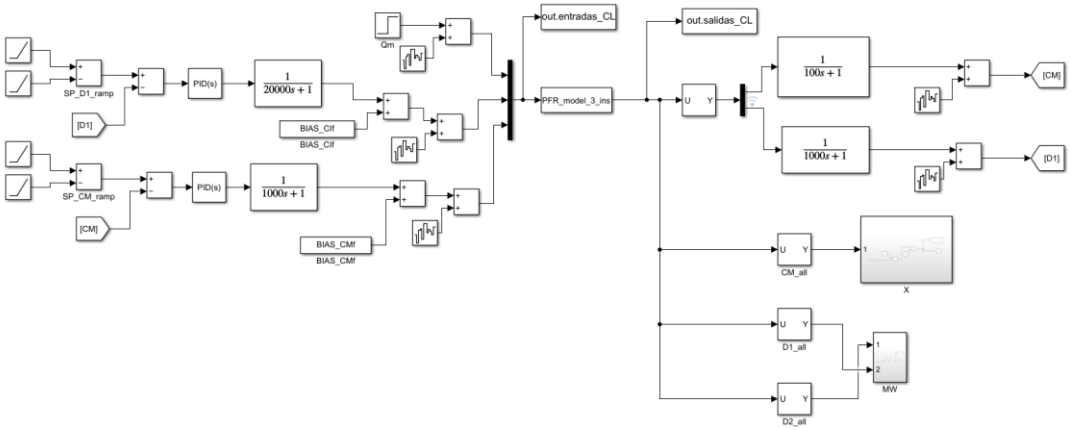

Figure 3-4: PFR PID implementation in Simulink®. Notice that the 'goto' block is used to simplify the closed loops implemented.

h) LQR control

As previously said in the tunning of LQG control, $\boldsymbol{Q}$ is normalized as described by Equation 2.31 and $\boldsymbol{R}$ is calculated by iteration, however, due to the high amount of states $\boldsymbol{Q}$ and $\boldsymbol{R}$ are not shown in the document. The final implementation of LQG control in Simulink® is shown in Figure 3-5.

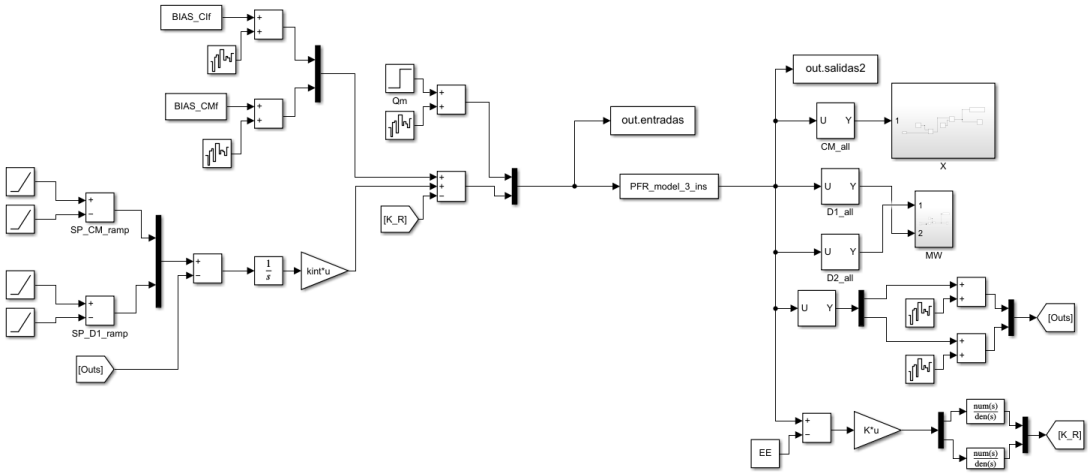

Figure 3-5: PFR Simulink® diagram for LQR controller with integral action. Notice that the 'goto' block is used to simplify the closed loops implemented.

i) LQG control

As the LQG control is an extension of the LQR control, the tunning is the same for both controllers. The Kalman filter tunning is not shown due to the same problem that $\boldsymbol{Q}$, $\boldsymbol{R_v}$ and $\boldsymbol{R_w}$ matrix are huge (250 states and 150 outputs for the

system implemented in the current controller). The final implementation of LQG control in Simulink® is shown in Figure 3-6.

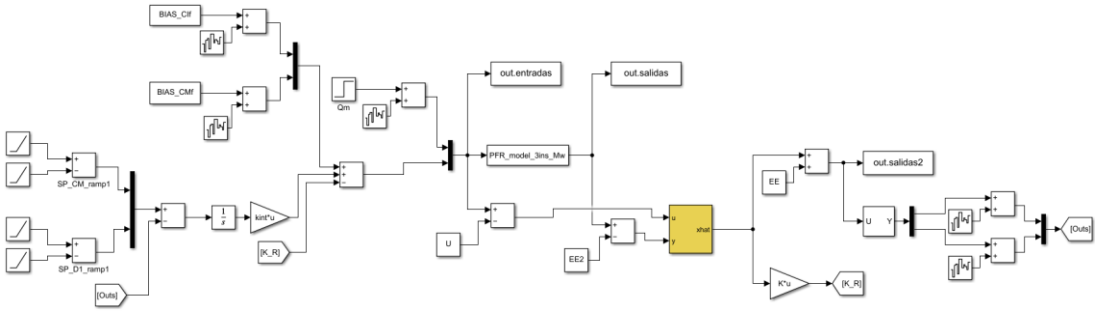

Figure 3-6: PFR simulink® diagram for LQG controller. Notice that the 'goto' block is used to simplify the closed loops implemented. The highlighted block is the Kalman filter implemented for state estimation.

3.4.3. Controllers' performance evaluation

Due to the problems presented in the last Chapter with higher values of setpoint, the current study case also used a ramp setpoint of 2% for the comparison between reactors. For the current section, just setpoint changes for C_M are shown, the other setpoint change (D_1) is presented in the PFR supplementary material section. For a better display of the controllers' actions, figures are used without the measurements noise Figure 3-8 and Figure 3-11. Besides, Figure 3-9 and Figure 3-12 show the system performance without the measurements noise and without the implementation of the filter to mitigate the integral noise. Also is presented the behavior of the system with filters and the measurements noise Figure 3-7 and Figure 3-10.

Interestingly, even the Kalman filter is unable to fully suppress the noisy signals in the systems but accomplishes the state estimation from measured states to unmeasured states. However, the other controllers also presented this kind of noise in a greater extend as was observed in the standard deviations presented above in Table 3-7.

For a better appreciation of changes in setpoint and performance indexes (t_s, t_r, t_p, O_S) for disturbances by changes in setpoint, all values are presented in Table 3-8 and Table 3-9.

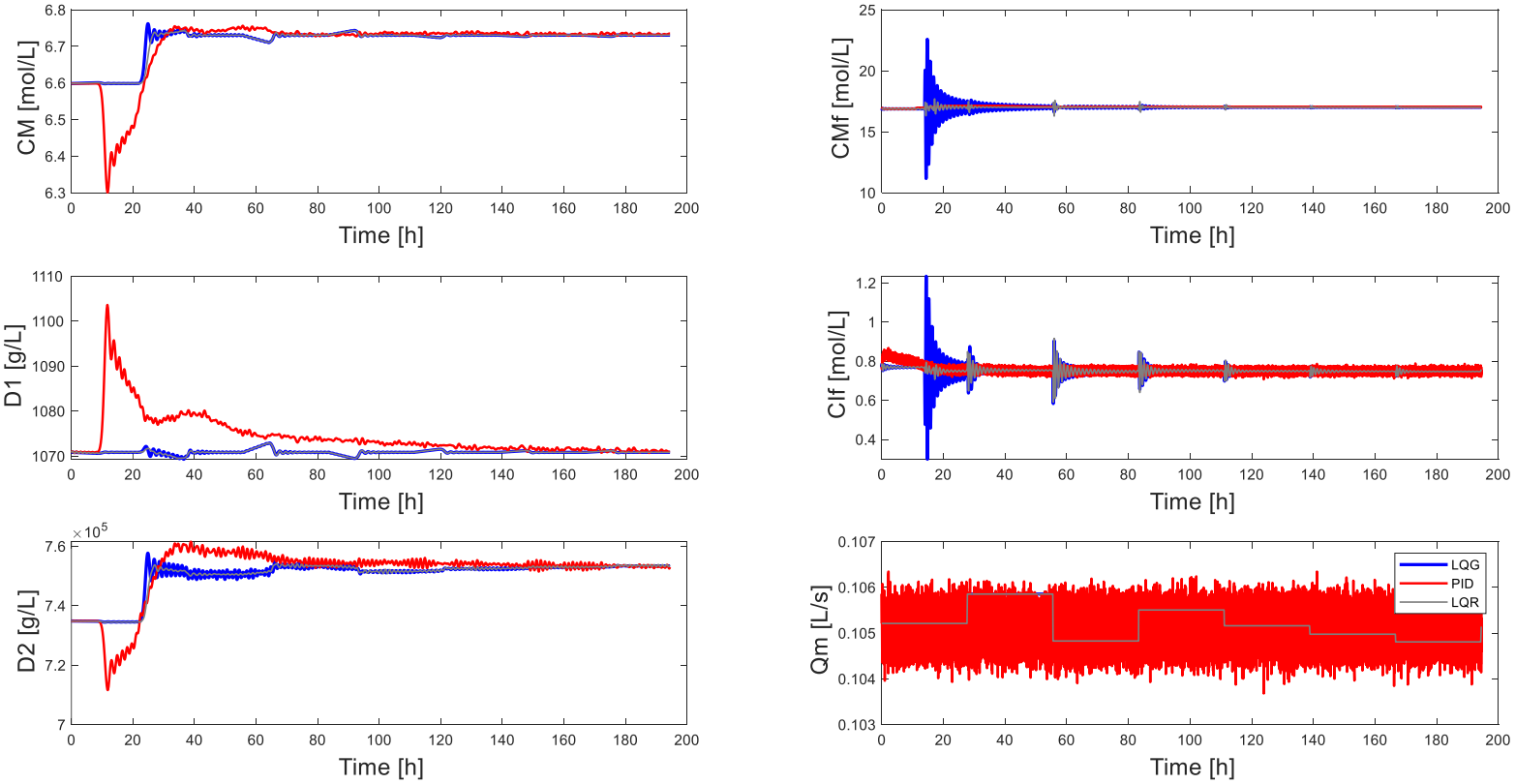

Figure 3-7: PFR system Response for setpoint change in C_M (2% above original setpoint) with filters and measurements noise implementation.

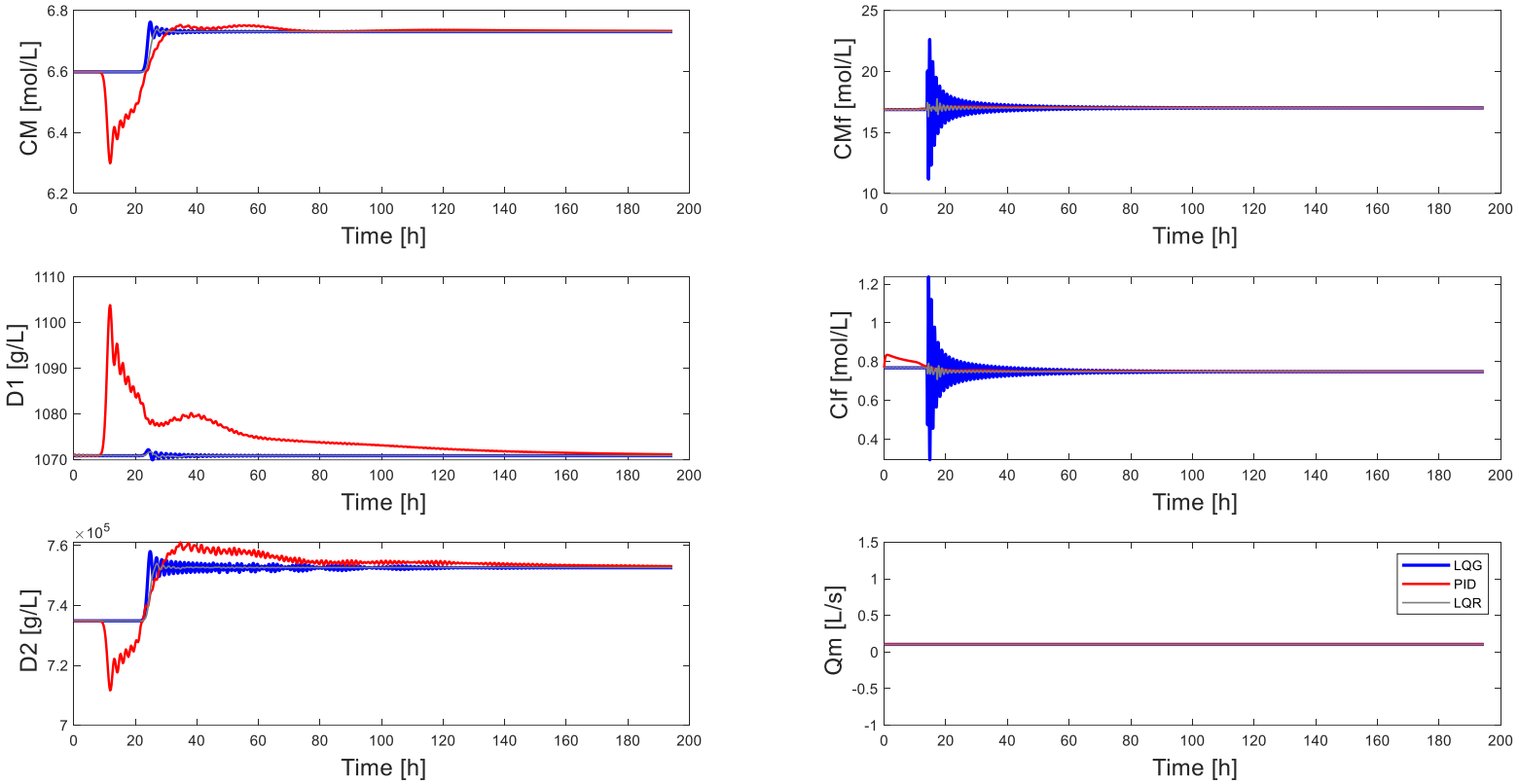

Figure 3-8: PFR system Response for setpoint change in C_M (2% above original setpoint) with filters implementation and without measurements noise implementation.

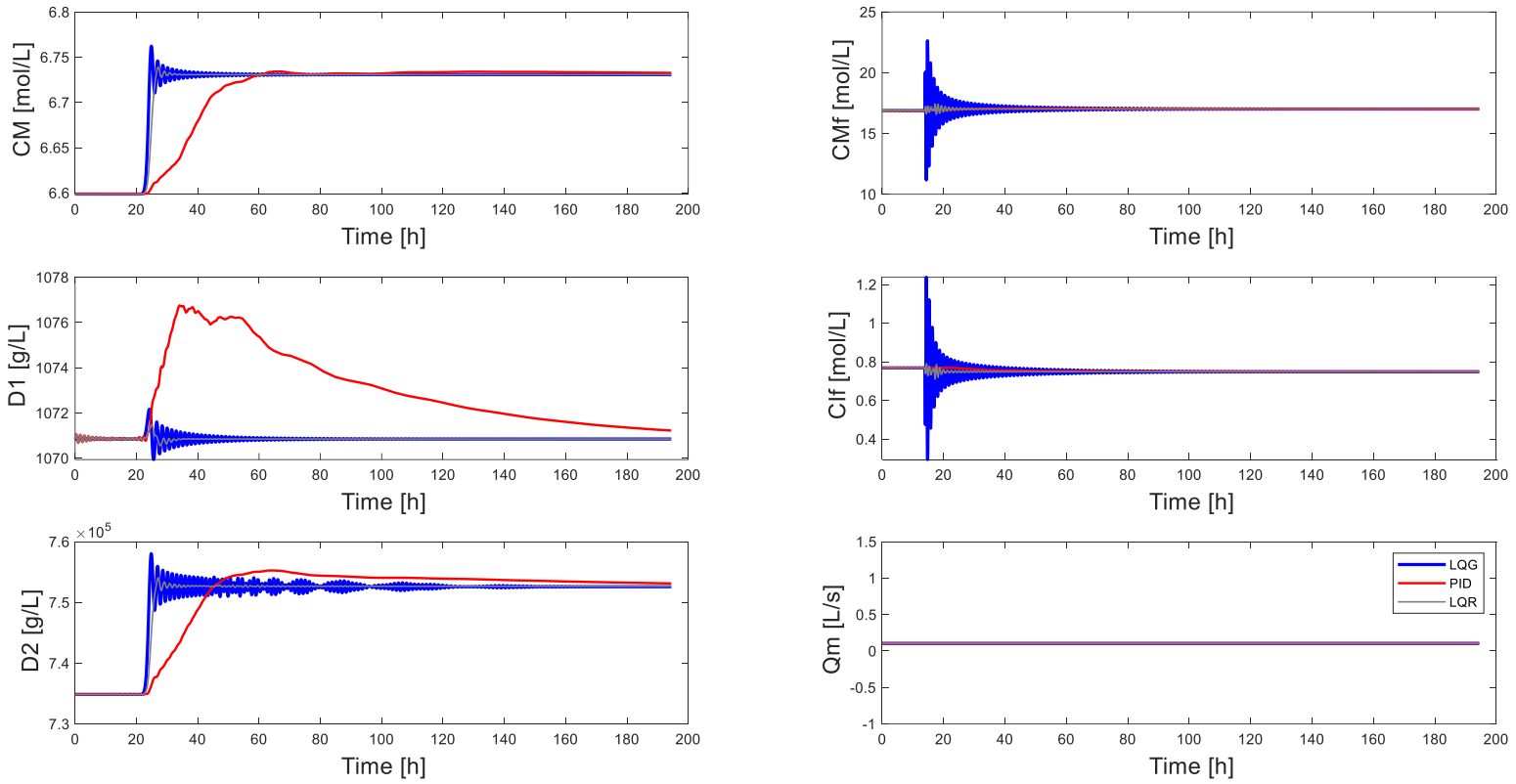

Figure 3-9: PFR system Response for setpoint change in C_M (2% above original setpoint) without filters implementation and without measurements noise implementation.

Table 3-8: PFR performance indexes for setpoint change of C_M.

Setpoint change	**C_M (6.59-6.72 mol/L)**		
Controller	**PID**	**LQR**	**LQG**
Rise time C_M [h]	47.63	12.55	10.41
Rise time D_1 [h]	180.56	13.04	11.04
Time to first peak C_M [h]	50.89	13.29	10.94
Time to first peak D_1 [h]	21.00	11.05	10.28
Settling time C_M [h]	82.65	21.77	36.34
Settling time D_1 [h]	180.56	30.28	66.68
Overshoot	0.03	0.06	0.23

Assessing the performance indexes, values of settling time are lower for the LQG control in the case of setpoint changes of D_1 (3.5 times lower than the PID controller and 1.17 times lower than the LQR). But not faster for setpoint changes of C_M (2.3 times lower than the PID controller but 1.7 times higher than the LQR). This could be attributed to the integral noise making the performance indexes present a deviation. Although that, the values for rise time are always lower for the LQG controller, with rise time values 4.6 to 10.6 times faster for PID and 1 to 1.2 times faster for LQR. Also, the time to first peak is faster for LQG (4.6-10 times lower than the PID controller and 1-1.21 times lower than the LQR). It is evident that there is a low difference comparing the LQR and LQG controllers.

All controllers present overshoot in the responses except the PID controller in the D_1 set point change according to Table 3-8 and Table 3-9 and easily corroborated in the previously mentioned figures. Meaning just for D_1 PID controller does not exceed the set point targeted. For the LQR and LQG controllers, the response of setpoint changes rise time and time to first are almost set at the same time, while the PID did not present this kind of behavior. Taking a closer look at responses for disturbance rejection in PID controller, it presents low values of time to first peak (21 hours) but high values of rise time (180 hours). This mean the PID controller presents an overshoot with no oscillation throughout the simulation, explaining the elevated values of settling time.

In summary, PID has shown a deficient performance compared tp the other two advanced controllers, where the responses for setpoint changes are almost 4-6 times slower than the best controller. Besides, the response for disturbances takes around 6 times to reach the steady state comparing the best controller.

According to the literature review, this is the first time D_1 is used as controlled variables, usually, literature is centered on controlling directly the temperature of the reactor and limiting reagent concentration. Taking into account that the temperature affects the kinetic parameters and that these in turn affect the energy balances. An approach where a parameter that has a direct effect on molecular weight is controlled, at least for PFR reactors (Li and Christofides, 2007; Flores-Tlacuahuac and Grossmann, 2010; Gharaghani, Abedini and Parvazinia, 2012; Padideh, Mohammad and Hossein, 2013). The most common controllers used in literature are the PID and PI, nevertheless, LQR controller is used to control a tubular reactor with axial dispersion (Li and Christofides, 2007). No information was found about LQG controller application in polymerization reactors, thus the approach used herein is novel.

Previous research has investigated LQR controller, where the settling time is approximately 8 hours to reach the new set point (Li and Christofides, 2007). Herein, LQR implementation takes around 22 hours to stabilize. In Mohsen Gharaghani, Abedini and Parvazinia, (2012), used PID controllers with values of 15 hours of the settling time for setpoint changes and 10 hours for disturbance rejection. Also, Padideh, Mohammad and Hossein, (2013) employed PID controllers, with response times of 2.5 hours for setpoint changes and 0.6 to 1.4 hours for disturbances. Comparing the PID herein times of almost 82 hours were obtained, however, this number is drastically reduced when compared to the LQG controllers have times of almost 36 hours. Observing that for the case proposed here the performance of the controllers is poorer, according to the setting time. However as previously mentioned, differences between the approaches in literature and this research reflected this abrupt difference. The change in reactor design parameters including kinetic parameters, consideration for the mass and energy balances, different state phases of the reaction, controlled variables, among others. So, the comparison for performance controllers is not equally balanced.

3.5. Conclusions

Here in, the styrene polymerization case has been investigated from multi-objective optimal design and control assessment for a PFR. From the design perspective, the implementation of two technical criteria (economical evaluation and the production capacity) as the objective functions in the system proves a robust way to obtain the operation point. Assessing important process variables to reach the operation point, enhancing the design of the system.

The pairing method employed for manipulated and controlled variables is the RGA methodology, a simple and powerful tool to design the control structure. Presenting a good association between the manipulated and the controlled variables. For this case, the pairing employed in this study case is the monomer concentration in the feed to control the monomer concentration and to manipulate the initiator concentration in the feed to control the first moment of the molecular distribution.

The best controller for the PFR study case is the LQG, despite LQR controller having a better settling time, at least with setpoint changes of C_M. Nevertheless, LQG controller obtained better results from the other 2 performance indexes and the capacity to transform measured states into unmeasured states, presenting more advantages for the present case. Even so, the controller selection depends on the objective that is required in the plant, changing the priorities on the performance indices, causing the best controller could be other than the LQG controller.

The better choice for the system production of styrene bulk polymerization by free radical at least in the economic and productive aspect is the PFR reactor system, due to the high performance of these designs. Easily comparing some indexes as the productivity, reaching almost 40 times the values achieved by the CSTR, the cost is almost 10 times lower than the CSTR study case. On the other hand, the CSTR reactor is the system that most resembles the reality of industrial systems, prioritizing the system with the least uncertainty. However, the results in this chapter showed the potential to further investigate PFR for future reactor implementations.

3.6. Nomenclature

A	Cross-sectional area in the tube.
A_d	Activation energy for initiator decomposition.
A_p	Activation energy for propagation reaction.
A_t	Activation energy for termination reaction.
c_p	Specific heat of monomer, polymer or mixture presented by Padideh, Mohammad and Hossein, (2013).
$c_{p,j}$	Specific heat of the service fluid presented by Padideh, Mohammad and Hossein, (2013).
C_A	Concentration of the limiting reagent A.
C_I	Concentratrion of the initiator.
C_{If}	Concentration of initiator in the feed.
C_M	Concentratrion of the monomer.
C_{Mf}	Concentration of monomer in the feed.
CO	Operation cost for styrene production.
C_P	Concentration of monomer intermediate.
D	Parameter D of the PID controller.
D_r	Reactor diameter.
D_0	Cero moment of molecular weight.
D_1	First moment of molecular weight.
D_2	Second moment of molecular weight.
E_p	Frequency factor for propagation reaction.
E_t	Frequency factor for termination reaction.
E_d	Frequency factor for initiator decomposition.
f	Initiator efficiency for AIBN.
$f'(x_i)$	Difference of the function in the position i.
$f(x_{i+1})$	Value of the fuction in the position $i+1$.
$f(x_{i-1})$	Value of the fuction in the position $i-1$.
F_A	Molar flow of the limiting reagent A.
F_j	Mass flow rate to the jacket presented by Padideh, Mohammad and Hossein, (2013).
h	Partition size value for the FDM.
h_i	Heat coefficient inside the reactor presented by Padideh, Mohammad and Hossein, (2013).
i	Position of the node that is used.
I	Parameter I of the PID controller.
k_d	Rate constant for decomposition reaction.
k_p	Rate constant for propagation reaction.
k_t	Rate constant for termination reaction.
L	Length of the reactor.
L_j	Jacket length presented by Padideh, Mohammad and Hossein, (2013).
N_A	Moles number of the limiting reagent A in the system.
M_m	Molecular weight of the monomer (styrene).

M_w	Mass average molecular weight in the reactor.
n	Number of nodes.
N	Parameter N of the PID controller.
O_S	Overshoot.
P	Parameter P of the PID controller.
PDI	Polydispersity index.
PR	Productivity.
PR_{ss}	Productivity in the steady-state.
Q	Weight that represents actuator performance in the LQR controller.
Q_i	Flow rate of initiator.
Q_m	Flow rate of monomer.
Q_s	Flow rate of solvent.
Q_t	Sum of all flows inning the reactor.
Q_V	Volumetric flow.
r_A	Reaction rate for the limiting reagent A.
R	Weight that represents actuator effort in the LQR controller.
R_o	Jacket radius presented by Padideh, Mohammad and Hossein, (2013).
R_p	Rate of polymerization presented by Padideh, Mohammad and Hossein, (2013).
R_v	Process noise covariance.
R_w	Measurement noise covariance.
R_1	Reactor radius presented by Padideh, Mohammad and Hossein, (2013).
t	Time.
t_p	Time to first peak.
t_r	Rise time.
t_R	Total time of reaction.
t_s	Settling time.
T	Reactor temperature.
T_j	Jacket temperature presented by Padideh, Mohammad and Hossein, (2013).
$T_{j,in}$	Jacket inlet temperature presented by Padideh, Mohammad and Hossein, (2013).
T_w	Reactor wall temperatura presented by Padideh, Mohammad and Hossein, (2013).
T_1	Reactor's temperature presented by Padideh, Mohammad and Hossein, (2013).
U_o	External overall heat transfer coefficient presented by Padideh, Mohammad and Hossein, (2013).
V	Reactor volume.
V_j	Jacket volume presented by Padideh, Mohammad and Hossein, (2013).
V_T	Total reactor volume.
V_Z	Axial velocity presented by Padideh, Mohammad and Hossein, (2013).
X	Reactor conversion.
z	Axial position presented by Padideh, Mohammad and Hossein, (2013).
Z	Length of the reactor.

3.6.1. Greek letters

ΔH	Heat of reaction presented by Padideh, Mohammad and Hossein, (2013).
ΔV	Amount of volume represented by the difference between two points along the axis coordinate in the tube.
η	Intrinsic viscosity.
ρ	Density of styrene_polyestirene mixture reacting mix presented by Padideh, Mohammad and Hossein, (2013).
ρ_j	Density of the service fluid presented by Padideh, Mohammad and Hossein, (2013).
π	Pi value.
ν	Linear velocity.
ω_m	Monomer weight fraction presented by Padideh, Mohammad and Hossein, (2013).

3.7. References

Alcocer García H (2018) Optimización multi-objetivo enfocada en la integración del diseño y control en secuencias intensificadas para la purificación de ácido levulínico

Alvarez LA, Odloak D (2012) Optimization and control of a continuous polymerization reactor. Brazilian J Chem Eng 29:807–820. https://doi.org/10.1590/S0104-66322012000400012

Asteasuain M, Bandoni A, Sarmoria C, Brandolin A (2006) Simultaneous process and control system design for grade transition in styrene polymerization. Chem Eng Sci 61:3362–3378. https://doi.org/10.1016/j.ces.2005.12.012

Chapra SC, Canale RP (2007) Métodos numéricos para ingenieros, Quinta edi. McGraw-Hill InteramerIcana

Chen CC (1994) A continuous bulk polymerization process for crystal polystyrene. Polym Plast Technol Eng 33:55–81. https://doi.org/10.1080/03602559408010731

Flores-Tlacuahuac A, Grossmann IE (2010) Simultaneous Cyclic Scheduling and Control of Tubular Reactors: Single Production Lines. Ind Eng Chem Res 49:11453–11463. https://doi.org/10.1021/ie1008629

Fogler HS (2006) Elements of Chenzicn 1 Reaction Engineering

Gharaghani M, Abedini H, Parvazinia M (2012) Dynamic simulation and control of auto-refrigerated CSTR and tubular reactor for bulk styrene polymerization. Chem Eng Res Des 90:1540–1552. https://doi.org/10.1016/j.cherd.2012.01.019

Hidalgo PM, Brosilow CB (1990) Nonlinear model predictive control of styrene polymerization at unstable operating points. Comput Chem Eng 14:481–494. https://doi.org/10.1016/0098-1354(90)87022-H

Koltzenburg S, Maskos M, Nuyken O (2017) Polymer Chemistry, Springer

Li M, Christofides PD (2007) An input/output approach to the optimal transition control of a class of distributed chemical reactors. In: Proceedings of the American Control Conference. pp 2042–2047

Luyben WL (2007) Chemical reactor design and control. John Wiley & Sons, Inc.

Padideh GM, Mohammad S, Hossein A (2013) Simulation, optimization & control of styrene bulk polymerization in a tubular reactor. Iran J Chem Chem Eng 32:69–79

Seborg DE, Edgar TF (2003) Process Dynamics and Control, second. Jhon Wiley and Sons, Inc.

The MathWorks Inc. (2013) Introduction to Model-Based PID Tuning in Simulink. https://www.mathworks.com/help/slcontrol/ug/introduction-to-automatic-pid-tuning.html#bsgra2e. Accessed 23 Dec 2022

Wallis JPA, Ritter RA, Andre H (1975) Continuous production of polystyrene in a tubular reactor: Part II. AIChE J 21:691–698. https://doi.org/10.1002/aic.690210408

Xu CZ, Wang JJ, Gu XP, Feng LF (2017) CFD modeling of styrene polymerization in a CSTR. Chem Eng Res Des 125:46–56. https://doi.org/10.1016/j.cherd.2017.06.028

3.8. PFR supplementary material

The following section contains the supplementary material as the Figures (with and without noise) and the table for values of the control performance for the system with changes in the setpoints D_1.

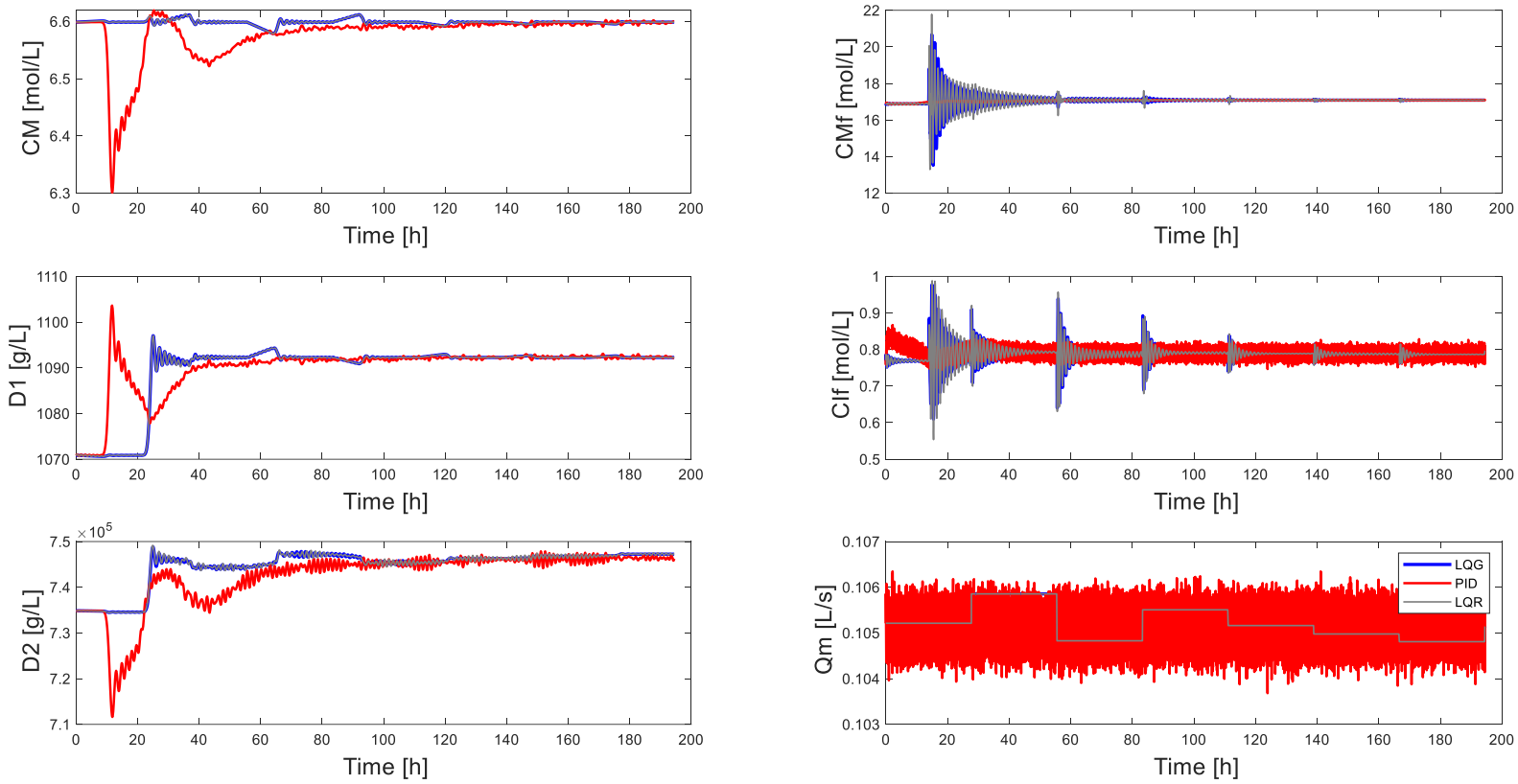

Figure 3-10: PFR system Response for setpoint change in $\boldsymbol{D_1}$ (2% above original setpoint) with filters and measuremets noise implementation.

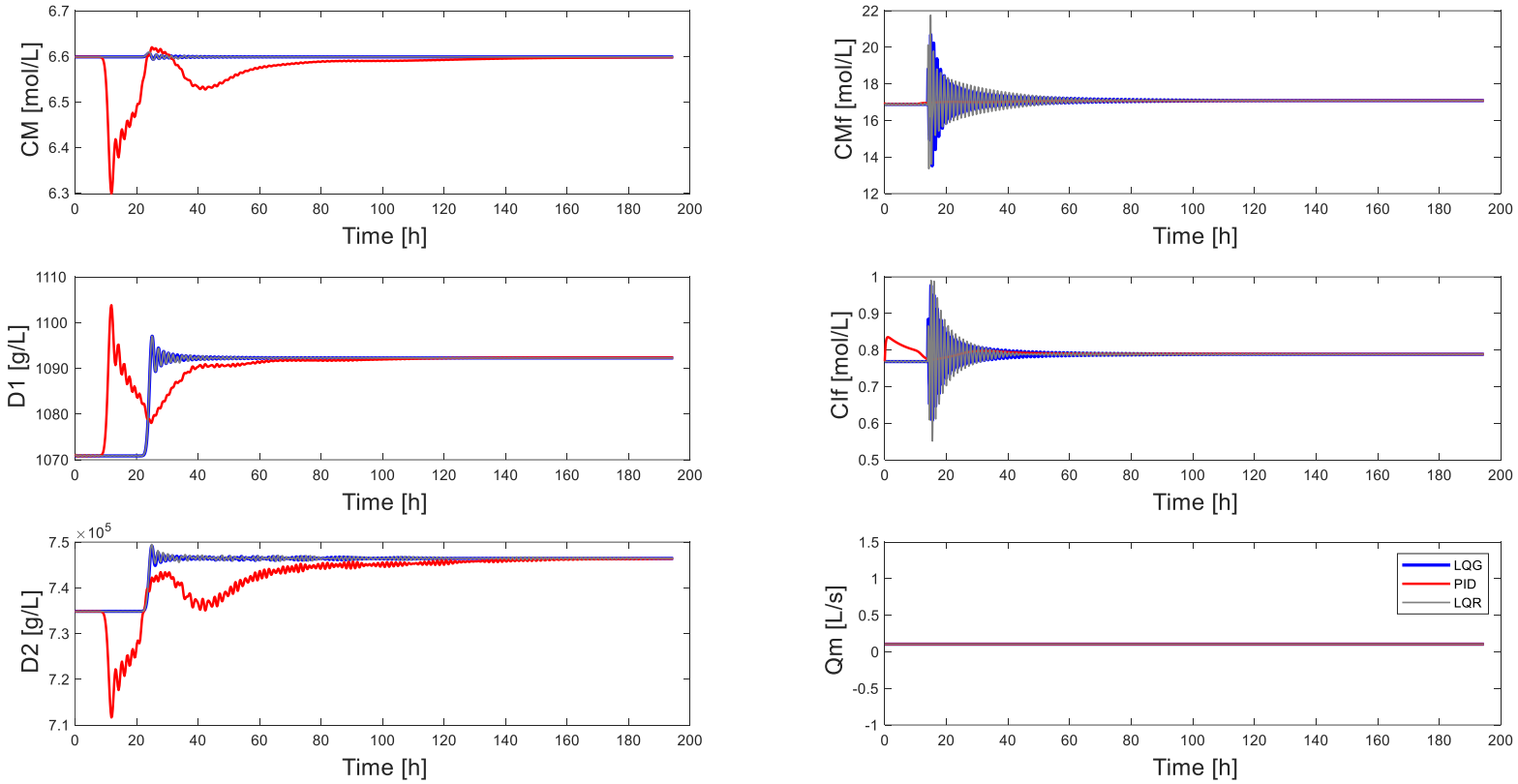

Figure 3-11: PFR system Response for setpoint change in $\boldsymbol{D_1}$ (2% above original setpoint) with filters implementation and without measurements noise implementation.

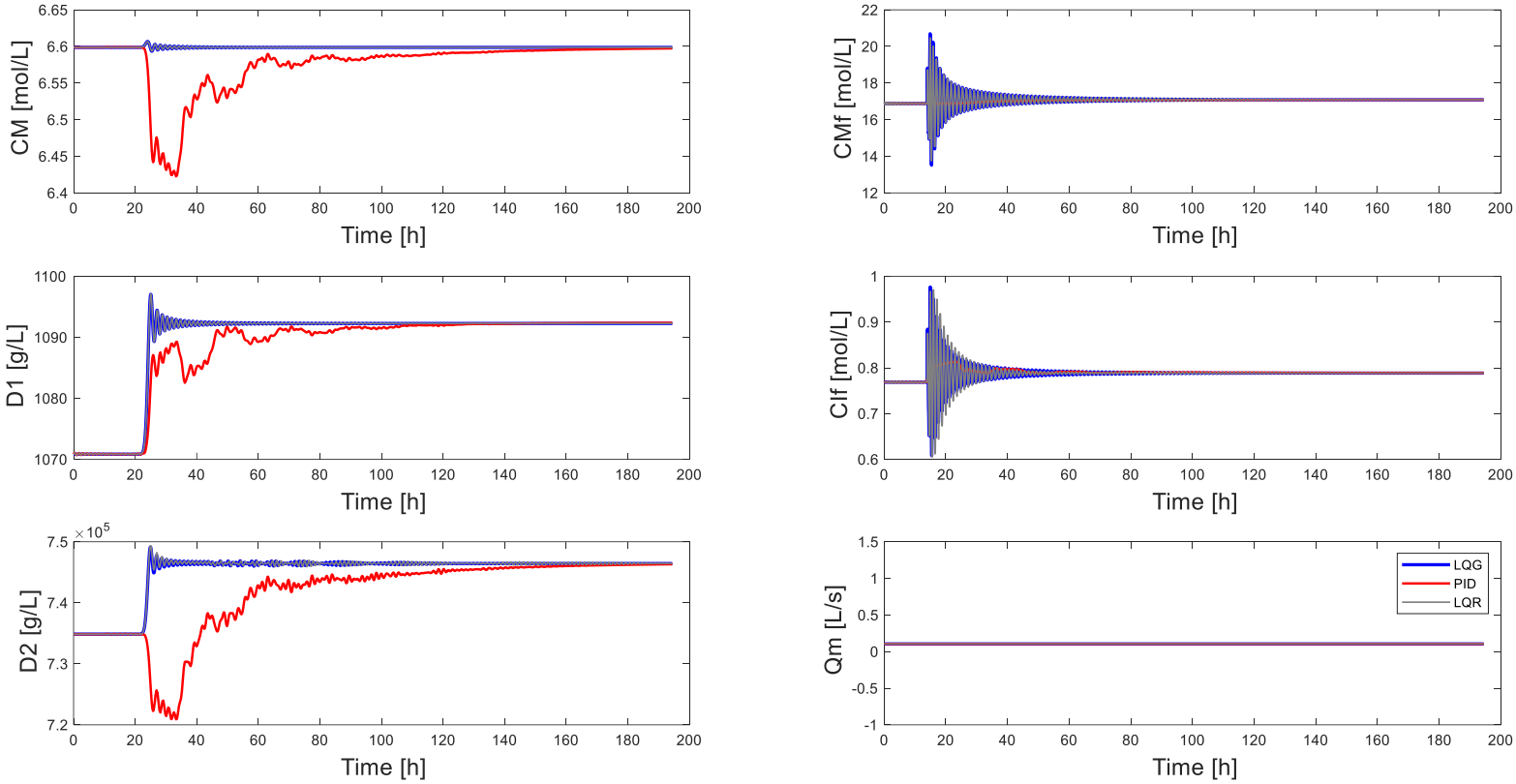

Figure 3-12: PFR system Response for setpoint change for $\boldsymbol{D_1}$ (2% above original setpoint) without filters implementation and without measurements noise implementation.

Table 3-9: PFR performance indexes for setpoint change of D_1.

Set point change	D_1 (1058.80-1079.98 g/L)		
Controller	**PID**	**LQR**	**LQG**
Rise time C_M [h]	156.07	10.98	10.61
Rise time D_1 [h]	112.96	10.66	10.63
Time to first peak C_M [h]	19.70	10.12	10.02
Time to first peak D_1 [h]	112.96	11.21	11.18
Settling time C_M [h]	156.07	66.08	50.23
Settling time D_1 [h]	112.96	37.33	31.78
Overshoot	-	0.23	0.22

3.9. Appendix

The following section presents some important information to complement the information presented in the document, including more data about the model used, the tunning for the PID, derivation of PID and LQR controller.

G. Mass balances

General mass balance:

$$In - Out = Accu - Gen \tag{3.19}$$

$$F_A|_V - F_A|_{V+\Delta V} = \frac{dN_A}{dt} - r_A \Delta V \tag{3.20}$$

Dividing by ΔV leads:

$$\frac{F_A|_V - F_A|_{V+\Delta V}}{\Delta V} = \frac{\partial C_A}{\partial t} - r_A \tag{3.21}$$

$$-\frac{\partial F_A}{\partial V} + (r_A) = \frac{\partial C_A}{\partial t} \tag{3.22}$$

Where F_A is the molar flow, also:

$$F_A = Q * C_A \tag{3.23}$$

$$\partial F_A = Q_v * \partial C_A \tag{3.24}$$

Where Q_v is the volumetric flow, replacing means:

$$-Q_v \frac{\partial C_A}{\partial V} + (r_A) = \frac{\partial C_A}{\partial t} \tag{3.25}$$

Where V is the volume in the reactor, also:

$$V = A * Z \tag{3.26}$$

$$\partial V = A * \partial Z \tag{3.27}$$

Where A is the cross-sectional area and Z is the length of the reactor, replacing means

$$-\frac{Q_v}{A}\frac{\partial C_A}{\partial Z} + (r_A) = \frac{\partial C_A}{\partial t} \tag{3.28}$$

$$-v \frac{\partial C_A}{\partial Z} + (r_A) = \frac{\partial C_A}{\partial t} \tag{3.29}$$

Where v is the ratio of volumetric flow and the cross-sectional area. Now for the 2 species entering the reactor.

$$-v \frac{\partial C_I}{\partial Z} + (r_I) = \frac{\partial C_I}{\partial t} \tag{3.30}$$

$$-v \frac{\partial C_M}{\partial Z} + (r_M) = \frac{\partial C_M}{\partial t} \tag{3.31}$$

H. Finite difference method (FDM)

The final styrene reactor model for a PFR is defined as follows:

$$\frac{\partial C_I}{\partial t} = -v \frac{\partial C_I}{\partial x} - k_d C_I \tag{3.32}$$

$$\frac{\partial C_M}{\partial t} = -\nu \frac{\partial C_M}{\partial x} - k_p C_M C_P \tag{3.33}$$

$$\frac{\partial D_0}{\partial t} = \left(0.5 * k_t * {C_P}^2\right) - \nu \frac{\partial D_0}{\partial x} \tag{3.34}$$

$$\frac{\partial D_1}{\partial t} = \left(M_m * k_p * C_P * C_M\right) - \nu \frac{\partial D_1}{\partial x} \tag{3.35}$$

$$\frac{\partial D_2}{\partial t} = \left(5 * M_m * k_p * C_P * C_M\right) + \left(\frac{5 * M_m * {k_p}^2 * {C_M}^2}{k_t}\right) - \nu \frac{\partial D_2}{\partial x} \tag{3.36}$$

Due to the system present PDEs, the finite difference method of first orden is used to solve the problem of the derivative with two dependent variables, depending on the approach. In the current work is used the 2 representations for the approximation to the first derivative difference are backward and central as follow:

Central difference:

$$f'(x_i) = \frac{f(x_{i+1}) - f(x_{i-1})}{2h} \tag{3.37}$$

Backward difference:

$$f'(x_i) = \frac{f(x_i) - f(x_{i-1})}{h} \tag{3.38}$$

Where i means the position of the node that is used, goes for 1 to n nodes, and h is the size of the current i node.

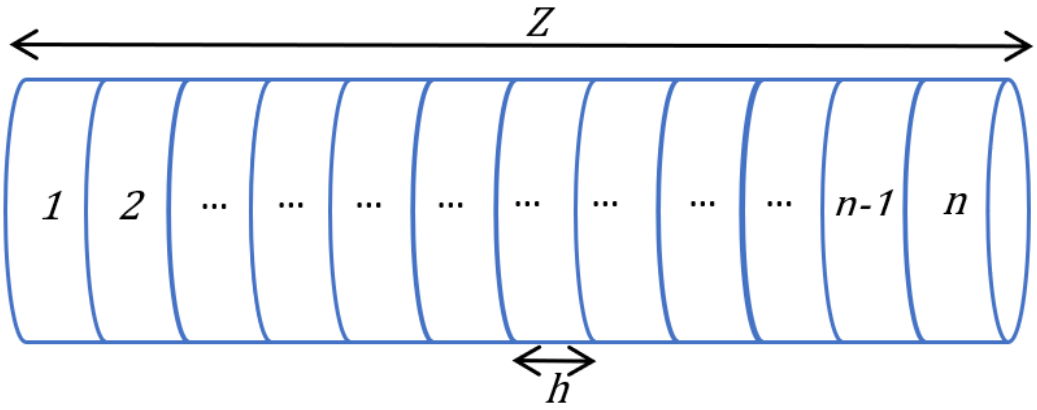

Figure 3-13: Finite difference method diagram.

Dividing all the length of the reactor into a total of 50 nodes where the first node is settled with the central form and also the subsequent nodes until the last node $(n-1)$, as shown in Figure 3-13 Where Z is the total size of the reactor, n is the total amount of nodes in the division, and h is the size of the current i node. For the first and the subsequent node until the $(n-1)$ node the central difference form is used, for the last node (n) is used the backward difference form.

As an example, the solution of a PFR has used the initiator concentration as follow:

First and middle nodes (central):

$$\frac{\partial C_I}{\partial x} = \frac{C_{I_{i+h}} - C_{I_{i-1}}}{2h} \tag{3.39}$$

Final node (backward):

$$\frac{\partial C_I}{\partial x} = \frac{C_{I_i} - C_{I_{i-1}}}{h} \tag{3.40}$$

Replacing for the first and middle nodes:

$$\frac{\partial C_I}{\partial t} = -\nu\left(\frac{C_{I_{i+h}} - C_{I_{i-1}}}{2h}\right) - k_d C_I \tag{3.41}$$

Replacing for the last node:

$$\frac{\partial C_I}{\partial t} = -v\left(\frac{C_{I_i} - C_{I_{i-1}}}{h}\right) - k_d C_I \tag{3.42}$$

Hence leads to the number n of ODEs that could easily solve. In the present work the number of nodes is 50 and solving ODEs by a modified Rosenbrock formula of order 2 solution in Matlab® (ode23).

4. Global conclusion

Considered the benchmark for control in polymerization systems, the bulk polymerization by free radical of styrene is selected as the reactive system. This process has high industrial relevance and could be considered as a benchmark for process design and control. For that reason, it is still extensively investigated in literature. For this reaction system, there is easy access to important information such as the steady state variables, parameter values, assumptions in the reactor for the mass and energy balances, and the step to step of the kinetic presented in the bulk polymerization by free radical of styrene. Interestingly, many of the referenced implementations present an ambiguity in the heat transfer coefficient parameter in the literature. Even the current model used shows issues that were corrected, as was exposed in the model correction implemented (Section 2.4.1.).

Process design optimization is carried out taking into account the inputs of the systems, the experience acquired with the purpose of the control objectives, and the evidence in the literature. Optimal design has shown that PFR has a better performance to be implemented for the production of styrene bulk polymerization by free radical. Obtaining operational costs values 6 times lower and almost 40 times productivity found values than the CSTR system. However, since PFR reactor key transport phenomena such as the gel effect and heat transfer are omitted. And also CSTR is the system that most resembles the reality of industrial systems, presenting the least uncertainty. However, the results showed the potential to further investigate PFR for future reactor implementations.

Three control structures were developed for each study case presented (PID, LQR, LQG), following the steps for the control structure design explained by the classic theory of control. Proving that automatic control not only can be implemented in this kind of system but target process enhancement process by reducing the off-specification production facilitating the transition times, thus reducing the enviromental impact and improving economic potential in the system. Results showed a better performance can be achieved by the advanced controller implementation (LQR and LQG). There, the settling time was lower for the advanced controller at least for the CSTR system (5-13 times faster). While for the PFR system

the settling time was lower in one of the two set point changes realized. Getting values of settling time 3-13 times faster than the conventional controller (PID).

It is necessary to remark on the importance of using the LQG controller since it can achieve state estimation from measured states to unmeasured states. A key aspect when it comes to this kind of system where the calculous of a variable employ a lot of time and effort. However, despite the PID has the worst performance, certain considerations need to be highlighted as the lack in the present thesis of an evaluation cost for the implementation of each controller and a fair comparison for each controller used. Since with the help of the economic evaluation, the effort made by each variable manipulated in the system can be evaluated, and thus the performance indices would be considered in their entirety for the evaluation of the three controllers. Considering the last installment as future work to continue the development of knowledge provided by this work. Also, the controller selection depends on the objective that is required in the plant, changing the priorities on the performance indices, and changing the choice of the best controller.

5. Recommendations

Through the realization of this thesis, some difficulties and problems were identified for future research in the same area to consideration:

- It is recommended to carry out experiments in the plant to validate the values of parameters found in the literature.
- Is recommended to employ the energy balances and the gel effect at least in the herein PFR system. Also is quite premature to define the PFR system as the best of the study case proposed for the production of polystyrene.
- It is recommended the use of thermic properties as variables, with the use of expressions dependent on temperature, to be a better system with fewer restrictions. Including the use of a better way to calculate the overall heat transfer coefficient due to some inconsistencies found in the literature presented in this work.
- It is important to know what is the purpose of the controller if the rejection of disturbances is not needed in the system another controller could be the best option. Besides the use of less controlled and manipulated variables is possible depending on the control goal. Even on some occasions the change for different manipulated variables used in the system.
- It is suggested to use an economic evaluation for the final product, in this case, the polystyrene because here is not used and is also an important item to decide controllers used in the system, controlled variables and manipulated variables.
- The installation of the automatic control proposed in this thesis in a plant may be an important choice decision item for the controller choose. Depending on the controller's installation price the decision made here may be affected. But regrettably, items like that surpass the objective in the present thesis.
- The recommended polymer used for this thesis is polystyrene, but the control structure design is built in such a way other polymers could be used (at least another polymer that uses bulk polymerization by free radical). Also, different arrangements of reactors could be used here to improve production in the process.

- According to the results obtained, the use of nodes in the PFR study case is key, it is supposed when a numeric method is used the more nodes presented the response is nearest to the real response. But with higher numbers of nodes make the system collapse because the high numbers of calculous need to be done. For this reason, 50 nodes were used but it can be used more nodes to ensure the accuracy of the method. However, the use of 100 nodes does not improve the responses obtained and with a high number the program crash.

- Is recommended not to use the herein PFR economic evaluation. Due is an arrangement using the information in the literature. Is better the use of an operational cost from a real PFR reactor in the polymer industry, to achieve veridical values in the evaluation.